Republic of Iraq

Ministry of Higher Education and Scientific Research

University of Karbala / College of Veterinary Medicine

Anatomy and Histology Department

Morphological and histochemical study of the impact of food preservative (sodium benzoate and pimaricin) on testicular tissues in albino male rats

A Thesis Submitted to the

Council of the Collage of Veterinary Medicine –University of Kerbala in Partial Fulfillment of Requirements for the degree of Master of (MSc) in Veterinary Medicine/ Anatomy and Histology

BY

Abdul-Ameer Ahmed Amoory kalash

Supervised by:

Supervised

Prof. Dr. **Muna Hussein Hassan**

Co. adviser

Prof. Dr.**Wefak Jbori Albazi**

1447 A.H **2025**. A.d

(فَتَعَالَى اللَّهُ الْمَلِكُ الْحَقُّ ۗ وَلَا تَعْجَلْ بِالْقُرْآنِ مِن قَبْلِ أَن يُقْضَىٰ إِلَيْكَ وَحْيُهُ ۖ وَقُل رَّبِّ زِدْنِي عِلْمًا)

صدق الله العلي العظيم

{114} سورة طه الآية

Supervisor Certificate

we certify that this thesis **(Histomorphological and Histochemical Study of the Impact of Preservatives on Testicular Tissues of male Wistar rats)** has been prepared by **Abdul-Ameer Ahmed kalash** under my supervision at the college of Veterinary Medicine, University of Kerbala in partial fulfillment of the requirements for the Degree of Master in the Sciences of Veterinary Medicine in Veterinary Anatomy and histology

Supervisors
Prof.Dr. Muna Hussain Hassan

Co- advisor

Prof.Dr. Wefak Jbori Albazi

Collage of Veterinary Medicine

University of Kerbala

Certification of examination committee

We the members of the examination committee, certify that after reading this thesis and have examined the students **Abdul-Ameer Ahmed Amoory kalash**, on its contents and that in our opinion, it is adequate as a thesis for the Degree of master (MSc) in veterinary Medicine/ Anatomy and Histology

Signature

Prof.Dr. Hussein Bashar Mahmood

College of Veterinary Medicine/ University of Kerbala

(Chairman)

Signature

Prof. Dr. Satar Abood Faris

(Member)

College of Sciences/ University of Thi Qar

Signature

Asst. Prof. Dr. Fateh Oudah AL-Shimmary

(Member)

College of Veterinary Medicine/ University of Kerbala

Signature

Prof.Dr. Wefak Albazi

(Member and supervisor)

College of Applied Medical Sciences / University of Kerbala

Signature

Prof.Dr. Muna Hussein Hassan

(Member and supervisor)

College of Veterinary Medicine/ University of Kerbala

Approved by the Council of the Collage of Veterinary Medicine / University of Kerbala

Signature

Prof. Dr. Hussein Bashar Mahmood

Head of Department \ Anatomy and Histology

Veterinary Medicine\ University of Kerbala

Signature

Assist. Prof. Dr. Mohammed Asaad Al-Kaabi

Dean of college of veterinary medicine /University of Kerbala

The recommendation of the Department

In the view of the above recommendation, I forward this thesis for scientific discussion by the examining committee

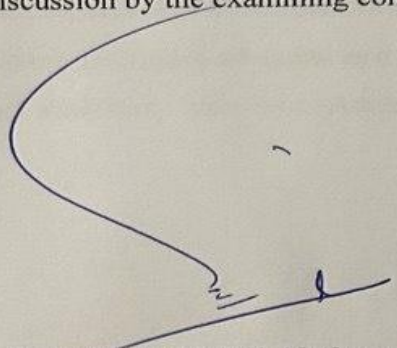

Prof.Dr. Ihab Ghazi Mahdi Al-shemmari

Vice Dean for Postgraduate studies and scientific Affairs

College of Veterinary Medicine

University of Kerbala

III

Certification of Linguistic Evaluator

We, the examining committee, certify that after reading this thesis and have examined the student Abdul-Ameer Ahmed kalash in its contents, and that in our opinion is adequate as a thesis for degree of Master in the Sciences of Veterinary Medicine / Anatomy and histology.

2025/9/1

أ.م. زينب فياض محمد حسن

Declaration

I hereby declare that this thesis is my origin work except for equations and citations which have been fully acknowledged. I also declare that it has not been previously, and is not concurrently, submitted for any other degree at University of Kerbala or other institutions.

Abdul-Ameer Ahmed kalash

DEDICATION

Praise be to Allah who granted me health, strength, and patience to complete this work.

My deepest gratitude and appreciation go to my beloved mother and father, whose unwavering support has been the backbone of my life.

I would like to express my sincere thanks to my supervisor, **Prof. Dr. Muna Hussein Hassan,** for her invaluable guidance, support, and encouragement throughout the course of this research.

Finally, I extend my appreciation to everyone who supported me, directly or indirectly, in the successful completion of this research.

.

Acknowledgments

First of all, I Would like to express my grateful thanks to Allah, who gives me everything.

I would like to express my sincere thanks and gratitude to the anatomy and histology Department especially my advisor, ***Prof. Dr. Muna*** who taught me a lot and helped to build up my academic background with her broad knowledge. Her strong support and patience are what made this dissertation possible and for her guidance and advice throughout the project

Great Thanks go to supervisor ***Prof.Dr. Wefak Albazi***

for support and her help in the study.

I am also profoundly grateful to **Prof.Dr. Hussein Bashar Mahmood** and **Asst. Prof. Dr. Ali Hussein Fadhil,** as well as all my esteemed teachers, for their continuous help, motivation, and academic guidance, without which this research would not have been possible.

My heartfelt thanks also go to **Asst. Prof. Dr. Fateh Oudah AL-Shimmary** and **Asst. Prof. Dr. Raeed Altaee** for their valuable support and encouragement during my study.

I would also like to extend my sincere gratitude and appreciation to Prof. **Dr. Mohammed Asaad Al-Kaabi**, the Dean of the College of Veterinary Medicine, as well as to the Department of Anatomy and Histology and all the respected academic staff members in the department, for their continuous support and valuable guidance throughout this work.

Finally, I wish to express my deep thanks to all the people who exerted all efforts in helping me with this work and those whose names do not come to my memory.

Abdul-Ameer Ahmed kalash

Abstract

This study aims to evaluate the histological and immunohistochemical impacts of sodium benzoate and pimaricin on the testes and epididymis of male albino rats, in order to determine their potential reproductive toxicity. The experiment was conducted in the laboratories of the Department of Anatomy and Histology, College of Veterinary Medicine / University of Kerbala, during the period from November 2024 to January 2025.

Forty male rats were randomly divided into four groups (10 rats/group): a control group and three experimental groups treated with sodium benzoate (600 mg/kg), pimaricin (0.3 mg/kg BW) and mixed group (sodium benzoate, pimaricin).Oral administration continued daily for 50 days. At the end of the experiment, Tissue samples were collected and processing for microscopic examination.

Histological analysis revealed degenerative and necrotic changes in the testes and epididymis of all treated groups. Sodium benzoate caused vascular thrombus, interstitial edema, degeneration of seminiferous epithelium, vacuolation of spermatogenic cells, and reduced Leydig cells, while the epididymis showed inflammatory infiltration, necrosis, and decreased sperm content. Pimaricin exposure induced focal testicular degeneration, vascular congestion, interstitial fibrosis, and impaired sperm maturation. The combined (mix) group exhibited the most severe alterations, including seminiferous tubular atrophy, spermatogenic cell necrosis, basement membrane disruption, extensive interstitial fibrosis, and tunica albuginea thickening, along with hyalinization and architectural distortion of epididymal ducts. PAS and Masson’s trichrome staining confirmed increased glycoprotein accumulation, basement membrane thickening, and marked collagen deposition, particularly in the mix group..

Immunohistochemical analysis: Malondialdehyde MDA marker was used to indicate oxidative stress, showed increased expression in all treated groups, with the most intense reaction in the mixed group, indicating clear oxidative damage in the reproductive tissues.

our hormone findings The results of the current investigation showed a discernible drop in serum levels of both Follicle-Stimulating Hormone (FSH) and Luteinizing Hormone (LH) across all treated groups compared to the control group. This hormonal suppression was progressed over time, with the most significant reductions observed in the mixed treatment group by day 50.

The study results suggest that exposure to long term of sodium benzoate and pimaricin, especially in combination, may lead to histological alterations in the testicular and epididymal tissues, accompanied by hormonal disruption, potentially impairing male fertility.

Table of Contents

Supervisor Certificate I
Certification of Linguistic Evaluator IV
Declaration V
DEDICATION VI
Acknowledgments VII
Abstract VIII
List of Figures XIII
List of Barograph XIX
List of Tables XIX
Chapter One Introduction .....
Chapter Two .....
Literature Reviews 3
2.1 Food Preservatives 3
2.2 Sodium benzoate 3
2.3 The adverse effects of Sodium Benzoate 4
2.4 Effect of Sodium Benzoate's on Embryos 5
2.5 The Impact of Sodium Benzoate's on the Liver and Kidney 6
2.6 The Impact of Sodium Benzoate on Alzheimer's Disease. 7
2.7 Sodium benzoate's Effect on Male Reproduction 8
2.8 The Impact Sodium Benzoate's on Hormone Levels 9
2.9 Natamycin 10
2.10 Acute and Chronic Toxicity of Pimaricin 10
2.11 The Effects of Natamycin on The Liver 11
2.12 Effect of natamycin on cytochrome P450 enzymes 11
2.13 Natamycin (E 235) as a Dietary Supplement 11
2.14 The Impact of Natamycin on Broiler Chicken Growth Performance 12
2.15 The effects of the antifungal natamycin on cholesterol 13

2.16 Atamycin (supplement) 14
2.17 Evaluating the Impact of Natamycin use in food preservative on the clinical efficacy of amphotericin B 14
2.18 Sensitivity to Natamycin (Pimaricin) 15
2.19 Plasma Level of LH and FSH 15
2.20 Serum LH, FSH, Prolactin and Progesterone from Birth to Puberty in Female and Male Rats 16
2.21 Health Benefits and Natural Alternatives 16
2.22 Potential Adverse Effects 17
2.23 Preservatives and Hormonal Balance in General 17
2.24 General Overview of Preservatives 18
2.25 Preservatives' Contribution in Oxidative Stress and Apoptosis . 18
Chapter Three Materials and methods 20
Methodology 20
3.1. Materials 20
3.1.1. Instruments and Equipment: 20
3.2 Experimental Design 23
3.3 The Experiment Protocol 23
3.4 Histological study 24
3.5 Immunohistochemistry 24
3.6 Blood Collection 25
3.7 Determination of Reproductive Hormones 26
3.8 Statistical Analysis 27
3.9 Ethical approval 27
Chapter Four .....
4-1- Histological findings of control group 28
4.2. Histological Changes in the Sodium Benzoate-Treated Group 29
4.3. Histological finding of Section in the Pimaricin-Treated Group ... 30
4.4. Histological Findings in the Mix-Treated Group 31
4.5 Immunohistochemistry Study of Experimental Animal with MDA Stain 33
4.5.1 Immunohistochemical Analysis of MDA in the Control Group . 33

4.5.2Immunohistochemical Analysis of MDA in the Sodium Benzoate Group 34
4.5.3 Immunohistochemical Analysis of MDA in the Pimaricin Group 35
4.5.4 Immunohistochemical Analysis of MDA in the Mix Group (Sodium Benzoate + Pimaricin)..... 36
Discussion Immunohistochemical assessment of MDA in treated group 37
4.6 Serum Follicle-Stimulating Hormone (FSH) and Luteinizing Hormone (LH) Levels..... 41
Discussion of Hormones..... 42
Discussion..... 72
Chapter Five.....
Conclusions and..... 73
Recommendations..... 73
References..... 73

List of Figures

Page No.	Title
46	Histological section of the testis form the **control group** showed seminiferous tubules that circular with regular contour (yellow arrow)&The interstitial tissue appeared as delicate loose C. T and Leydig cells (white arrow) (H&E stain 10 X
	Histopathological section of testis in **control group** showed normal seminiferous tubules that lined with series of spermatogenic cells: spermatogonia , primary spermatocytes, round spermatids (blue arrow), Sertoli cells (red arrow) with attached sperms & interstitial cell of Leydig (black arrow) (H&E stain 40 X).
47	Histopathological section in the epididymis of **control group** showed epididymal tubule that lined by ciliated pseudostratified columnar epithelium with few spermatozoa in the lumen (yellow arrow) (H&E stain 10 X).
	Histopathological section of epididymis from control group showed columnar cells with basal nuclei and stereocilia (yellow arrow), basal cells resting on the basal lamina & clear cells with pale cytoplasm (black arrow) with thin layer of smooth muscle fibers surrounds each epididymal duct (white arrow), numerous spermatozoa were seen in the epididymal lumen (green arrow), (H&E stain 40 X).
48	Histological section of the testis from control group demonstrated well-preserved testicular architecture, with normal seminiferous tubules, The Tunica Albuginea and basement membranes of the tubules are distinctly PAS- staining affinity indicating normal glycoprotein structures (yellow and green arrows) respectively (PAS stain 10 X)
	Histological section of the testis from the control group showed Periodic acid–Schiff staining affinity in the basement membrane (yellow arrow) & elongated spermatids with acrosomal caps in some developing spermatids (white arrows) (PAS stain 40 X)
49	Histological section of the epididymis from the control group showed PAS reaction in the basal lamina of the epididymal ducts (white arrow) with intact thin apical PAS reaction in the lining epithelial cells (yellow arrow) (PAS stain X40).
	histological section in the epididymis of control group showed purple stained collagen fibers surrounding the epididymal ducts (yellow arrow)(PAS stain 10 X)

50	histological section in the testis of control group showed positive masson reaction for tunica Albuginea stained blue color (yellow arrow) (masson trichrome stain 10 X)
	Histological section in the epididymis of control group showed masson trichrome +ve for tunica Albuginea that stained blue color (yellow arrow) (masson trichrome stain 10 X)
51	Histological section of the testis after 50 days post exposed to sodium benzoate showed thrombus of blood vessels (yellow arrow) with edema in interstitial tissue and sub tunica albuginea (black arrows) (H&E stain 10 X).
	Histological section of the testis in rat group that exposed to sodium benzoate after 50 days, showed moderate increase in the thickness of tunica albuginea (black arrow) and vacuolation of spermatogenic cell (yellow arrow) with few Leydig cells interstitial (white arrow), (H&E stain 10 X).
52	Histological section of the epididymis in the sodium benzoate group at 50 days post-exposure showed disorganized tubular structure with marked expansion of interstitial tissue and infiltration of mononuclear inflammatory cells mainly lymphocytes (yellow arrow), (H&E Stain10 X, 40X)
	Histological section of the epididymis from sodium benzoate group at 50 days post exposure, revealed hydropic degeneration of epithelial lining cells (red arrow), luminal dilatation, oligospermia (green arrow) with mild interstitial edema, detached of stereocilia (yellow arrow), (H&E stain 40 X).
53	Histological section of the testis from group treated with sodium benzoate at 50 days post exposure, showed lumen full of abundant PAS +ve elongated spermatids (yellow arrow) with increase in thickness of the basement membrane that stained purplish (white arrow),(PAS stain 10 X)
	Histological section of epididymis from sodium benzoate group at 50 days post exposure, showed moderate increase in the thickness of basal lamina (yellow arrow) with strong PAS reaction in the apical parts of the lining epithelial cells (white arrow) (PAS stain 10 X).
54	Histopathological section of the testis from sodium benzoate exposed group at 50 days post exposure, showed moderate increase in the thickness of tunica Albuginea due to proliferation of fibrous connective tissue that stained with blue color (yellow arrow) (Masson trichrome stain 10 X).

54	Histopathological section of epididymis from sodium benzoate exposed group after 50 days, showed moderate increase in fibrous connective tissue in tunica Albuginea & collagen fibers in the connective tissue surrounding the epididymal ducts which stained with blue color (yellow arrow), (Masson trichrome stain, 10 X).
55	Histological section of the testis from pimaricin group after 50 days of exposure, showed degenerative & necrosis of spermatic cells (yellow arrow) with decrease Leydig cells in the interstitial (green arrow), congestion of blood vessels (white arrow), (H&E stain 10 X +40 X).
	Histological section of the testis from the pimaricin treated group at 50 days post-exposed are showed degenerative changes and necrosis of spermatogenic epithelium (white arrow) & some lumens have few mature spermatozoa (yellow arrow) and other lumen filled with sloughed immature cells, (blue arrow) (H&E stain 10 X)
56	Histological section of the epididymis from the pimaricin treated group at 50 days post-exposed are showed vascular congestion (white arrow) & large number of degenerative sperm(red arrows) (H&E stain 10 X)
	Histological section of the testis from the pimaricin trated group at 50 days post-exposed are showed degenerative changes with vaculations of cells (white arrow)(PAS stain 10 X)
57	Histological section of epididymis from pimaricin treated group at 50 days post exposure, showed obvious increase in the thickness of basement membrane (blue arrow) with loose of normal tissue appearance intact thin apical PAS reaction in the lining epithelial cells (white arrow), (PAS stain, 10 X).
	Histological section of the testis from the pimaricin treated group at 50 days post exposure, showed disorganization in the seminiferous tubules with increase in the thickness of tunica Albuginea due to overproduction of fibrous connective tissue stained with blue color (yellow arrow), (Masson Trichrome stain, 10 X).
58	Histological section of the epididymis from the pimaricin treated group at 50 days post exposure, showed irregular outlines with degeneration of the ductal epithelium and increased collagen fibers surrounding the epididymal ducts stained with blue color (yellow arrows), (Masson Trichrome stain, 10 X).
	Histological section of the epididymis from the pimaricin treated group at 50 days post exposure showed increased fibrous connective tissue in the tunica Albuginea stained with blue color (yellow arrow) with irregular tubules structure (Masson Trichrome stain 10 X)

59	Histological section of the testis from the mixed treated group at 50 days post-exposure, exhibited seminiferous tubules atrophy with clear dilatation of interstitial spaces (yellow arrows) and decrease in number of Leydig cells (H&E stain 10 X)
	Histological section of the epididymis from the mixed treated group at 50 days post-exposed showed hyalinization of epididymal lumen (yellow arrows) (H&E stain 10 X))
60	Histological section of the cauda epididymis from the mixed treated group at 50 days post exposure showed irregular arrangement of tubules surrounded by stroma with an increase thickness of basement membrane (black arrow) (H&E stain 10 X).
	Histological section of the testis from the mix treated group at 50 days post-exposed are showed edema (yellow arrow) and a marked increase in thickness of interstitial tissues and basement membrane with stained purplish color (black arrow) with low number of Leyding cells(PAS& 10 X)
61	Histological section of the epididymis from the mixed treated treatment group at 50 days post exposure showed irregular tubular structure and marked increase in thickness of tunica albuginea & basement membrane stained with purplish color (black arrow), (PAS stain ; 10 X).
	Histological section of the testis from the mix treated group at 50 days post-exposure are showed loose of normal tissue appearance and a marked increase in the thickness of tunica Albuginea due to increased fibrous connective tissue stained with blue color (black arrow), (Masson Trichrome stain 10 X).
62	Histological section of the epididymis from mixed treatment group at 50 days post-exposure, showed marked fibrosis in tunica Albuginea and proliferation of collagen fibers surrounding the epididymal ducts (black arrow) and small blood vessels stained with blue color (red arrow), (Masson Trichrome stain 40 X).
	Immunohistochemistry analysis of MDA in formalin fixed testis sections from the normal control rats at day 50 of experiment. Representative photomicrographs showing no immune reactive cells in the negative control without primary antibody. (Negative MDA immunostaining 40 X +10 X)
63	Immunohistochemistry analysis of MDA in formalin fixed testis sections from the normal control rats at day 50 of experiment. Representative photomicrographs demonstrated the presence of MDA immunoexpression in the spermatogenic (white arrow), Sertoli cells (blue arrow)in the seminiferous tubules& Leydig cells in the interstitial tissue (black arrow) (MDA immunostaining 40 X)

63	Immunohistochemistry analysis of MDA in formalin fixed cauda epididymis sections from the normal control rats at day 50 of experiment. Representative photomicrographs showing no (MDA) immunostaining in the negative control without primary antibody. (Negative MDA immunostaining 40 X +10 X).
64	Immunohistochemistry analysis of MDA in formalin fixed cauda epididymis sections from the normal control rats at day 50 of experiment. Representative photomicrographs demonstrate the presence of MDA in the nuclear and cytoplasm of the epithelial cells lining the epididymal ducts (white arrow). (MDA immunostaining 40 X).
	Immunohistochemistry analysis of MDA in formalin fixed testis sections from the sodium group at day 50 of experiment. Representative photomicrographs showing positive (MDA) immunoexpression in the spermatogenic in the seminiferous tubules (white arrow).(MDA immunostaining, 40 X)
65	Immunohistochemistry analysis of MDA in formalin fixed testis sections from the sodium group at day 50 of experiment. Representative photomicrographs showing positive (MDA) immunoexpression in Leydig cells in the interstitial tissue (white arrow) (MDA immunostaining 40 X)
	Immunohistochemistry analysis of MDA in formalin fixed cauda epididymis from the sodium group at day 50 of experiment. Representative photomicrographs showing no (MDA) immunostaining in the negative control without primary antibody. (Negative MDA immunostaining 40 X +10 X).
66	Immunohistochemistry analysis of MDA in formalin fixed cauda epididymis from the sodium group at day 50 of experiment. Representative photomicrographs showing mild nuclear and cytoplasmic MDA immunoreaction in the epithelial cells lining the epididymal ducts(white arrow). (MDA immunostaining 10 X +40 X).
	Immunohistochemistry analysis of MDA in formalin fixed testis sections from the pimaricin group rats at day 50 of experiment. Representative photomicrographs showing no immune reactive cells in the negative control without primary antibody. (Negative MDA immunostaining 10 X)
67	Immunohistochemistry analysis of MDA in formalin fixed cauda epididymis from the pimaricin treated group at day 50 of experiment. Representative photomicrographs showing mild (MDA) immunoexpression in the spermatogenic (white arrow) when compared with other treated group, and moderate reaction Sertoli cells (blue arrow) in the seminiferous tubules& Leydig cells in the interstitial tissue (black arrow) (MDA immunostaining 40 X)

68	Immunohistochemistry analysis of MDA in formalin fixed cauda epididymis from the pimaricin group at day 50 of experiment. Representative photomicrographs showing no (MDA) immunostaining in the negative control without primary antibody.(negative MDA immunostaining 40 X +10 X)
68	Immunohistochemistry analysis of MDA in formalin fixed cauda epididymis from the pimaricin group at day 50 of experiment. Representative photomicrographs showing moderate nuclear and cytoplasmic MDA immunoreaction in the epithelial cells lining the epididymal ducts(white arrow) when compared with mix group (MDA immunostaining 10 X +40 X)
69	Immunohistochemistry analysis of MDA in formalin fixed testis sections from the mix group (Sodium + Pimaricin) at day 50 of experiment. Representative photomicrographs showing no immune reactive cell (negative MDA immunostaining) in the negative control without primary antibody. Magnification 40 X +10 X.
	Immunohistochemistry analysis of MDA in formalin fixed cauda epididymis from the mix group (Sodium + Pimaricin) at day 50 of experiment. Representative photomicrographs showing strong nuclear and cytoplasmic MDA immunoreaction in the epithelial cells lining the epididymal ducts (white arrow). (Magnification 10 X +40 X).
70	Immunohistochemistry analysis of MDA in formalin fixed testis sections from the mix group (Sodium + Pimaricin) at day 50 of experiment. Representative photomicrographs showing no (MDA) immunostaining in the negative control without primary antibody. Magnification 10 X.
	Immunohistochemistry analysis of MDA in formalin fixed testis sections from the mix group (Sodium + Pimaricin) at day 50 of experiment. Representative photomicrographs showing strong nuclear and cytoplasmic positivity staining for MDA in germ cells (red arrow) & Sertoli cells (white arrow) in seminiferous ducts. Magnification 40 X).
71	Immunohistochemistry analysis of MDA in formalin fixed cauda epididymis from the mix group (Sodium + Pimaricin) at day 50 of experiment. Representative photomicrographs showing no (MDA) immunostaining in the negative control without primary antibody. (Magnification 10X +40X).
	Immunohistochemistry analysis of MDA in formalin fixed cauda epididymis from the mix group (Sodium + Pimaricin) at day 50 of experiment. Representative photomicrographs showing strong nuclear and cytoplasmic MDA immunoreaction in the epithelial cells lining the epididymal ducts (white arrow). Magnification 10 X +40 X.

List of Barograph

Page No.	Title
44	Barograph (4-1): Changes in serum FSH levels in control and treated groups at 0, 20, and 50 days. A progressive decline in FSH is observed in all treated groups compared to the control, with the most significant suppression in the mix group (sodium benzoate + pimaricin).
44	Barograph (4-2): shows a significant decrease in Luteinizing Hormone (LH) levels over time, particularly in the sodium benzoate, pimaricin, and mix groups compared to the control group. The mix group exhibited the most pronounced reduction by day 50.
45	Barograph (4-3): Serum Follicle-Stimulating Hormone (FSH) Levels in Different Experimental Groups at 0, 20, and 50 Days.This chart shows a significant time-dependent decrease in FSH levels in all treated groups compared to the control. The most pronounced suppression is observed in the mix-treated group (sodium benzoate + pimaricin), suggesting a synergistic inhibitory effect on the hypothalamic-pituitary-gonadal axis
45	Barograph (4-4): shows the effects of different treatments on Follicle-Stimulating Hormone (FSH) levels over time (0, 20, and 50 days). The control group maintains stable FSH levels, while all treatment groups—sodium benzoate, pimaricin, and especially the mix group—exhibit a significant and progressive decline in FSH levels, with the mix group showing the most dramatic drop by day 50.

List of Tables

Page No.	Title
18	Table(3-1): Chemicals and kits were used in the study.
19	Table (3-2) shows the instruments utilized in this investigation, as well as the providers and sources.
	Table (4-1)Thickness of tunica albuginea in mane and Standard deviation (µm)

List of abbreviation

abbreviation	meaning
SB	Sodium benzoate
MDA	Malondialdehyde
PAS	Periodic acid- shifft
EFSA	European Food Safety Authority
ANS	Additives and Nutrient Sources added to Food
NMDA	The N-methyl-D-aspartate
TNF-α	Tumor Necrosis Factor-alpha
IL-6	Interleukin-6
17β-HSD	17-beta-hydroxysteroid dehydrogenase deficiency
17-KSR	17-ketosteroid reductase

Chapter One
Introduction

Introduction

Food preservatives are extensively used in food and pharmaceutical industries, raising serious concerns about their safety. The antifungal and antibacterial qualities of sodium benzoate and pimaricin make them popular preservatives. A natural antifungal agent called pimaricin is used to prolong the shelf life of a variety of food products, while sodium benzoate is frequently used to prevent the growth of molds and yeasts in acidic foods. **(Cinar and Onbaşı, 2019).** Because of its antibacterial and antifungal qualities Sodium benzoate is used as a preservative in food at precisely measured dosages **(Davidson, Sofos and Branen, 2005)** although these compounds are effective in preserving food quality, new data shows that these compounds may have adverse impact on human health, notably reproductive functions **(Moniruzzaman and Min, 2020)**. Research has indicated that exposure to various chemicals can induce histopathological changes in testicular and epididymal tissues, impacting spermatogenesis and hormone levels**, (Rezaei, Amirahmadi and Poozesh, 2022).** The FDA has certified that sodium benzoate, a popular food preservative, is generally recognized as safe when used at authorized quantities **(Food and Drug Administration, 2016)**. However Recent studies, indicate that it might negatively impact the reproductive system as well as other organ systems. For instance,**(Kehinde, Christianah and Oyetunji, 2018)** revealed that sodium benzoate caused oxidative stress in rat liver and kidney cells, which raised concerns about the possible effects on other organs, such as the tests' naturally occurring antifungal substance, pimaricin (PIM), commonly referred to as natamycin (E235), is frequently employed as a food preservative, particularly in cheese and other dairy products **(Cinar and Onbaşı, 2019).**

While its usefulness in food preservation is well-established, the potential influence of pimaricin on male reproductive health, especially testicular tissue, remains completely unexplained **(Silva and Lidon, 2016).** Pimaricin, generated by Streptomyces natalensis, is a polyene macrolide antifungal that functions by attaching to ergosterol in fungal cell membranes, causing cell death **(Te Welscher *et al.*, 2008).**Regulatory agencies worldwide have approved its use as a food additive. However, safety assessments of food additives frequently focus on broad toxicity and carcinogenicity, with less emphasis on specific organ systems such as the male reproductive tract. The male reproductive system, including the testes, is known to be exposed to many environmental toxicants and chemical exposures **(Creasy, 2001).** Testicular tissue, responsible for spermatogenesis and hormone production, can be adversely affected by xenobiotics, leading to impaired fertility and hormonal imbalances **(Mathur and D'cruz, 2011)**. While numerous studies have examined the impact of different dietary additives on testicular function, research specifically addressing the impact of pimaricin on testicular tissue remains limited.

The aims of the current study are as follows:

1. To analyze the histological effects of long term exposure to sodium benzoate and pimaricin, both individually and in combination(mix) , on the testicular and epididymal tissues of adult male albino rats.
2. To evaluate the immunohistochemical alterations induced by these preservatives, using specific markers (MDA) to identify signs of oxidative damage in the reproductive tissues.
3. To investigate the potential hormonal disruptions caused by sodium benzoate and pimaricin by measuring serum levels of Follicle-Stimulating Hormone (FSH) and Luteinizing Hormone (LH), aiming to assess their impact on male reproductive function.

Chapter Two
Literature Reviews

2. Literature Review

2.1 Food Preservatives

Preservatives, also referred to as antimicrobial agents, are a category of food additives used to extend the shelf life of food products by preventing spoilage caused by microorganisms. Within the European Union, the use of 45 specific substances as preservatives is authorized, with their applications and purity standards strictly regulated. These additives, whether naturally derived or synthetically produced, are added in small amounts to achieve technological purposes, such as maintaining color, enhancing sweetness, or more commonly, inhibiting microbial growth to prolong freshness **(Silva and Lidon, 2016).**

2.2 Sodium benzoate

Sodium benzoate is the sodium salt of benzoic acid, with the chemical formula C_6H_5COONa, commonly appearing as a white, crystalline powder that is highly soluble in water. It is one of the most widely used food preservatives worldwide, effectively inhibiting the growth of molds, yeasts, and certain bacteria, particularly in acidic foods and beverages such as soft drinks, pickles, and fruit juices. Beyond the food industry, sodium benzoate is used in cosmetics, pharmaceuticals, and personal care products as a stabilizer and preservative, and it also serves in industrial applications including corrosion inhibition and as a laboratory reagent. Globally, regulatory authorities such as the Joint FAO/WHO Expert Committee on Food Additives (JECFA) have established an Acceptable Daily Intake (ADI) of up to 5 mg/kg body weight per day, which means its use within recommended limits is considered safe for consumers **(Shahmohammadi, Javadi and Nassiri-Asl, 2016)**

2.3 The adverse effects of Sodium Benzoate

Sodium benzoate is regarded as a preservative with a high safety. Some studies claim that it is detrimental, while others demonstrate that it may be used to treat ailments including depression, pain, autism spectrum disorders, schizophrenia, and neurodegenerative diseases. For instance, oxidative stress, hormone disruption, mutagenesis consequences, and decreased fertility were all discovered. The goal of this study is to thoroughly examine sodium benzoate's safety profile and its applications in neurodegenerative illnesses, particularly in major depressive disorder, autistic spectrum disorder , schizophrenia, and pain management, in light of these inconsistent findings **(Walczak-Nowicka and Herbet, 2022)**. Particularly when combined with vitamin C, benzoate is thought to be capable of decarboxylation into poisonous benzene, which can further develop into a highly toxic, mutagenic, and teratogenic chemical **(Walczak-Nowicka and Herbet, 2022)** . Sodium benzoate is also said to have a mild genotoxic impact. In vitro, it was also demonstrated to enhance DNA damage in human cells. The substance decreased the mitotic rate but had no effect on the rate of replication. **(Altunkaynak and Avuloglu-Yilmaz, 2024)** Mutagenic and genotoxic effects were also demonstrated in another study on human lymphocytes (Mohiuddin *et al.*, 2021) **.**

Sodium benzoate (SB) is a commonly used food preservative, however excessive intake may cause neurotoxic effects. Rats treated with (SB) showed anxiety-like behavior, reduced memory, movement, and exploration. Biochemical tests revealed increased oxidative stress, inflammation, and brain enzyme activity, along with reduced antioxidant levels. Histological analysis showed brain cell damage. However, co-treatment with (AA) reversed these behavioral and biochemical changes, reduced neuronal damage, and improved brain function. These findings

suggest (AA) may protect against SB-induced neurotoxicity in the brain. **(Asejeje *et al.*, 2022)**

2.4 Effect of Sodium Benzoate's on Embryos

In a zebrafish model, sodium benzoate found to be teratogenic. The embryos showed a 100% survival rate at low dosages (1–1000 ppm), while the larvae were deformed at higher concentrations. Using a similar paradigm, another study similarly showed that both duration and dosage affected embryo survival. Additionally, the larvae showed lower locomotor activity and expression of the dopamine transporter and tyrosine hydroxylase. According to a different study, benzoate's effects on hormones may intensify with time **(Sabour and Ibrahim, 2019).**Such an effects may be observed for other parameters as well. Furthermore, sodium benzoate at concentrations of 0.5, 1, and 1.5 mg/mL was given to pregnant female rats in several tests . No harmful effects were seen, although this substance had minimal influence on the weight increase of the mother. The 1% and 1.5% benzoate dosage groups showed a significant increase in perinatal mortality. But there were no signs of weight loss or foetal abnormalities. Additionally, benzoate exhibited genotoxic effects on maternal and foetal liver tissue. However, in another research, rats' foetal weight fell and their mortality rose when given sodium benzoate at dosages of 9.3 and 18.6 mmol/kg b.w. **(Taheri and Sohrabi, 2002).**

In addition, a study by **(Afshar *et al.*, 2014)** reported fetal deformities after prior treatment of pregnant females with benzoate (280 and 560 mg/kg b.w.) These included limb malformations, spine problems, neural tube anomalies, skin haemorrhages, and craniofacial deformities.

These foetuses were found to have ocular development abnormalities, including malformed lenses and retinal folds with underdeveloped layers that

accompanied by hemorrhages. The detrimental effects of sodium benzoate on the fetus are also confirmed by another study **(Afshar *et al.*, 2012) .** Contrasting results regarding the teratogenicity of benzoate were observed in chickens (5–200 mg/kg b.w.) **(Emon *et al.*, 2015)** These embryos' neural tube development was unaffected by this substance. However, because of its possible teratogenic effects, its usage should be restricted.

2.5 The Impact of Sodium Benzoate's on the Liver and Kidney

Sodium benzoate affected the lipid profiles and liver and renal indicators of the animals. Furthermore, at dosages ranging from 150 to 700 mg/kg b.w., histological and dose-dependent changes in the biochemical markers of liver damage were observed. **(Khan *et al.*, 2022) (Khodaei *et al.*, 2019)**. Notably, it was found that sodium benzoate may affect the kidneys more significantly than the liver **(Zeghib and Boutlelis, 2021)** . For 15 weeks, this substance (100 mg/kg bw) was added to drinking water. The rats displayed histological alterations, such as glomerular and tubular necrosis and atrophy, along with elevated levels of urea and creatinine and impaired antioxidant defense, just like in the earlier study. A rise in the blood liver enzymes (aspartate aminotransferase (AST) and alkaline phosphatase indicated that study had verified its detrimental effects on the liver **(Ibekwe, Uwakwe and Monanu, 2007)** .In a rat model of schizophrenia, also affected liver indicators; for instance, alanine transaminase and AST increased while total protein and albumin decreased **(Mahmoud *et al.*, 2019).** Furthermore, the detrimental effects of benzoate were demonstrated in the livers of B6C3F1 mice and F344 rats (sodium benzoate was provided at a rate of 3.0% for mice and 2.40 percent for rats. **(Fujitani, 1993)** Sodium benzoate was found to have negative effects on the liver and kidneys, as evidenced by changes in liver parameters such as albumin, total protein, γ-

glutamyltranspeptidase, serum phospholipids, and cholesterol. It also increased absolute liver weight in both animal species and absolute kidney weight in rats. Histological alterations were also found, which are consistent with earlier investigations. **(Oyewole, Dere and Okoro, 2012)(Agarwal *et al.*, 2016) (Radwan *et al.*, 2020) .**

2.6 The Impact of Sodium Benzoate on Alzheimer's Disease.

Sodium benzoate (250–1500 mg/day) was tested on patients with mild cognitive impairment, as well. The impact of regional homogeneity (ReHo) on brain activity—more especially, local functional connectivity (FC)—was evaluated. The change in nonverbal (spatial) working memory was positively correlated with ReHo in the right precentral gyrus and right middle occipital cortex in the group that received sodium benzoate treatment. Furthermore, a favourable association between verbal learning and memory and ReHo in the left precuneus was noted in this group **(Caldinelli *et al.*, 2010)**

In another investigation, benzoate (250-750 mg/day) was administered for 24 weeks to individuals with severe Alzheimer's disease and mild amnestic cognitive impairment **(Stoy *et al.*, 2005)**. This substance had a positive effect on the patients' overall health and cognitive performance. These alterations were ascribed by the researchers to NMDA receptor activation. overall, sodium benzoate was well tolerated. Routine blood morphology and biochemical assays from the baseline evaluation were unchanged. Relevantly, tryptophan breakdown is also inhibited by sodium benzoate **(Maier *et al.*, 2010)** .Cognitive impairment is caused by low levels of tryptophan, which are decreased in AD patients **(Weaver *et al.*, 2020).**

2.7 Sodium benzoate's Effect on Male Reproduction

Both the food and pharmaceutical sectors make extensive use of sodium benzoate (SB), a synthetic food preservative. while negative consequences of SB on human health are becoming increasingly apparent, remains unclear its how long-term SB use affects the reproductive system. The study examines how the reproductive systems of male rats given oral SB for 90 days in a row are affected by varying dosages of SB (1000 mg/kg BW)**(Shahmohammadi, Javadi and Nassiri-Asl, 2016)**The findings showed that increasing SB dosages dramatically changed the weight of reproductive organs, increased the proportion of defective sperm, and lowered sperm motility and count. The testes' 17β-HSD and 17-KSR enzyme activity decreased, plasma testosterone and FSH levels significantly decreased, and plasma LH levels increased concurrently. The considerable rise in TNF-α and IL-6 levels, the suppression of antioxidant enzyme activity and GSH levels, the increase in NO and TBARS levels, and the increased protein expression of mtTFA and UCP2 in the testes all demonstrated the induction of inflammation and oxidative stress. Remarkably, the testes showed increased p53 expression and caspase-3 activity, indicating apoptotic induction. In addition to confirming apoptosis, histopathological analysis of the testes showed degenerative changes to their architecture and disruption of spermatogenesis. These results demonstrated the dangers of long-term exposure to both low and high doses of SB on male reproductive health, with the no observed adverse effect threshold of SB on the reproductive system being found to be less than 1 mg/kg BW/day **(El-Shennawy *et al.*, 2020).**

study is designed to investigate the effect of NaB and ascorbic acid on the testicular function of adult Wistar rats. The medication was administered orally, and the course of therapy lasted for 28 days. The change in body weight was tracked. Histological examination, biochemical test, and

semen analysis were carried out.Testicular endocrine function, sperm quality, oxidative stress status, and testicular tissue cytoarchitecture were all markedly changed by NaB treatment **(Kehinde, Christianah and Oyetunji, 2018).**

2.8 The Impact Sodium Benzoate's on Hormone Levels

It impacted the levels of sex hormones and altered the reproductive organs. Additionally, sodium benzoate had an impact on the male reproductive system in a different study. In comparison to the control group, the chemical resulted in a 50% decrease in sperm count and an increase in oxidative stress**. (Jewo *et al.*, 2020).** Another study found that rats given sodium benzoate at a dose of 100 mg/kg body weight for 28 days experienced testicular impairment. **(Al-Shelash and Gomaa, 2023)** This was associated with changes in the testes, endocrine function, and semen quality. Follicle-stimulating hormone (FSH), luteinizing hormone (LH), and free testosterone were among the sex hormones that were impacted by the chemical (0.01 mg/kb b.w.) in another in vivo investigation **(Mahmoud *et al.*, 2019)** . The decline in FSH, LH, and testosterone levels (sodium benzoate: 280 mg/kg/day) was associated with a similar finding**. (Sohrabi, Alipour and Gholami, 2008)** .Furthermore, there was an increase in thyrotropin and a reduction in triiodothyronine and thyroxine. However, another research found that thyroxine and thyrotropin levels decreased when sodium benzoate was administered at a dosage of 50–200 mg/kg/day **(Sabr & Ibrahim, 2015)**

2.9 Natamycin

Streptomyces natalensis strains generate the natural antibacterial peptide natamycin. It is an efficient antifungal preservative for a variety of foods, including yoghurt, khoa, sausages, juices, wines, and more. It is categorised as a widely acknowledged safe component for a variety of food applications and has also been utilised as a biopreservative.. Knowing the scientific aspects of the synthesis of natamycin is also essential **(Meena *et al.*, 2021).**

2.10 Acute and Chronic Toxicity of Pimaricin

In a comprehensive evaluation of pimaricin toxicity across various animal models, the oral LD50 values indicate significant differences between genders in rats, with male rats exhibiting an LD50 of 2.73 g/kg and female rats showing a higher value of 4.67 g/kg. Notably, following high single dosages, no acute toxicity symptoms were observed, and post-mortem examinations revealed no significant abnormalities linked to pimaricin intake. In fasted male albino rabbits, the oral LD50 was determined to be 1.42 g/kg, with adverse effects such as diarrhea manifesting at doses of 0.5 g/kg and above. Animals succumbing to high doses displayed congested and hemorrhagic gastric mucosa, while those euthanized two weeks post-administration appeared normal. Dermal toxicity assessments indicated mortalities of 0/10, 3/10, and 1/5 for single dermal doses of 1.25, 2.5, and 5.0 g/kg, respectively, although an LD50 could not be calculated; it is posited that the dermal LD50 exceeds 1.25 g/kg. Importantly, no systemic toxicity or skin irritation was noted after topical application, and the ocular safety profile was favorable, with only mild discomfort from small quantities of the dry product, resolving within a day. Overall, pimaricin demonstrated a low toxicity profile, warranting further investigation into its safety and efficacy**(Shaffer, 1966).**

2.11 The Effects of Natamycin on The Liver

A food preservative called natamycin is used to stop the growth of fungus and yeast on cheese and sausages. Using a blood enzyme activity test, the current study examined the effects of natamycin on the levels of liver enzymes and total protein in mice. Male and female mice received intraperitoneal injections of natamycin at 200, 400, and 800 mg/kg for six, twelve, and twenty-four hours. A spectrophotometer was used to measure the levels of alanine aminotransferase, aspartate aminotransferase, alkaline phosphatase, lactate dehydrogenase, and total protein in blood samples. When compared to the negative control, the current results showed a substantial rise in the levels of ALT in both male and female mice treated with varying dosages of natamycin. Additionally, natamycin caused **(RasGele and Kayma, 2013).**

2.12 Effect of natamycin on cytochrome P450 enzymes

This study investigated the impact of natamycin on drug-metabolizing enzymes in rat liver microsomes. Rats were given oral doses of 0.3, 1, 3, and 10 mg/kg body weight per day for six days. Enzyme activity assays revealed that higher doses (1, 3, and 10 mg/kg) significantly reduced the activity of key cytochrome P450 enzymes, including CYP2E1, CYP1A1/2, CYP2B1/2, and CYP4A1/2, while the lowest dose (0.3 mg/kg) had no notable effect. These results suggest that natamycin, while not directly increasing toxicity via reactive metabolite accumulation, may interfere with the metabolism and clearance of other compounds processed by these enzymes. This raises potential concerns about its broader implications for food safety and drug interactions **(Martínez *et al.*, 2013).**

2.13 Natamycin (E 235) as a Dietary Supplement

following a request from the European Commission requested it from EFSA, the Scientific Panel on Food Additives and Nutrient Sources Added to Food (ANS) was asked to provide a scientific opinion on the safety of using natamycin (E 235) as a food additive, as well as the issue of natamycin-induced antibiotic resistance. Natamycin is a polyene macrolide antifungal approved under Directive 95/2/EC for surface treatment of dry, cured sausages and semi-hard or semi-soft cheeses, with a limit of 1 mg/dm² in the outer 5 mm.

While the SCF (1979) found no safety concerns, it could not establish an ADI due to limited data. JECFA later proposed an ADI of 0.3 mg/kg bw/day. However, EFSA's ANS Panel identified weaknesses in the available studies, including small sample sizes, lack of carcinogenicity data, and insufficient human data, making the ADI uncertain. Estimated exposure for high-consuming children was below 0.1 mg/kg bw/day, which was considered safe given natamycin's minimal absorption. The Panel concluded that its proposed use does not pose health risks or contribute to antibiotic resistance. **((Additives and Nutrient Sources), 2009, 2010)**.

2.14 The Impact of Natamycin on Broiler Chicken Growth Performance

A recent study evaluated the effects of dietary natamycin supplementation on broiler health over a 42-day period, using 360 birds divided into three groups: a control group (CON) receiving a basal diet, and two treatment groups supplemented with 10 mg/kg (T1) and 50 mg/kg (T2) of natamycin, respectively. The findings revealed dose-dependent physiological responses. At the higher dosage (T2), broilers exhibited significantly elevated blood urea nitrogen and alanine aminotransferase levels by day 42, alongside reduced alkaline phosphatase activity at day 21, indicating potential hepatic stress. Additionally, serum globulin (day 21) and total protein (day 42) levels were lower in the T2 group compared to the

control. In contrast, the lower natamycin dose (T1) was associated with beneficial outcomes. Broilers in the T1 group showed increased serum total antioxidant capacity and reduced malondialdehyde levels at day 21, as well as elevated glutathione peroxidase activity and reduced liver malondialdehyde levels at day 42. These results suggest that low-dose natamycin supplementation may enhance antioxidant status and support liver function in broilers, whereas higher doses could pose metabolic risks **(Hu *et al.*, 2018).**

2.15 The effects of the antifungal natamycin on cholesterol

Natamycin stands out among antimicrobial agents due to its broad-spectrum antifungal activity and the absence of known resistance. Importantly, it exhibits low toxicity in humans when administered either orally or topically, a property likely linked to its limited interaction with mammalian cell membranes. To explore the biophysical basis of this selectivity, recent studies have employed Langmuir monolayers as model membranes to investigate natamycin's interactions at the molecular level. Findings indicate that natamycin exerts significant effects on cholesterol monolayers, causing expansion of the surface pressure isotherm and a decrease in compressibility modulus, indicative of structural disruption. These effects are attributed to natamycin's penetration into the hydrophobic core of the cholesterol layer, as demonstrated by polarization-modulated infrared reflection absorption spectroscopy (PM-IRRAS). In contrast, natamycin had negligible influence on dipalmitoyl phosphatidylcholine (DPPC) monolayers. Notably, strong interactions were only observed in mixed cholesterol/DPPC monolayers at cholesterol concentrations of 50 mol% or higher—levels significantly above those typically present in mammalian membranes (around 25 mol%). This differential membrane interaction likely underlies natamycin's selective toxicity and its safe profile for treating superficial fungal infections **(Arima *et al.*, 2014).**

2.16 Atamycin (supplement)

Natarnycin is a member of the broad class of antibiotics that are polyene antifungal. This group is characterised by a macrocyclic lactone ring that has many conjugated carbon-carbon double bonds. Researchers have succeeded in elucidating the full stereostructure of natamycin by the use of advanced 2D NMR investigations, the production of certain hydrogenated derivatives, and the use of D-mycosamine as an internal chiral reference. The parameters were 4R, 5R, 7S, 9R, llS, 12R, 13R, 15R, 25R, and 1R. The whole stereo structure of natamycin is included in the structural formula. Natamycin with gamma-cyclodextrin create an inclusion complex, just as a number of other polyenes. In comparison to the parent antibiotic, the complex exhibits biological activity and is significantly more soluble in water. The findings of the natamycin retroaldol reaction, several of its breakdown products (with or without a mycosamine group), borohydrid-reduced natamycin, and mycosamine itself—specifically, whether or not ethanal is present in the volatile fractions—make it clear that ethanal comes from both the lactone ring and the amino sugar .**(Brik, 1994)**

2.17 Evaluating the Impact of Natamycin use in food preservative on the clinical efficacy of amphotericin B

Natamycin is considered safe for use in solid and semi-solid foods, with typical exposure levels well below the acceptable daily intake (ADI). However, concerns have been raised about its potential to promote polyene resistance in gut Candida spp., particularly in elderly or immunocompromised individuals. This risk is heightened with high-exposure products, such as beverages containing natamycin–cyclodextrin complexes, which may exert stronger selective pressure in the gut. While Natamycin is safe in conventional food use, caution is warranted for formulations that increase systemic exposure **(Dalhoff and Levy, 2015).**

2.18 Sensitivity to Natamycin (Pimaricin)

Molds and yeasts isolated from cheese warehouses where natamycin has been used for varying lengths of time were tested for natamycin sensitivity. No molds or yeasts that were insensitive to natamycin were discovered after years of consistent natamycin usage. It was impossible to reduce the sensitivity for natamycin in 26 mold strains that were isolated from cheese warehouses under laboratory conditions. In addition to the fungi's susceptibility to natamycin, the isolated molds' ability to produce mycotoxins was examined. Under experimental circumstances, strains of Penicillium viridicatum, Aspergillus versicolor, and Penicillium eye/opium that were isolated from the warehouses generated penicillic acid, ochratoxin A, and sterigmatocystin, respectively **(De Boer and Stolk-Horsthuis, 1977).**

2.19 Plasma Level of LH and FSH

A study examining the plasma levels of luteinizing hormone (LH) and follicle-stimulating hormone (FSH) in developing male and female rats using radioimmunoassay (RIA) revealed distinct sex-specific patterns. While LH concentrations followed a similar age-related trend in both sexes from 5 to 45 days, FSH levels showed marked differences. Female rats exhibited a sharp peak in plasma FSH around days 15, followed by a rapid decline, whereas male FSH levels remained relatively stable. Hemigonadectomy at days 10 of age produced a rapid and significant increase in FSH levels in males, reaching 240% of control values within two days. In contrast, the female response was delayed by at least 10 days and involved only a modest FSH increase, with no significant change in LH. These findings suggest that in males, gonadotropin regulation is influenced by gonadal steroids from early infancy, while in females, ovarian hormones

begin affecting FSH regulation only after 20 days of age **(Ojeda and Ramirez, 1972).**

2.20 Serum LH, FSH, Prolactin and Progesterone from Birth to Puberty in Female and Male Rats

In prepubertal male and female rats, serum levels of prolactin, progesterone, FSH, and LH show distinct developmental patterns. At birth, both sexes exhibited elevated levels of FSH and LH, with females consistently showing higher levels than males. Prolactin and progesterone were low in both sexes during the neonatal period. Between days 10 and 20, an unusual LH pattern was observed in females, where 10–15% showed elevated LH levels, unlike males who displayed only slight variations. During the same period, FSH levels increased in both sexes, again with higher values in females. Progesterone rose slightly in both males and females, while prolactin remained low. These results suggest early sex differences in hormone regulation, with female rats exhibiting greater fluctuations in LH and FSH during prepuberty **(DOHLER and WUTTKE, 1974).**

2.21 Health Benefits and Natural Alternatives

Natural preservatives—such as plant extracts, essential oils, bacteriocins, enzymes, and bacteriophages—offer safer alternatives to synthetic chemicals. They often provide both antimicrobial and antioxidant properties. For instance, plant-derived phenolic compounds can inhibit bacterial growth and neutralize free radicals, which may reduce oxidative stress and inflammation . Such biopreservatives are increasingly being explored for their synergistic effects and lower toxicity in food preservation .**(Cedillo-Olivos *et al.*, 2024)**

2.22 Potential Adverse Effects

Despite their utility, preservatives—especially synthetic ones—can carry risks. For example, nitrites used in processed meats may contribute to cancer formation, sodium benzoate can form benzene when combined with vitamin C, and certain antioxidants like BHA and BHT have been linked to health concerns . Artificial preservatives are also associated with asthma, behavioral issues in children, heart tissue weakening, obesity, headaches, reduced mental concentration, and even GERD-like symptoms (heartburn, bloating) .**(Cedillo-Olivos et al., 2024)**

2.23 Preservatives and Hormonal Balance in General

Preservatives, while essential for extending product shelf life, are increasingly studied for their potential effects on endocrine health. Many of them are considered endocrine-disrupting chemicals (EDCs), capable of mimicking or blocking natural hormones such as estrogen, testosterone, and thyroid hormones. For example, some commonly used preservatives (e.g., parabens, phthalates, and sodium benzoate) can bind to hormone receptors, altering cellular signaling and hormone regulation. Over time, these disruptions may affect reproductive functions, metabolic processes, and even stress-response pathways. Long-term, low-dose exposure is particularly concerning because it may not cause immediate toxicity but can contribute to cumulative hormonal imbalance and chronic disorders.**(Silva and Lidon, 2016)**

2.24 General Overview of Preservatives

Preservatives are extensively applied in food, pharmaceuticals, and cosmetics to prevent microbial growth and chemical degradation, thereby extending product shelf life. According to the World Health Organization, preservatives such as nitrates, benzoates, and parabens are among the most frequently used additives in global food systems. While these compounds provide essential protection against foodborne pathogens, studies have highlighted possible toxicological risks associated with chronic exposure, including oxidative stress, DNA damage, and potential carcinogenicity. Thus, preservatives are viewed as a double-edged sword—essential for safety but raising concerns for long-term health effects.**(Altunkaynak and Avuloglu-Yilmaz, 2024)**

2.25 Preservatives' Contribution in Oxidative Stress and Apoptosis

A previous experimental study investigated the cytotoxic effects of different preservatives on a continuous human conjunctival cell line. The cells were exposed to various concentrations of benzalkonium chlorides (BACs), benzododecinium bromide (BOB), cetrimide (Cet), phenylmercuric nitrate (PM), thimerosal (Thi), methyl parahydroxybenzoate (MPHB), chlorobutanol (Clb), and EDTA. The results revealed that quaternary ammonium compounds (BAC, BOB, and Cet) caused the greatest cytotoxicity, with significant loss of membrane integrity and chromatin condensation at concentrations ≥0.005%, effects that were amplified after 24 hours of recovery. While all preservatives induced hydrogen peroxide production, superoxide anion generation was particularly high in quaternary ammoniums. The study concluded that quaternary ammonium preservatives

are the most harmful to ocular surface cells, inducing apoptosis at low concentrations and necrosis at higher concentrations, with oxidative stress playing a central role in tissue damage.**(Debbasch *et al*., 2001)**

Chapter Three Materials and methods

Methodology

3.1. Materials

3.1.1. Instruments and Equipment:

Table(3-1): Chemicals and kits were used in the study.

NO.	Chemicals and Kits	Origin and Company/supply
1.	**Alcohol**	**India**
2.	**Dpx**	**India**
3.	**Ethanol absolute 99.5%**	**Merck, Germany**
4.	**Formalin10%**	**Chemanol Saudi arabia**
5.	**Haematoxylin and Eosin (H&E) stain kit**	**Merck, Germany**
6.	**Immunohistochemistry (MDA)**	**Elabasxience, USA**
7.	**Masson trichrome stain kit**	**vectorLab,UK**
8.	**Natassen, pimaricin (E235) purity 99.7 %**	**Uk shelf life**
9.	**Paraffin wax**	**Merck, Germany**
10.	**Periodic acid-Schiff (PAS) kit**	**BioGnost,Croatia**
11.	**Sodium benzoate purity 99.7 %**	**ALPHA CHEMIKA Made in India**
12.	**Sterile water**	**Baxter**
13.	**Xylazine**	**Randlab Ltd,australia**
14.	**Xylole**	**Scharlau, Spain**
15.	**Isoflurane 100%**	**Isospire UK**
16.	**Ketamine**	**Randlab Ltd,australia**

Table (3-2) shows the instruments utilized in this investigation, as well as the providers and sources.

NO.	Instrument	Suppliers and sours
1.	Water bath	Yamato scienitic japan
2.	Test tubes	China
3.	Sterile Syringe	China
4.	Slide and cover slide	China
5.	Rotary microtome	Germany
6.	Oven	China
7.	Light microscope	Lieca/China
8.	Insulin syringes	Italy
9.	Incubator	Japan
10.	Gel tubes	Jordan
11.	Freezer	Hitachi/Japen
12.	Dissection set	China
13.	Digital Camera	Top Cam/China
14.	Centrifuge	Hettich Roto fix11/Japan
15.	Balance for animals	Shimadu company-Japan
16.	Analytical Sensitive Balance	Sartorius/ Germany
17.	ELISA reader	Biotek/USA
18.	ELISA washer	Biotek/USA

Experimental design

Forty albino male rats will be divided into four groups (10 rats in each group)

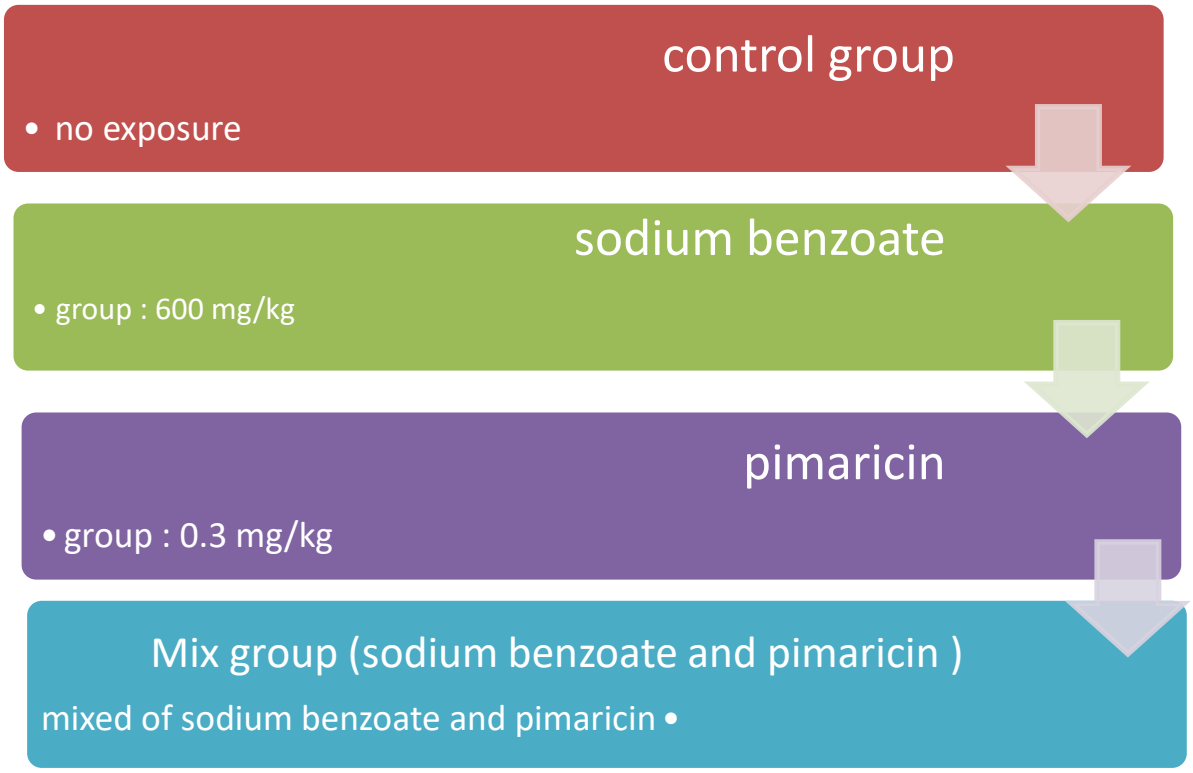

The Experiment Protocol

Parameters: Histochemical Stains, Immunohistochemistry & Hormonal Assays

- **Haematoxylin and Eosin (H&E) stain**
- **Periodic acid-Schiff**
- **Masson trichrome stain**
- (MDA) immunohistochemistry
- **Serum LH levels**
- **Serum (FSH) levels**

3.2 Experimental Design

The research is conducted between November 2024 and January 2025. Forty male albino rat was housed in an animal home for two months to get used to the conditions of the laboratory. From the animal house of the college of pharmacy at Karbala University, forty healthy adult male albino rat weighing between 300 and 350 g were acquired. They were housed at the veterinary medical college's animal house at Karbala University. The temperature was kept at 21 to 25 degrees Celsius, the air in the room was continuously changed using a ventilation vacuum, and the animals were given a newly made feed pellet for 12 hours every day.

3.3 The Experiment Protocol

Forty male (40) rats were randomly divided into four groups each group contains ten rat .The dosages were administered at the start of the trial by oral intubation (gavage) ensuring precise delivery of the tested compounds directly into the stomach and providing accurate and consistent dosing across all animals (Turner *et al.*, 2011)**.**

1. G I: (control) Rats were fed without supplementation for 50 days.
2. G II: Rats were given 600mg/kg B.W daily oral intubation of sodium benzoate, dissolved in water for 50 days .The dosage was selected based on the protocol reported by (El-Shennawy *et al.*, 2020)**.**
3. GIII: Rats were given 0.3 mg /kg B.W daily oral intubation of pimaricin for 50 days. The dosage was selected based on the protocol reported by ((ANS), 2009)**.**
4. G IV: Rats were given 600mg/kg B.W daily oral intubation of sodium benzoate dissolved by water and given 0.3 mg /kg BW of pimaricin to evaluate the potential cumulative toxic effects of both compounds on male reproductive tissues.

3.4 Histological study

Animals were sacrificed by the end of the experimental period using isoflurane 100 % (2 mg/Kg BW or equal 2% inhaled in dictator). and For a histological analysis, their testes will be removed., after removing the testes right away, the adhering fat and connective tissues were removed and the testes were cleaned with a saline solution (0.9%).

Further the rat testicles were extracted, fixed with 10% formalin right away, treated with xylol and regular grade alcohol, embedded in paraffin, and then sectioned.

Haematoxylin and Eosin (H&E) stain (Bancroft and Gamble, 2008): Widely used for general tissue structure; Haematoxylin stains nuclei blue/purple, while eosin stains cytoplasm and extracellular matrix pink, offering clear contrast **(Appendix 1).**

Periodic acid-Schiff (PAS) stain (RD, 1948) :Highlights carbohydrates and glycogen stains structures such as basement membranes and mucins magenta **(Appendix 2).**

Masson trichrome stain (Foot, 1933)**:** Differentiates muscle, collagen, and fibrin; collagen appears blue or green, muscle red, and nuclei black, making it valuable for assessing fibrosis and connective tissue **(Appendix3)**

3.5 Immunohistochemistry

Polyclonal Antibody (MDA) immunohistochemistry was carried out on tissue blocks that were embedded in formalin-fixed paraffin in each instance. Thin 5 mm tissue slices were deparaffinized by using xylene, and rehydrated by series of alcohol, and then subjected to a series of graded alcohol. The antigen retrieval process was then conducted in an autoclave using 5 mm citrate buffer (pH 6.0). After blocking the sections, the primary

antibody (E-AB-17209) was added and incubated for two hours at 37°C. subsequently, a goat anti-mouse linker and rabbit antibody.were added followed by washing and then the secondary antibody using the enzyme (peroxides) after 30 minutes. Following the manufacturer's instructions, further procedures were carried out using the Immunohistochemistry Kit (Elabasxience, USA). Only negative controls were sections that were treated with phosphate-buffered saline (PBS) (Paradis *et al.*, 1997) (Qian *et al.*, 2013) (Jarjees, 2022) **(Appendix4).** Immunohistochemistry for MDA (Malondialdehyde) was performed to detect lipid peroxidation and evaluate oxidative stress in tissue sections. MDA is a well-established biomarker of oxidative damage, and its accumulation indicates the extent of cellular membrane injury. The intensity and distribution of MDA immunoreactivity were assessed to determine the degree of oxidative stress in different experimental groups.

3.6 Blood Collection

Blood samples were collected at three time points: day 0, day 25 (midpoint), and day 50 (end of the experiment) , using the cardiac puncture technique with a 10 ml disposable syringe, and 2 ml of blood was extracted slowly and gently. and collected in gel test tubes for serum preparation. The sample were left for 30 minutes at room temperature before being centrifuged at 3000 rpm for 15 minutes to separate serum, which was then placed in Eppendorf tubes and frozen at -20C. Eppendorf tube stored in the freezer at -20 degrees Celsius **(Bielohuby, Popp and Bidlingmaier, 2012).**

3.7 Determination of Reproductive Hormones

1- Serum LH levels were measured using an ELISA kit,

Following the method described by (Tietz, 1995) This assay employs a solid-phase, two-site enzyme immunometric technique in a microplate format, allowing for the quantitative detection of LH in serum. The method detects both intact LH heterodimers and free β-subunits due to its cross-reactivity. Streptavidin-coated wells were used to capture a complex formed by excess biotinylated monoclonal anti-LH antibodies and enzyme-labeled LH antibodies. The sandwich complex, involving the LH antigen, was bound to the plate via streptavidin interaction. Tetramethylbenzidine (TMB) and hydrogen peroxide (H_2O_2) served as substrates for the enzyme reaction, which generated a color change proportional to LH concentration. Absorbance was recorded at 450 nm, with 620 nm as a reference, using a Tecan Infinite F50 microplate reader (Tecan Group, Switzerland).

2. Serum levels of follicle-stimulating hormone

Plasma FSH levels were measured using a direct enzyme immunoassay (EIA) kit specific for human serum follicle-stimulating hormone, following the manufacturer's protocol as modified by (Tietz, 1995).All reagents and samples were equilibrated to 25°C before use. The required number of coated microwells was prepared, with an additional well (FSH1) designated for the substrate blank. Fifty microliters of standards, controls, and test samples is added to the respective wells, excluding FSH1, within a 5-minute window. Subsequently, 100 µL of FSH-HRP conjugate was added to each one (except FSH1), gently mixed for 30 seconds, covered, and incubated at 37°C for one hour. After incubation, the contents were discarded, and wells were blotted dry.

Wells were washed five times with 350 µL of wash buffer and dried. Then, 50 µL each of TMB substrate and hydrogen peroxide were added to all wells, mixed for 20 seconds, and left to react at room temperature for 15 minutes. The enzymatic reaction was terminated by adding 50 µL of 1 N HCl to each well, followed by gentle mixing. Absorbance was read at 405 nm within 15 minutes using a microplate reader.

3.8 Statistical Analysis

Biochemical data in this study were analyzed and reported as mean ± SD. tow-way ANOVA was performed usngn GraphPad Prism® (version 6.01, GraphPad Software, Inc.) to examine significant variance among groups. Turkey's multiple comparisons test was used for multiple compatibility, with p-values < 0.05 considered significant **(corp,2011).**

3.9 Ethical approval

Under the reference number UOK.VET.AN2024.092, this research was carried out in the anatomical laboratory of the College of Veterinary Medicine at the University of Kerbala – Iraq

Chapter Four
Results and Discussion

4.-Results and Discussion

4-1- Histological findings of control group

Histological examination of testicular and epididymal tissues from the control group revealed normal architecture with no histopathological alterations, The testicular sections demonstrated well-preserved seminiferous tubules with circular profiles and regular contours as well as lined with stratified epithelium and Sertoli cells were also clearly identifiable, supporting the developing germ cells within the tubules. The interstitial spaces contained delicate loose connective tissue interspersed with prominent interstitial (Leydig) cells.

Special Histochemical staining revealed a normal structure integrity in the basement membrane of seminiferous tubules and in the acrosomal caps spermatids, that appeared purplish in color reflecting a normal distbution of glycoprotein content in these structures. As well as Trichrome staining verified an intact tunica albuginea with well-organized collagen fibers.

The epididymal ducts were lined by Pseudostratified columnar ciliated epithelium composed of tall columnar cells with stereocilia, basal cells resting on the basal lamina, and clear cells with pale cytoplasm. The lumen of these ducts contained abundant spermatozoa, and each duct was surrounded by a thin layer of smooth muscle fiber. PAS staining showed faint affinity in the basal lamina of the epididymal ducts, with dye purplish hue, along with a thin but distinct apical reaction in the lining epithelial cells. Collagen fibers surrounding the ducts and the tunica albuginea of the epididymis yielded a prominent blue coloration, further highlighting the collagen content. **(Figures 4-1 to 4-10 illustrate the above findings.)**

4.2. Histological Changes in the Sodium Benzoate-Treated Group

Histological examination of testicular and epididymal tissues from male albino rats treated with sodium benzoate for 50 days revealed widespread tissue–level alterations characterized by pronounced structural disruption and degenerative changes. These included marked tissue disorganizations, inflammatory infiltration, and a reduction in normal spermatogenic activity compared to the control group.

The testicular sections exhibited vascular thrombus of blood vessels and interstitial edema, particularly evident beneath the tunica albuginea, along with a mild degree of tunica albuginea thickening was observed (table 4-1) The seminiferous tubules showed signs of spermatogenic cell vacuolation, and degeneration of seminiferous epithelium, Furthermore a pronounced decrease in the number of interstitial tissue Leydig cells was observed.

Collectively these alterations are inductive of disrupted spermatogenesis and impaired testicular function induced by sodium benzoate exposure.

Moreover, the epididymal epithelium showed a disorganized tubular structure with clear expansion of interstitial tissue and infiltration of mononuclear inflammatory cells, mainly lymphocytes accompanied by degenerative changes and focal areas of necrosis. These alterations were accompanied by disruption of the normal tissue architecture and loss of the germinal epithelium. A noticeable reduction in luminal sperm content was also observed, indicating impaired spermatogenesis.

Histochemical Staining using periodic Acid-Shift(PAS) staining demonstrated degenerative changes with loss of normal spermatogenic germ layers and reduction of mature sperm, which stained with a more intense purplish color. Enhanced staining of The basement membrane and apical parts of the lining epithelial cells suggested increased

glycoprotein content and possible cellular stress.

Masson's Trichrome staining demonstrated increase in the thickness of tunica Albuginea attributed to the proliferation of fibrous connective tissue, as indicated by intense blue staining-consistent with fibrotic changes. Similarity enhanced blue coloration was observed in the collagen fibers surrounding the epididymal ducts, suggesting elevated fibrotic activity and increased extracellular matrix deposition in the interstitial area.**(Figures 4-11 to 4-18 illustrate these histological changes.)**

4.3. Histological finding of Section in the Pimaricin-Treated Group

Histological evaluation of testicular and epididymal tissues from albino male rats treated with pimaricin for 50 days revealed histological alterations. Testicular tissue exhibited pronounced degenerative, necrotic, and fibrotic depostion with a noticeable low of interstitial Leydig cells density, reflecting considerable testicular damage and disruption of normal spermatogenesis. Prominent congestion of interstitial blood vessels was observed, suggesting vascular involvement. Additionally, vascular congestion was evident, along with the presence of a fibrin network and a substantial accumulation of degenerative spermatozoa , suggesting impaired sperm maturation and transport.

Histochemical Staining PAS Stain: showed cellular and tissue degenerative changes with vacuolation of testicular cells, reactivity to stain purplish color.

Assessment of the epididymal sections indicated an increase in the thickness of basement membrane and loose of normal tissue appearance. despite this a thin apical PAS reaction remained visible in the lining epithelial cells.

Masson's Trichrome Stain: demonstrated disorganization in the

seminiferous tubules with increase in the thickness of tunica Albuginea (table 4-1) due to overproduction of fibrous connective tissue as indicated by Intense blue staining, In addition irregular outlines with degeneration of the ductal epithelium were observed accompanied by increased collagen fibers surrounding the epididymal ducts which stained prominently blue, suggesting fibrotic reaction. **(Figures 4-19 to 4-26 illustrate these findings.)**

4.4. Histological Findings in the Mix-Treated Group

Microscopic evaluations of testicular and epididymal tissues of albino male rats treated with the combined agents (Mix Group) highlight noticeable structural disruptions, inflammation, and fibrotic remodeling affecting both testicular and epididymal architecture.

The testicular sections showed significant thickening of the tunica albuginea, accompanied by edema within the interstitial tissue and sub-tunica regions. those represented atrophy of the seminiferous tubules, with significant interstitial dilation. Focal regions lacking seminiferous tubules were also observed, indicating advanced testicular deterioration.

The seminiferous tubules exhibited degenerative changes and necrosis of the spermatogenic epithelium, along with lumen filled with sloughed immature cells. Further notable findings included distortion and partial detachment of the basement membrane, along with congestion of blood vessels, reflecting significant tissue injury and compromised testicular function.

The structural integrity of the epididymal ducts was also impaired with irregular arrangement of ducts surrounded by a fibrotic stroma matrix, along with a marked increase in the thickness of the basement membrane.

Epididymis tissues sections revealed with intense hyalinization within the

epididymal lumina, suggesting marked epithelial and luminal degeneration. These changes were associated with disrupted ductal organization and impaired epithelial wholeness.

Histochemical analysis using periodic acid schift PAS Staining: displayed evident interstitial accompanied by a notable thickening of the interstitial and basement membrane. These regions exhibited a distinct purplish stain, suggestive abnormal alterations, likely associated with increased extracellular matrix deposition or early fibrotic changes A reduced number of Leydig cells, indicating significant accumulation of glycoprotein substances. The tunica albuginea in the epididymis also showed irregular tubular structure and marked increase thickness of tunica albuginea and basement membrane, suggesting altered extracellular matrix components. Masson's Trichrome Staining: demonstrated extensive fibrosis in the tunica albuginea, confirmed by marked increase in its thickness due to increased fibrous connective tissue that stained with blue color.

Additional fibrotic changes were observed in the tunica Albuginea and proliferation of collagen fibers surrounding the epididymal ducts and small blood vessels. These regions also exhibited intense blue staining, indicating chronic fibrotic remodeling. **(Figures 4-27 to 4-33 illustrate these histological alterations)**

4.5 Immunohistochemistry Study of Experimental Animal with MDA Stain

4.5.1 Immunohistochemical Analysis of MDA in the Control Group

Immunohistochemistry was performed to evaluate the localization of malondialdehyde (MDA), an established marker of lipid peroxidation and oxidative stress, in formalin-fixed testicular and epididymal tissues from normal control rats after 50 days of the experiment.

The testicular tissue negative control sections, which were incubated without the primary antibody showed no MDA immunoreactive cells, validating the specificity of the staining protocol, In contrast, experimental sections showed MDA immunoexpression in several testicular cell populations. Positive staining was detected in spermatogenic cells, Sertoli cells, within the seminiferous tubules, and Leydig cells, in the interstitial tissue, suggesting basal oxidative activity under physiological conditions.

Similarly, negative control sections of the cauda epididymis demonstrated no MDA staining in the absence of primary antibody. In contrast Experimental staining revealed MDA immunoreactivity in both the nucleus and cytoplasm of the epithelial cells lining the epididymal ducts, primarily localized in the columnar cells , indicative of normal oxidative metabolic activity. **(Representative photomicrographs shown in Figures 4-34 to 4-37.)**

4.5.2Immunohistochemical Analysis of MDA in the Sodium Benzoate Group

Immunohistochemistry was conducted to investigate the distribution and intensity of malondialdehyde (MDA) expression—an established marker of lipid peroxidation and oxidative stress—in testicular and epididymal tissues of rats treated with sodium benzoate for 50 days. In the sodium benzoate-treated group, MDA immunostaining revealed positive immunoreactivity in spermatogenic cells of the seminiferous tubules, indicating a mild increase in oxidative stress compared to other treated group, Furthermore, Leydig cells in the interstitial tissue also displayed profound MDA expression, suggesting that sodium benzoate exposure notable affected steroidogenic activity through oxidative pathways Compared to the control group.

In epididymal tissue, the negative control section of the cauda epididymis, processed without the primary antibody, showed no MDA immunostaining, confirming the specificity of the antibody used. In contrast, the experimental section demonstrated mild nuclear and cytoplasmic MDA immunoreaction in the epithelial cells lining the epididymal ducts , indicating localized oxidative stress in the epididymal tissue compared to other treated group.

(Representative photomicrographs shown in Figures 4-38 to 4-41.)

4.5.3 Immunohistochemical Analysis of MDA in the Pimaricin Group

Immunohistochemical staining for malondialdehyde (MDA) was performed to assess oxidative damage in testicular and epididymal tissues of rats treated with pimaricin for 50 days.

In testicular tissue, Negative sections of the testicular tissue, processed without the primary antibody showed no MDA immunostaining.

However, other sections revealed moderate MDA immunoexpression in spermatogenic cells, Sertoli cells and Leydig cells within the interstitial tissue. These findings indicate a moderate level of oxidative stress within the testis, likely reflecting pimaricin-induced cellular injury and accumulation of reactive oxygen species, Compared to other treated group.

In epididymal tissue, negative control sections of the cauda epididymis, processed without the primary antibody, showed no MDA immunostaining, confirming the specificity of the immunohistochemical protocol. In contrast, moderate nuclear and cytoplasmic MDA immunoreactivity was observed in the epithelial cells lining the epididymal ducts, supporting a moderate oxidative stress effect in the epididymal tissue compared to other treated group. **(Representative photomicrographs shown in Figures 4-42 to 4-45.)**

4.5.4 Immunohistochemical Analysis of MDA in the Mix Group (Sodium Benzoate + Pimaricin)

Immunohistochemical staining for malondialdehyde (MDA) was performed on testicular and epididymal tissues of rats treated with a combination of sodium benzoate and pimaricin for 50 days to assess the extent of oxidative stress.

In testicular tissue negative, control sections prepared without the primary antibody confirmed staining specificity by showing no MDA immunoreactivity. In contrast, treated sections exhibited strong nuclear and cytoplasmic MDA immunoexpression in both germ cells and Sertoli cells, within the seminiferous tubules, highlighting a pronounced oxidative effect at the cellular level.

Similarly epididymal Tissue, negative control sections of the cauda epididymis revealed no MDA immunostaining, validating the staining protocol.

However, the treated epididymal sections demonstrated strong nuclear and cytoplasmic MDA immunoreaction in the epithelial cells lining the epididymal ducts, indicating substantial oxidative damage to the epididymal structure. **(Representative photomicrographs shown in Figures 4-46 to 4-51.)**

Discussion Immunohistochemical assessment of MDA in treated group

In the present study, Immunohistochemical analysis of MDA in the testicular and epididymal sections from the control group at 50 days post-exposure showed nuclear and cytoplasmic immunoreaction in germ cells and Sertoli cells within the seminiferous tubules.

To date little information exists on the specific effect of sodium benzoate and pimaricin on MDA expression in testicular and epididymal tissues. However, MDA (malondialdehyde) is a well-established biomarker of lipid peroxidation, representing a terminal product of polyunsaturated fatty acid degradation under oxidative stress conditions. An increase in free radicals leads to excessive lipid peroxidation and, consequently, overproduction of MDA, which reflects the extent of oxidative damage **(Kurutas, 2015).**

MDA is a highly reactive dialdehyde with a short biological half-life. It preferentially binds to amino groups of proteins, resulting in the formation of both intramolecular and intermolecular cross-links, thereby disrupting normal protein structure and function (**Paradis *et al.*, 1997)**.This molecular damage contributes to cellular dysfunction, apoptosis, and tissue degeneration.

Apoptosis is a physiological mechanism of controlled cell deletion that plays a critical role in maintaining homeostasis in testicular tissue. It regulates the number of germ cells and helps eliminate damaged or unnecessary cells. However, excessive apoptosis, especially when induced by oxidative stress and elevated MDA levels, can impair spermatogenesis and lead to reduced male reproductive capacity **(John, 2000).**

In the sodium benzoate-treated group, mild MDA immunopositivity was observed in germ cells and Leydig cells, with nuclear and cytoplasmic

expression also noted in the epithelial lining of the epididymal ducts. Similarly, the pimaricin-treated group exhibited moderate nuclear and cytoplasmic expression of MDA. In the mix-treated group, intense MDA staining was observed both in the testicular tissue and in the epididymal ducts, suggesting synergistic oxidative stress effects. These findings align with **(Adelakun *et al.*, 2019),** who demonstrated that exposure to nitrite significantly elevated MDA levels in testicular tissue, accompanied by tubular atrophy, hypocellularity, and degeneration of spermatogenic cells. The elevated MDA was indicative of increased lipid peroxidation and oxidative stress, which play a major role in impairing spermatogenesis. Interestingly, co-administration of antioxidant-rich walnut oil in their study led to a significant reduction in MDA levels, highlighting the role of MDA as a sensitive biomarker of oxidative testicular damage.

In a separate study **(Davoodi *et al*., 2021)** , the antioxidant effect of Hirudo medicinalis (leech therapy) was investigated in the context of chemically induced oxidative stress. The findings revealed that administration of leech extract significantly reduced malondialdehyde (MDA) levels in liver tissues following carbon tetrachloride (CCl_4) exposure. Elevated MDA levels, which are indicative of lipid peroxidation, were notably decreased in the treated group compared to the untreated toxic group. This reduction was accompanied by histopathological improvements, suggesting that MDA is a sensitive and reliable biomarker of oxidative injury. The study supports the broader concept that monitoring MDA expression can effectively reflect tissue damage caused by oxidative stress and may be modulated by antioxidant therapies, even in non-reproductive organs.

In support of the role of MDA as a sensitive indicator of oxidative damage in reproductive tissues, a study investigating the effects of lead acetate

toxicity reported a significant increase in MDA levels within the testes. This biochemical elevation corresponded with clear histopathological changes such as degeneration of germ cells and disruption of seminiferous tubule architecture. The authors attributed these alterations to lipid peroxidation and reactive oxygen species activity induced by lead exposure.**(Mohammed AL-Haar, 2011)** The findings mirror the current study's observations, where elevated MDA expression in sodium benzoate- and pimaricin-treated groups coincided with structural impairment in both testicular and epididymal tissues. These similarities highlight a common oxidative mechanism shared across different toxicants, including industrial pollutants like lead and chemical preservatives

The current study revealed that the sodium benzoate-treated group showed marked MDA immunopositivity in both the nuclei and cytoplasm of germ cells within the seminiferous tubules, in addition to Leydig cells. Furthermore, the epithelial lining of the epididymal ducts exhibited dual nuclear and cytoplasmic expression. This extensive distribution of MDA suggests a considerable level of lipid peroxidation and oxidative stress affecting both spermatogenic and somatic cells of the male reproductive system. These findings are consistent with the fundamental concept that sodium benzoate increases oxidative burden, leading to membrane damage and activation of lipid peroxidation cascades. Similar oxidative stress patterns were also reported by **(Rezaei, Amirahmadi and Poozesh, 2022),** who noted mild to moderate MDA expression in reproductive tissues following chemical exposure, supporting the notion that lipid peroxidation plays a key role in testicular damage.

In the mix-treated group, which received both sodium benzoate and pimaricin, the testicular and epididymal tissues showed the strongest MDA immunoreactivity among all groups. The staining was intense and observed

in both nuclear and cytoplasmic compartments of the seminiferous epithelium and the epididymal lining. This suggests that co-exposure to these agents may produce a synergistic or additive effect in generating free radicals, thus enhancing lipid peroxidation and oxidative tissue damage. The co-localized nuclear and cytoplasmic expression indicates that both genomic material and organelles were affected. These results are in line with oxidative damage mechanisms described by **Kurutas (2015**), who emphasized that excessive reactive oxygen species result in elevated MDA production and widespread intracellular damage.

On the other hand, the group treated with pimaricin alone exhibited a milder oxidative response, as evidenced by mild to moderate MDA expression in the nuclei and cytoplasm of testicular and epididymal cells. Although lipid peroxidation was still present, its extent was noticeably less than in the sodium benzoate or combined-treatment groups. This indicates that pimaricin has a relatively weaker pro-oxidative effect on the male reproductive tissues when used alone. Comparable findings were reported by **(Rezaei, Amirahmadi and Poozesh, 2022),** who documented moderate oxidative changes and localized MDA positivity in antifungal-exposed tissues. Their results support the interpretation that MDA levels directly reflect the degree of chemical-induced oxidative stress in reproductive organs.

4.6 Serum Follicle-Stimulating Hormone (FSH) and Luteinizing Hormone (LH) Levels

Figures 4-53 to 4-56 present the serum levels of Follicle-Stimulating Hormone (FSH) and Luteinizing Hormone (LH) in different experimental groups—control, sodium benzoate-treated, pimaricin-treated, and mix-treated (sodium benzoate + pimaricin)—measured at 0, 20, and 50 days.

In the control group, both FSH and LH levels remained relatively stable over the 50-day period. In contrast, all treated groups exhibited a significant, time-dependent reduction in the levels of both hormones compared to the control group ($p < 0.05$). The most substantial decreases were observed in the mix-treated group, indicating a potential synergistic inhibitory effect of sodium benzoate and pimaricin on the hypothalamic-pituitary-gonadal (HPG) axis.

By day 20, animals in the sodium benzoate and pimaricin groups showed moderate but statistically significant declines in both FSH and LH levels. These reductions progressed further by day 50. The mix-treated group, however, demonstrated a markedly sharper decline in both hormone levels over time, suggesting an amplified endocrine-disrupting effect when both compounds were administered in combination.

These findings suggest that exposure to sodium benzoate and pimaricin—either individually or in combination—impairs the regulation of gonadotropins. The combined treatment exerts the most pronounced suppressive effect, likely due to a synergistic mechanism affecting the HPG axis and associated hormonal signaling pathways.

Discussion of Hormones

The primary androgen for males is testosterone, typically regulated by FSH and LH from the anterior pituitary gland. FSH and LH also promote the production of steroids and the growth of testicles. These sex hormones are crucial in the physiological roles of both reproductive and nonreproductive tissues. The harmful effects of food additives/preservatives and bacterial infections have been reported to hurt the reproductive organs which in turn, affect the levels of sex hormones(**Ogunro and Babatunde, 2023).**In our study reported reduced levels of FSH and LH were observed in the sodium benzoate, pimaricin and mix groups However, the reduction in the concentrations of FSH, LH, in NaB or pimaricin- treated rats was in tandem with the findings of **(Kehinde, Christianah and Oyetunji, 2018)**.In this study, the significant reduction in FSH and LH levels following individual administration of sodium benzoate, pimaricin, or both may have been caused by the hypothalamic-pituitary gonad axis functioning normally or by increased systemic oxidative stress, which may have inhibited the gonadotrophic cells' responsiveness to gonadotropin-releasing hormone and, as a result, inhibiting the secretion of gonadotropin (Oyola and Handa, 2017)**.**To better understand the aberrant sperm cell induction process, the gonadotropic hormone levels that control spermatogenesis were evaluated in mice subjected to certain chemicals. **(Alabi *et al.*, 2022)** showed that presence of dietary additives led to decreased luteinizing hormone (LH) levels while those of follicle-stimulating hormone (FSH) and total testosterone (TT) increased. Spermatogenesis and testicular development depend heavily on FSH, which is also a good predictor of Klinefelter's syndrome, oligozoospermia, azoospermia, and primary testicular failure **(Merino *et al.*, 1999).** Consequently, it is suggested that damage to germinal cells is associated with a significant increase in FSH levels according to

decreased testicular activity and a lack of testicular components involved in negatively feedback on FSH secretion **(Matsumoto *et al.*, 1983)**

Table :4-1 Thickness of tunica albuginea in mean and Standard deviation (µm)

Thickness of tunica albuginea in mean and Standard deviation (µm)	
Control group	36.45 ± 1.5
Sodium benzoate group	40.43 ± 1.7
Pimaricin group	40.23 ± 1.2
Mix group (Sodium benzoate , Pimaricin)	46.03 ±0.1

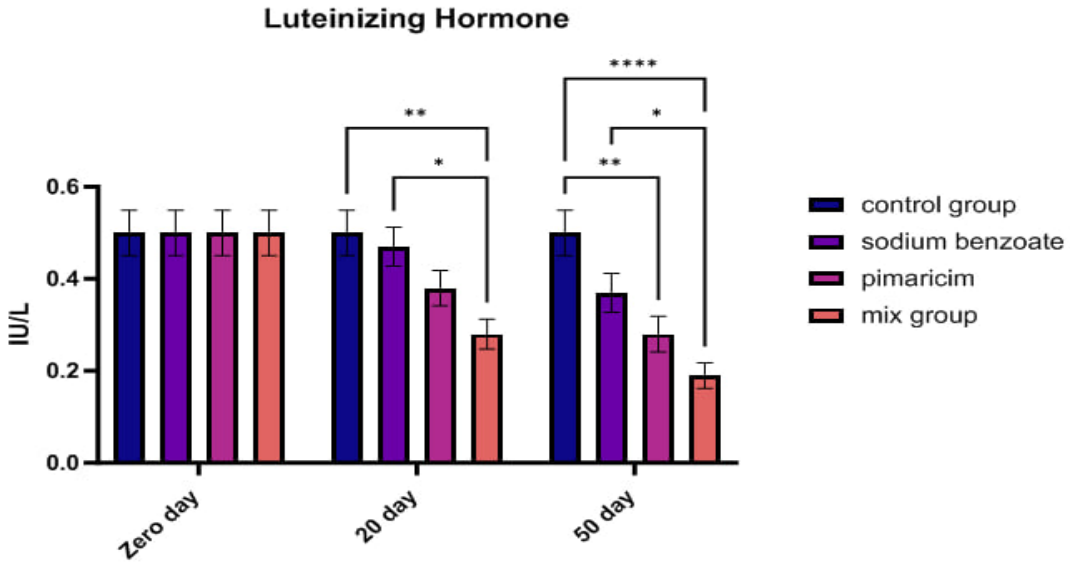

Barograph (4-1): Changes in serum **(LH)** levels in control and treated groups at 0, 20, and 50 days. A progressive decline in **(LH)** is observed in all treated groups compared to the control, with the most significant suppression in the mix group (sodium benzoate + pimaricin). Mean ± SD

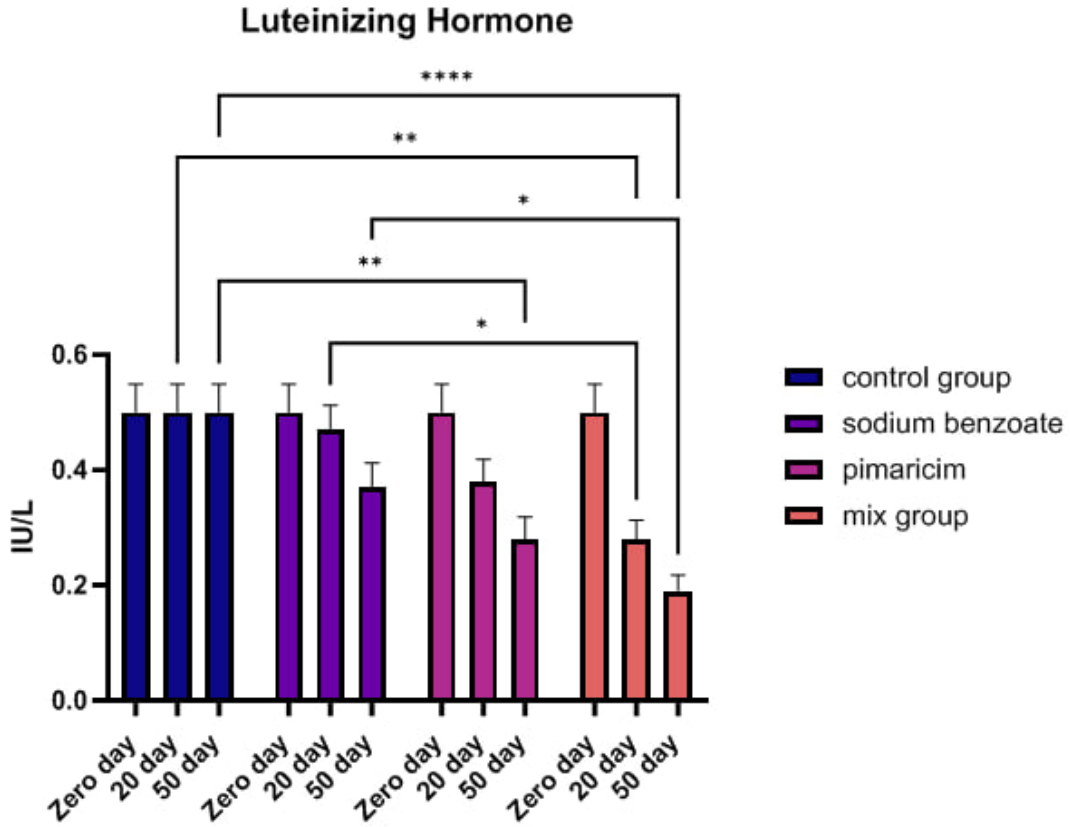

Barograph (4-2): shows a significant decrease in Luteinizing Hormone (LH) levels over time, particularly in the sodium benzoate, pimaricin, and mix groups compared to the control group. The mix group exhibited the most pronounced reduction by day 50. Mean ± SD

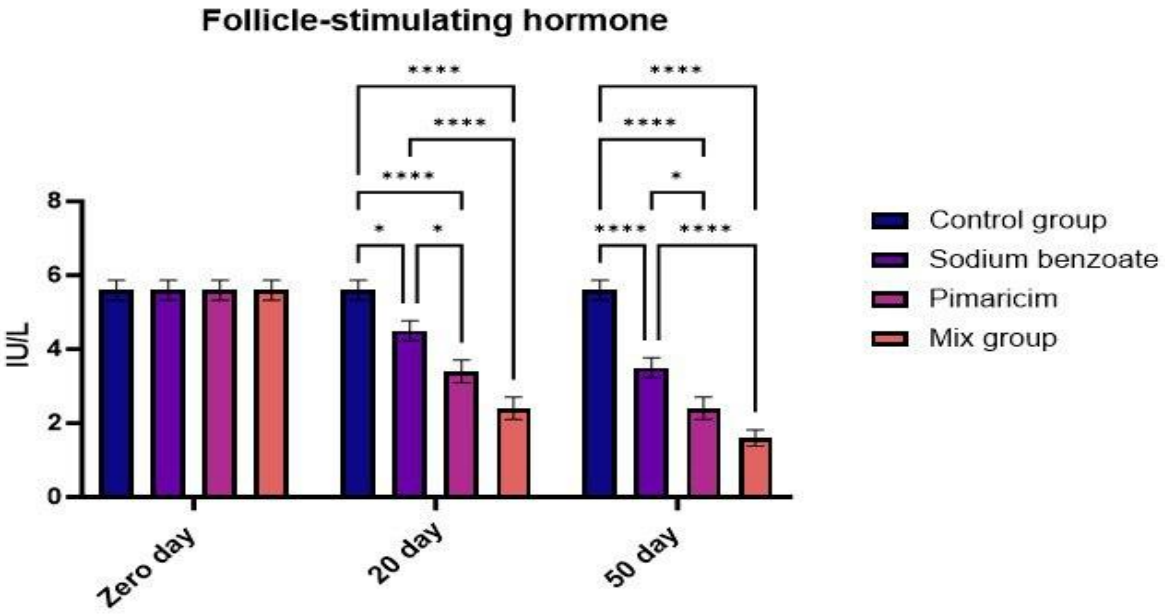

Barograph (4-3): Serum Follicle-Stimulating Hormone (FSH) Levels in Different Experimental Groups at 0, 20, and 50 Days.This chart shows a significant time-dependent decrease in FSH levels in all treated groups compared to the control. The most pronounced suppression is observed in the mix-treated group (sodium benzoate + pimaricin), suggesting a synergistic inhibitory effect on the hypothalamic-pituitary-gonadal axis. Mean ± SD

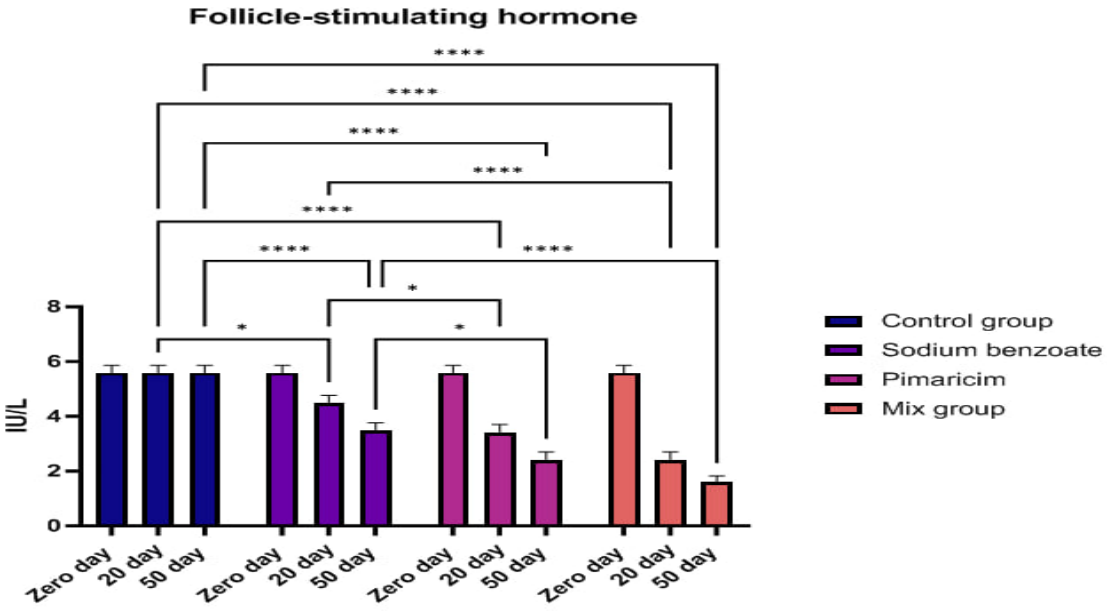

Barograph (4-4): shows the effects of different treatments on Follicle-Stimulating Hormone (FSH) levels over time (0, 20, and 50 days). The control group maintains stable FSH levels, while all treatment groups—sodium benzoate, pimaricin, and especially the mix group—exhibit a significant and progressive decline in FSH levels, with the mix group showing the most dramatic drop by day 50. **Mean ± SD**

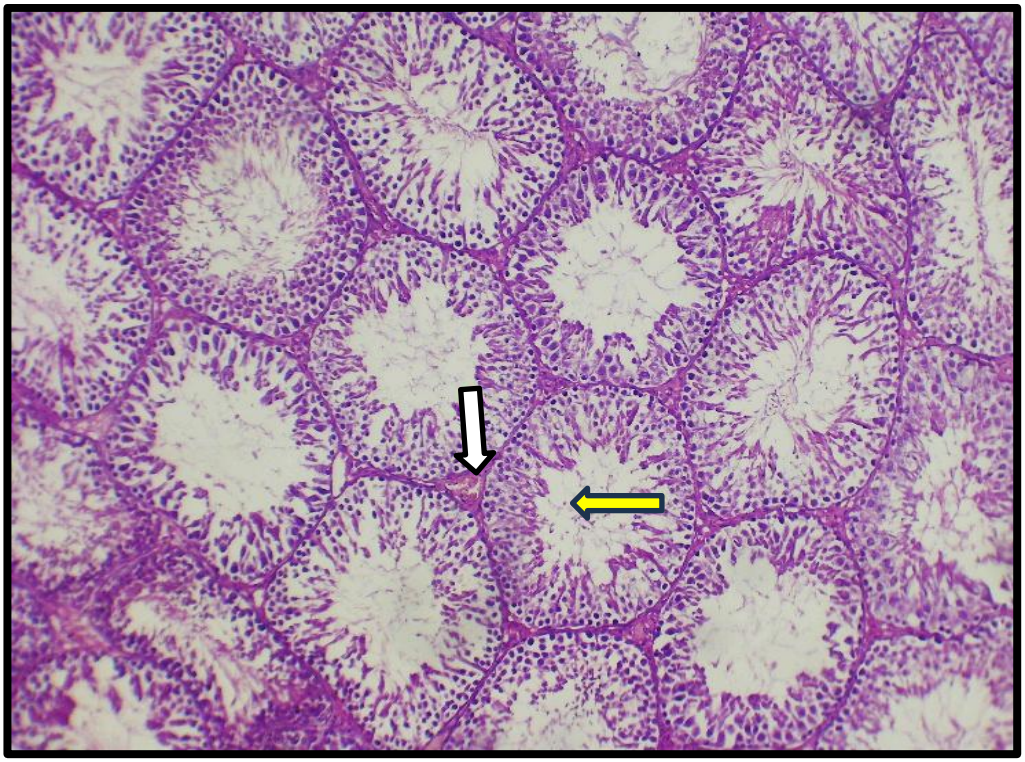

Figure (4-1): Histological section of the testis from the **control group** showed normal seminiferous tubules that circular with regular contour **(yellow arrow)** The interstitial tissue appeared as delicate loose C. T and Leydig cells **(white arrow)** (H&E stain10X)

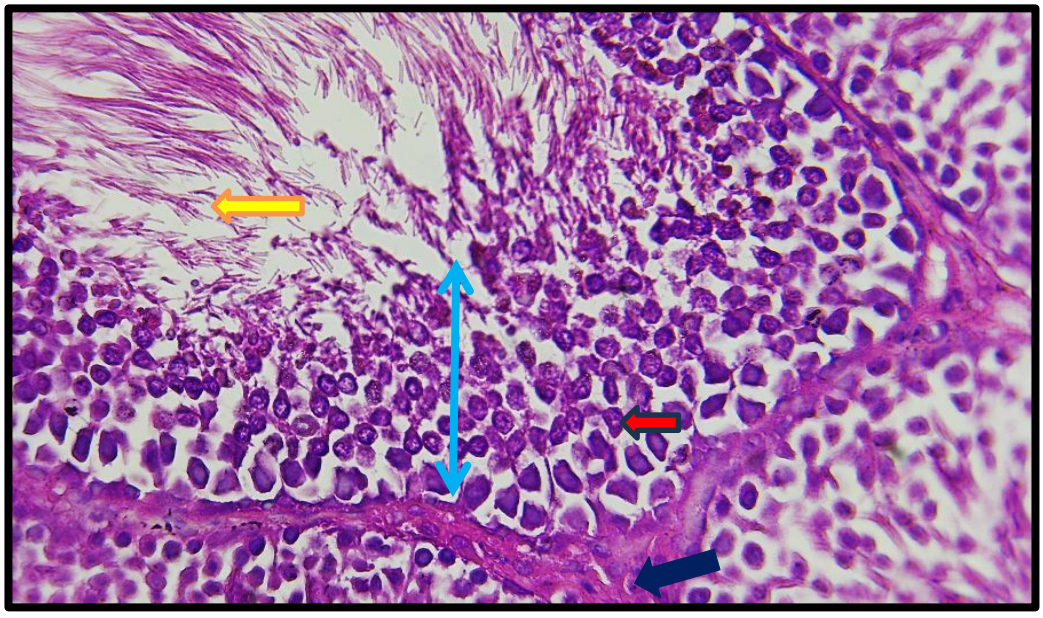

Figure (4- 2): Histological section of testis from the **control group** showed normal seminiferous tubules lined with a series of germinal epithelium (**blue arrow**) and Sertoli cells **(red arrow)** with attached sperms **(yellow arrow**) & interstitial cell of Leydig **(black arrow)** (H&E stain 40 X).

Figure (4-3): Histological section in the epididymis **of control group** showed epididymal tubule lined by ciliated Pseudostratified columnar epithelium with lumens filled with spermatozoa **(yellow arrows)** (H&E stain 10 X).

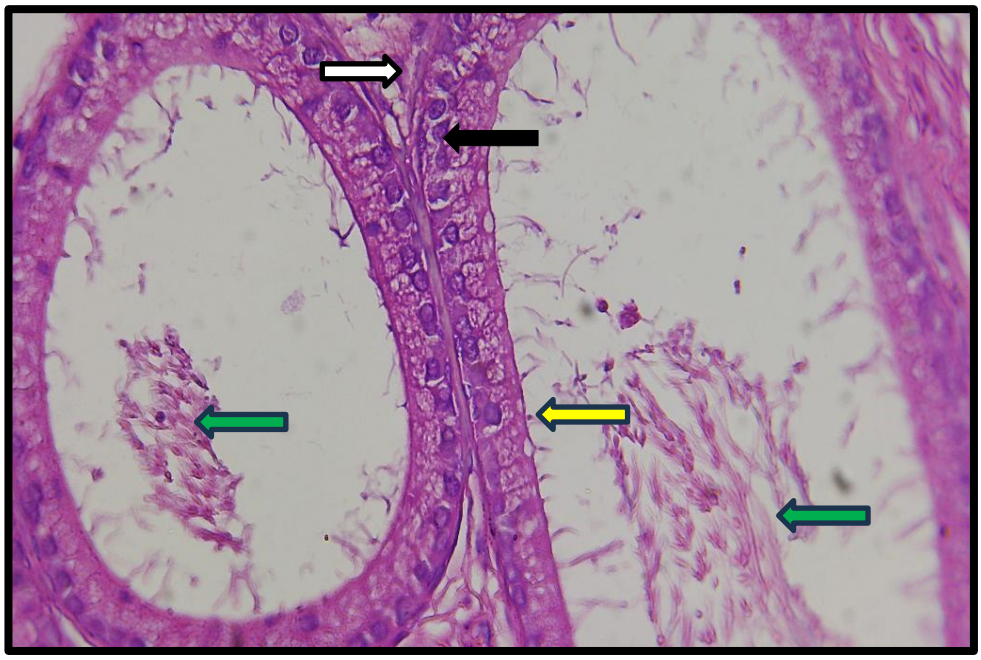

Figure (4-4): Histological section of epididymis from the **control group** showed columnar cells with basal nuclei and stereocilia **(yellow arrow),** basal cells resting on the basal lamina & clear cells with pale cytoplasm **(black arrow).** Also a thin layer of smooth muscle fibers surrounds each epididymal duct **(white arrow),** and numerous spermatozoa were seen in the epididymal lumen **(green arrows),** (H&E stain 40 X).

Figure (4-5): Histological section of the testis **from control group** demonstrated well-preserved testicular architecture, with normal seminiferous tubules, The Tunica Albuginea and basement membranes of the tubules are distinctly PAS- staining affinity indicating normal glycoprotein structures **(yellow and green arrows)** respectively (PAS stain 10 X)

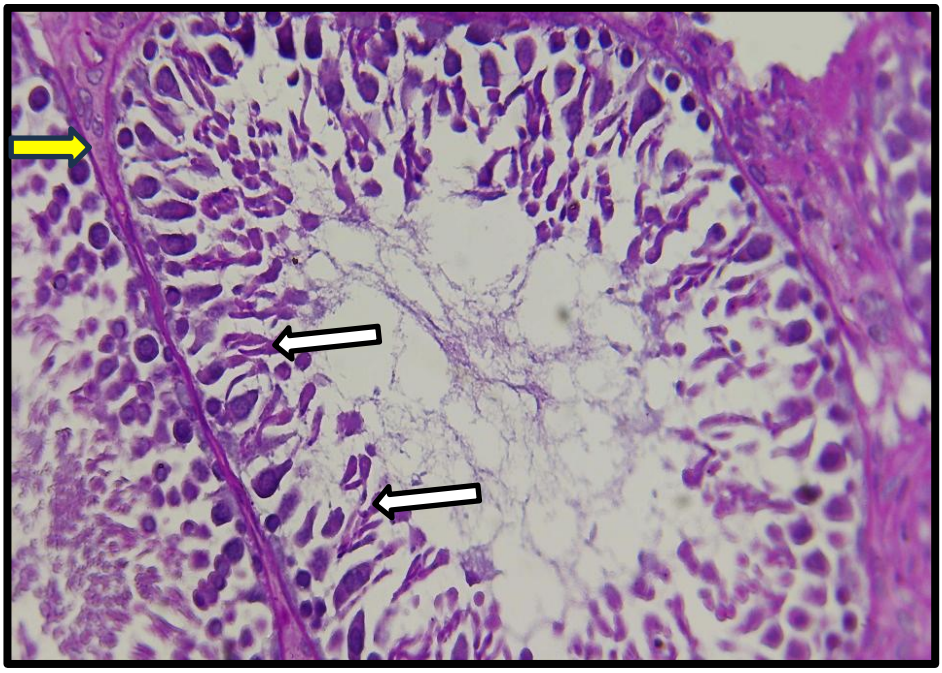

Figure (4-6): Histological section of the testis from the **control group** showed Periodic acid–Schiff staining affinity in the basement membrane **(yellow arrow)** & elongated spermatids with acrosomal caps in some developing spermatids **(white arrows)** (PAS stain 40 X)

Figure (4-7): Histological section of the epididymis from the **control group** showed PAS stain uptake in the basal lamina of the epididymal ducts **(white arrow)** with intact thin apical PAS reaction in the lining epithelial cells **(yellow arrows)** (PAS stain 40 X).

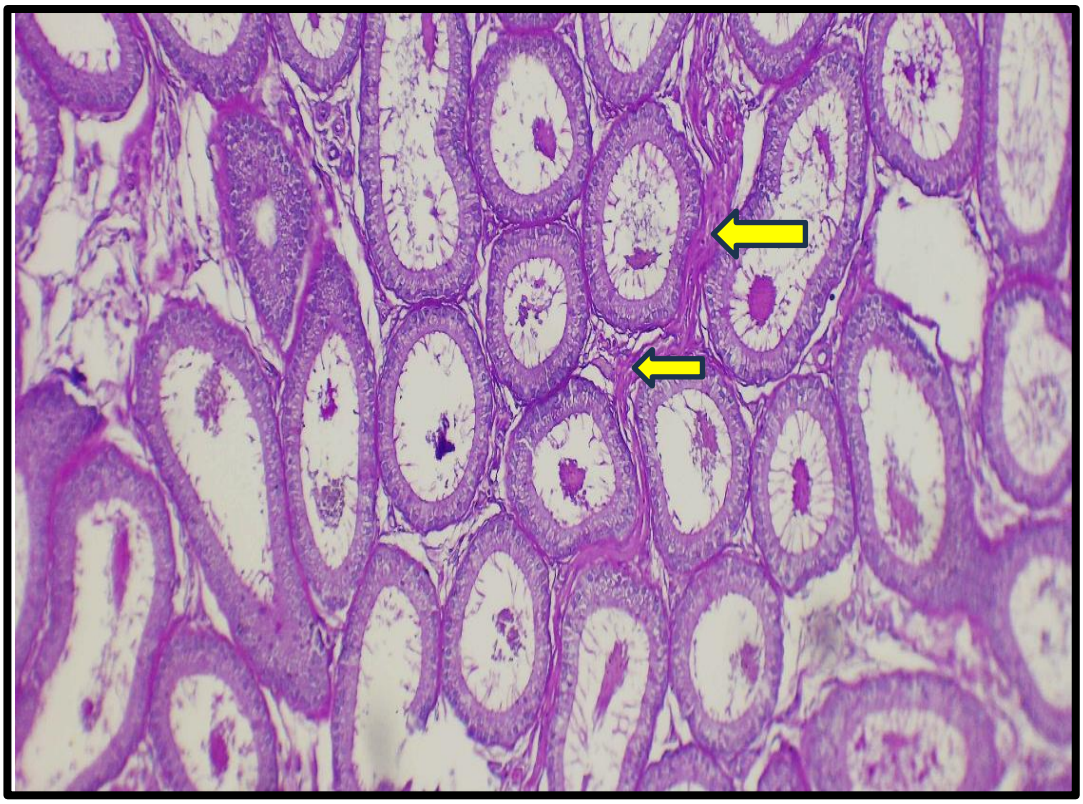

Figure (4-8): Histological section of the epididymis from the **control group** showed purple stained collagen fibers surrounding the epididymal ducts **(yellow arrows)** (PAS stain 10 X)

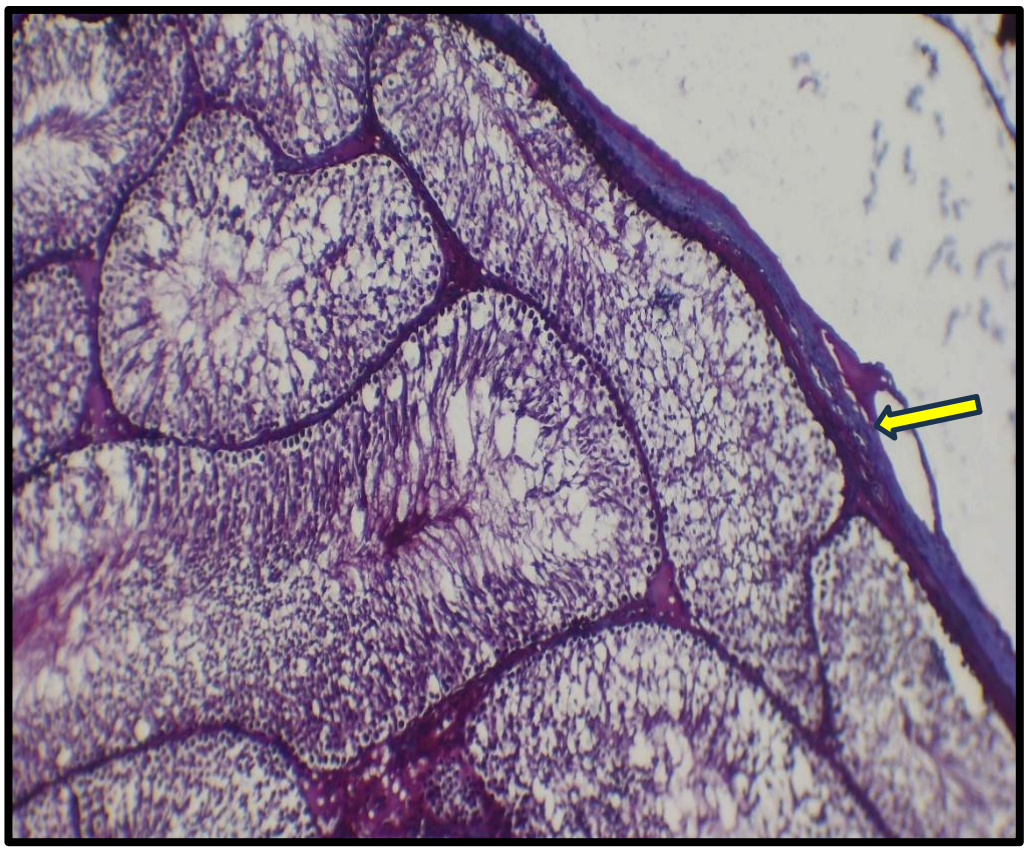

Figure (4-9): Histological section of the testis from the **control group** showed susceptibility Masson stain for tunica Albuginea stained blue color **(yellow arrow)** (Masson Trichrome stain 10 X)

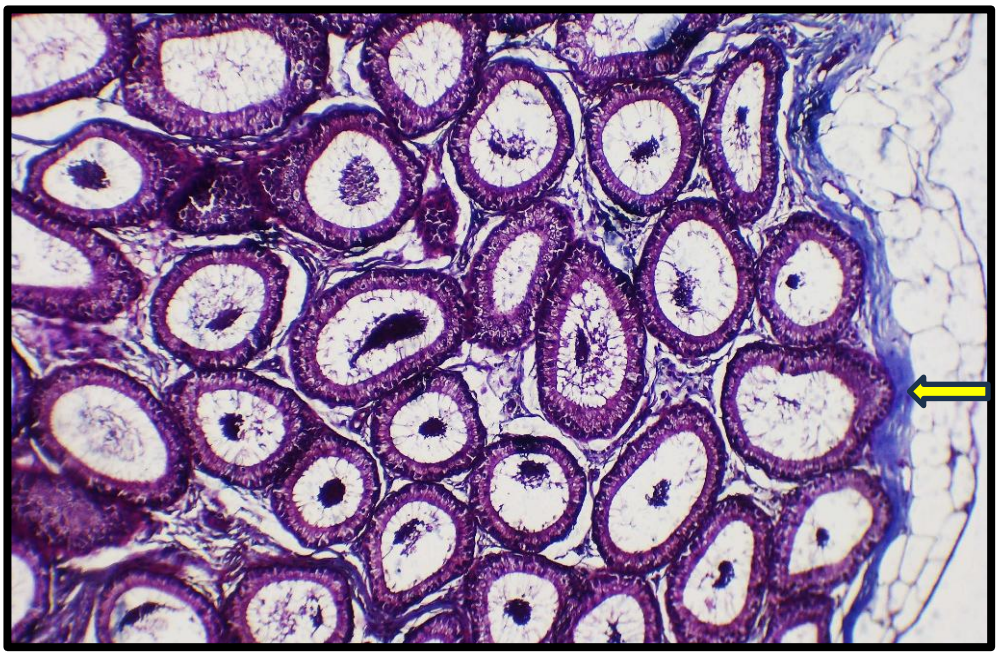

Figure (4-10):Histological section of the epididymis from the **control group** showed Masson Trichrome stain reaction for tunica Albuginea stained with blue color **(yellow arrow)** (Masson Trichrome stain 10 X)

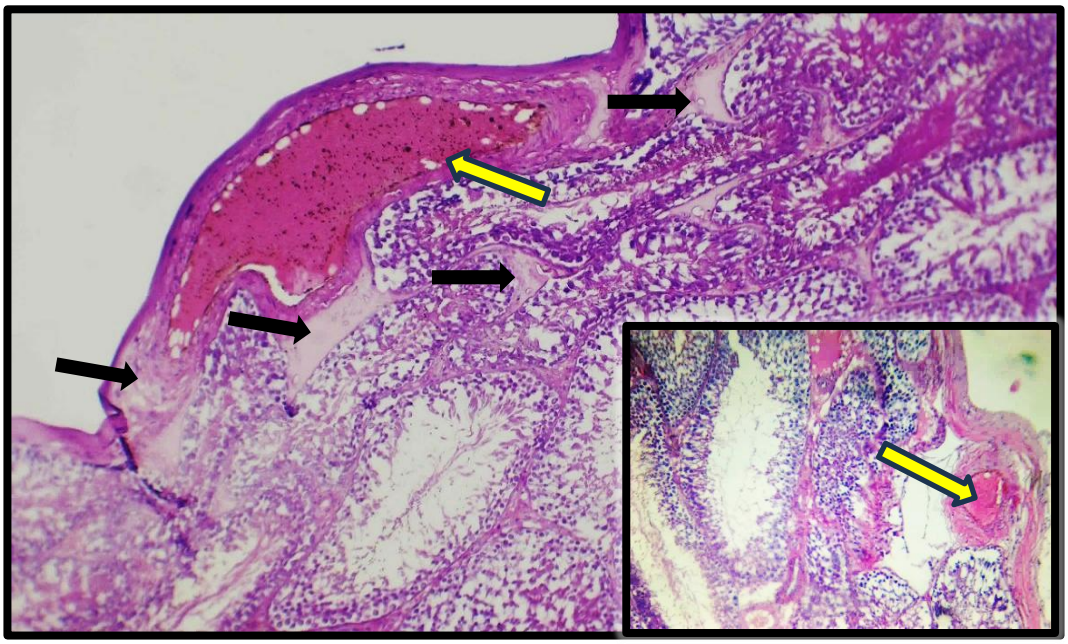

Figure (4-11): Histological section of the testis after 50 days post exposed t**o sodium benzoate** showed thrombus of blood vessels **(yellow arrows)** with edema in interstitial tissue and sub tunica albuginea **(black arrows)** (H&E stain 10 X).

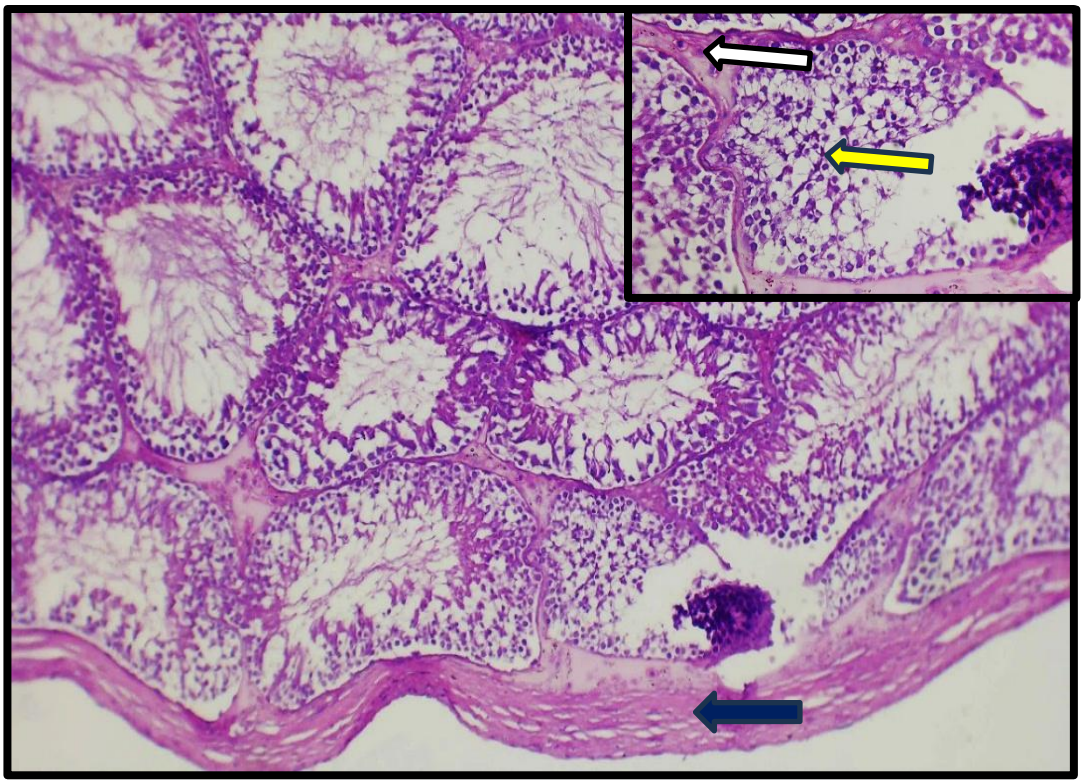

Figure (4-12): Histological section of the testis from the rat group exposed to **sodium benzoate** for 50 days, showed increase in the thickness of tunica albuginea **(black arrow)** and edema with vacuolation of spermatogenic cell **(yellow arrow)** and few Leydig cells interstitial **(white arrow),** (H&E stain 10 X,40 X).

Figure (4-13): Histological section of the epididymis in the **sodium benzoate group** at 50 days post-exposure showed disorganized tubular structure with marked expansion of interstitial tissue and infiltration of mononuclear inflammatory cells mainly lymphocytes **(yellow arrow),** (H&E Stain10 X, 40X)

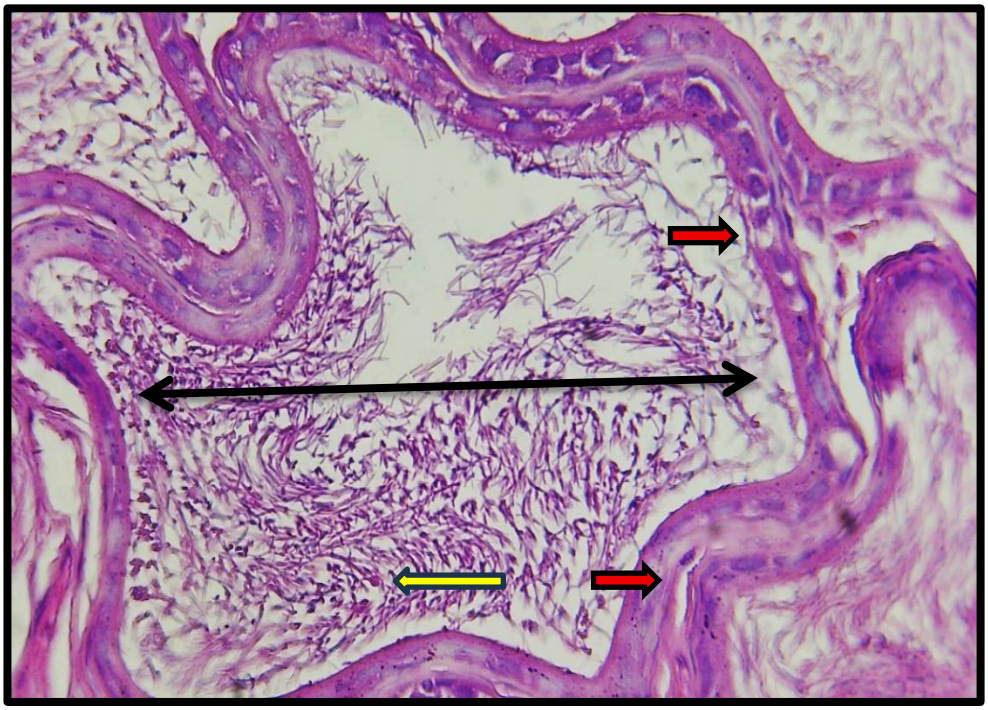

Figure (4-14): Histological section of the epididymis in the **sodium benzoate treated group** at 50 days post-exposure reveled abnormal tubular architecture due to degenerative alterations with necrosis of epithelial lining cells **(red arrows)** and interstitial edema with detached stereocilia **(yellow arrow)** ,along with reduced sperm count, (H&E stain, 40 X)

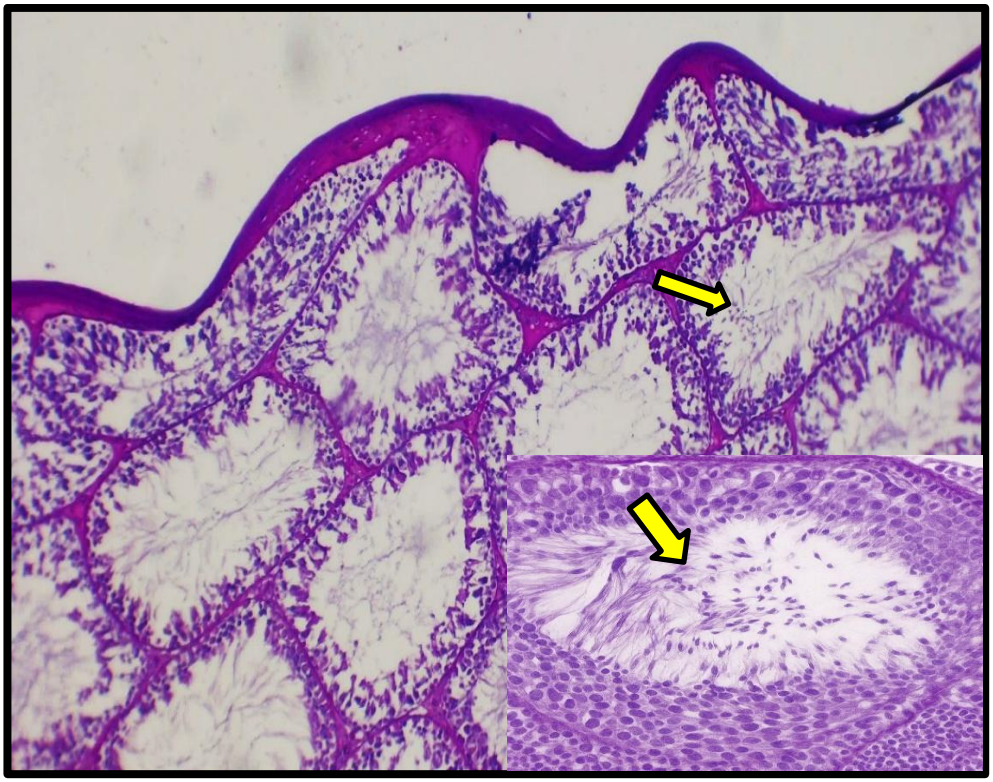

Figure (4-15): Histological section of the testis **of group treated with sodium benzoate** at 50 days post exposure, showed degenerative changes with loss of normal spermatogenic germ layers and reduction of mature sperm **(yellow arrows),(**PAS stain 10 X)

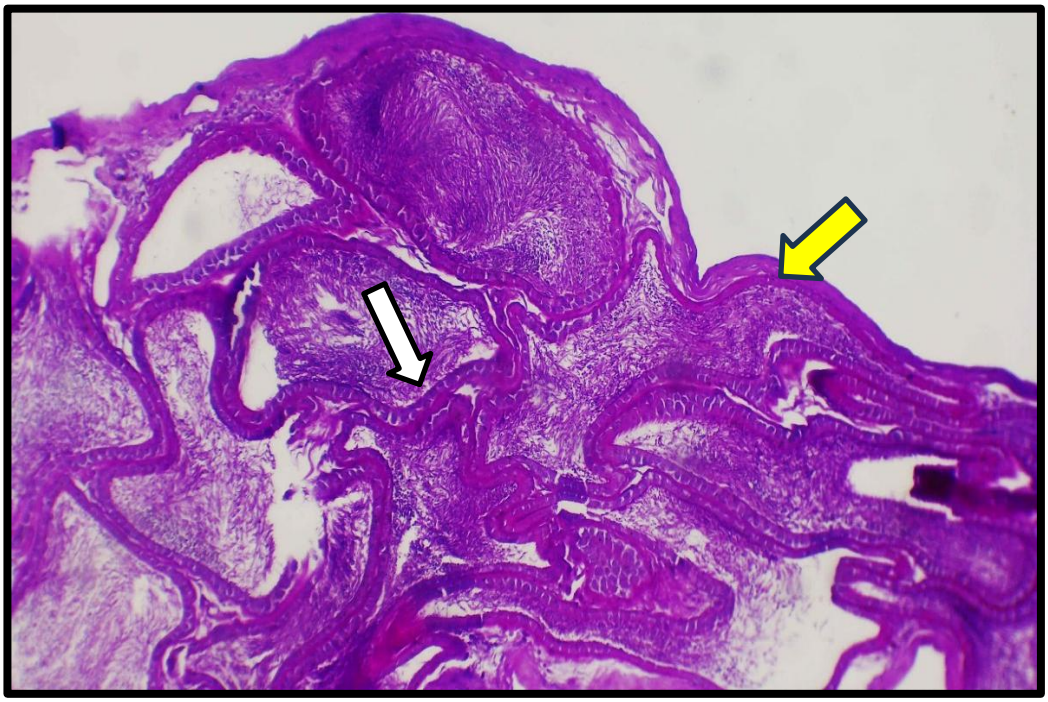

Figure (4-16): Histological section of epididymis **of sodium benzoate group** at 50 days post exposure, showed modest increase in the thickness of basal lamina **(yellow arrow)** with marginal gain PAS reaction in the apical parts of the lining epithelial cells **(white arrow)** (PAS stain 10 X).

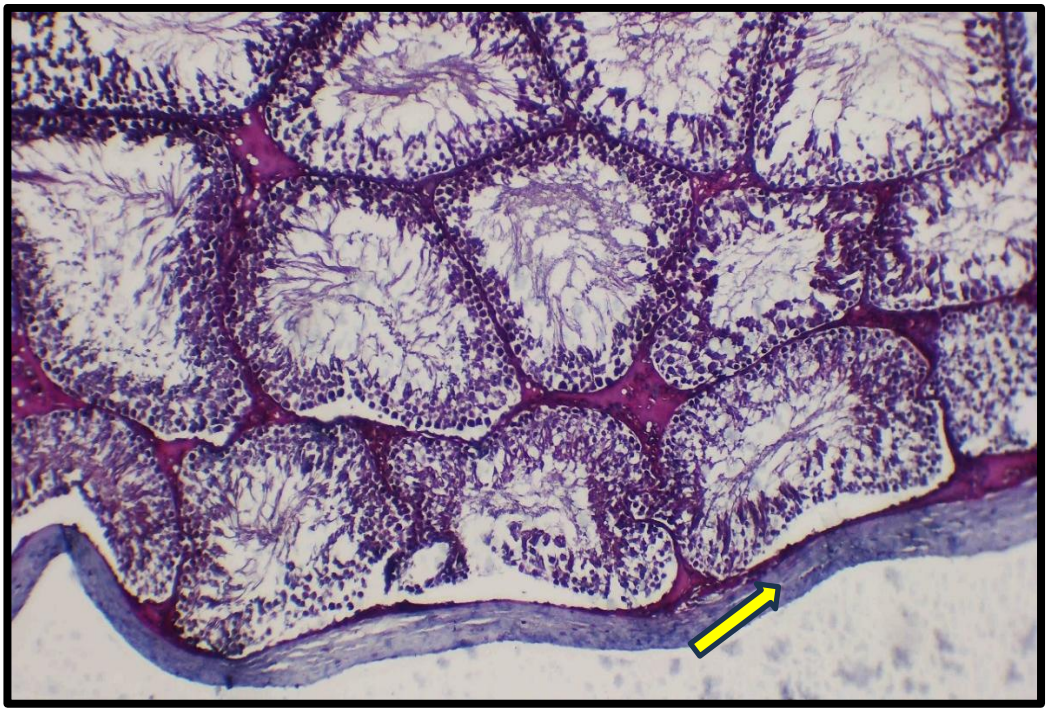

Figure (4-17): Histological section of the testis **in sodium benzoate exposed group** at 50 days post exposure, showed incremental increase in the thickness of tunica Albuginea due to proliferation of fibrous connective tissue stained with blue color **(yellow arrow) (Masson Trichrome stain 10** X**).**

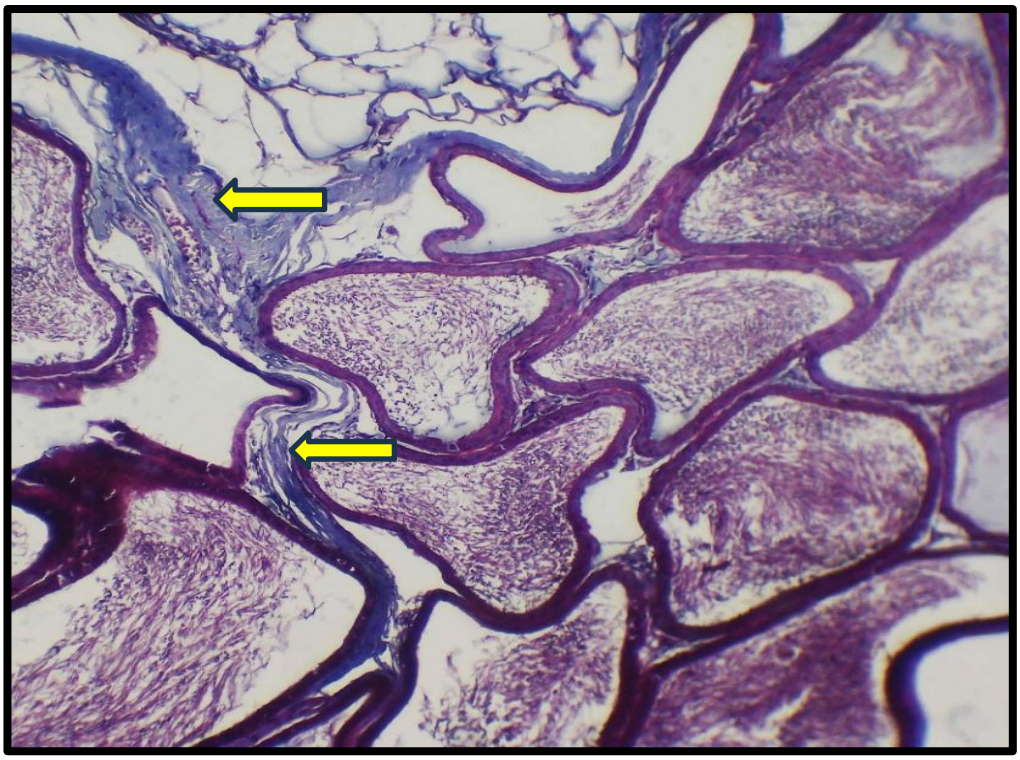

Figure (4-18): Histological section of epididymis **in the sodium benzoate exposed group** after 50 days, showed minor increase in fibrous connective tissue in tunica Albuginea & collagen fibers in the connective tissue surrounding the epididymal ducts stained with blue color **(yellow arrows), (Masson Trichrome stain, 10 X).**

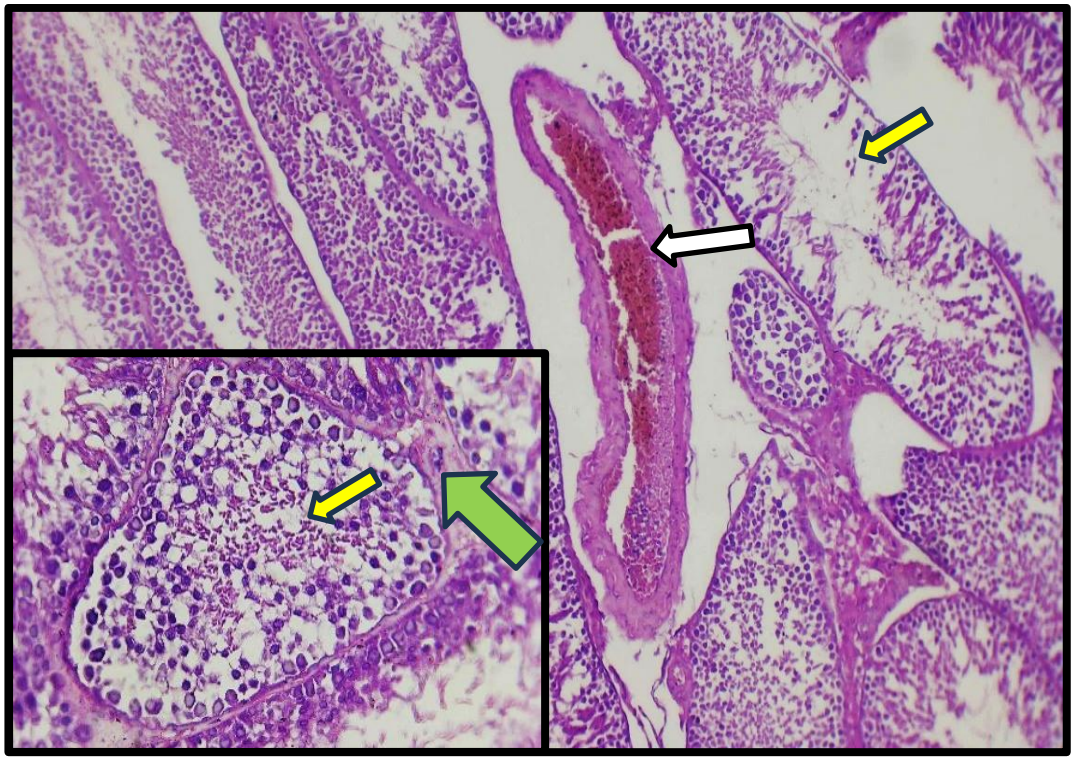

Figure (4-19): Histological section of the testis **from the pimaricin treated group** after 50 days of exposure, showed degenerative & necrosis of spermatic cells **(yellow arrows)** with a reduced of interstitial Leydig cell count **(green arrow),** and congestion of blood vessels **(white arrow), (H&E stain 10 X +40 X).**

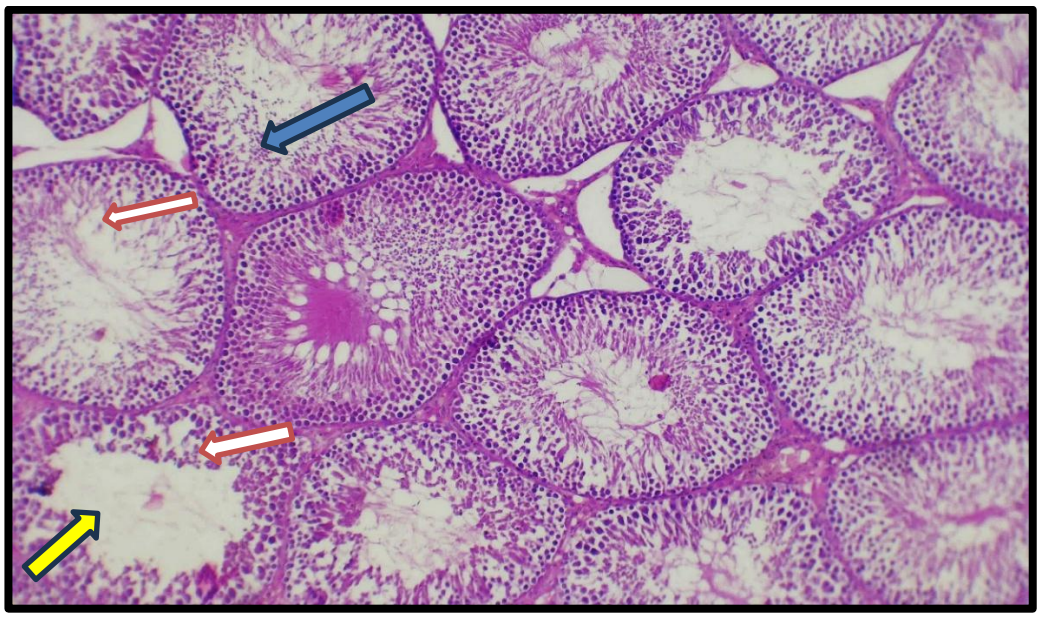

Figure (4-20): Histological section of the testis **from the pimaricin treated group** at 50 days post-exposed are showed degenerative changes and necrosis of spermatogenic epithelium **(white arrow)** & some lumens have few mature spermatozoa **(yellow arrow)** and other lumen filled with sloughed immature cells, **(blue arrow)** (H&E stain 10 X)

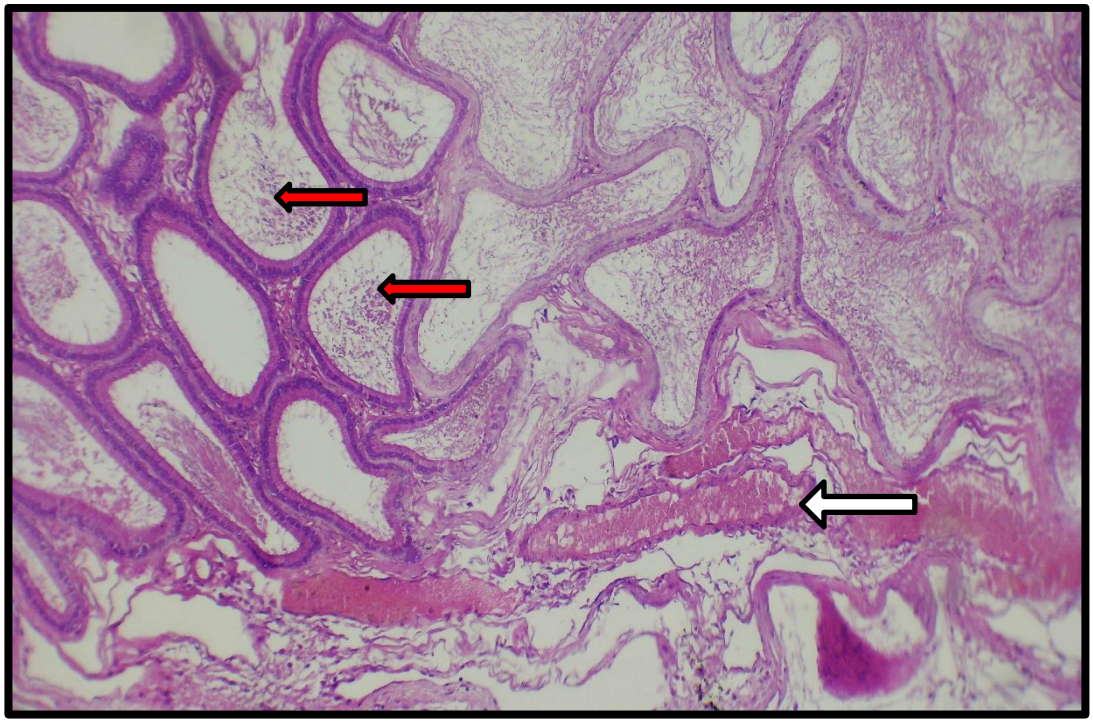

Figure (4-21): Histological section **of the epididymis from the pimaricin treated group** at 50 days post-exposed are showed vascular congestion **(white arrow)** & large number of degenerative sperm**(red arrows) (H&E stain 10 X)**

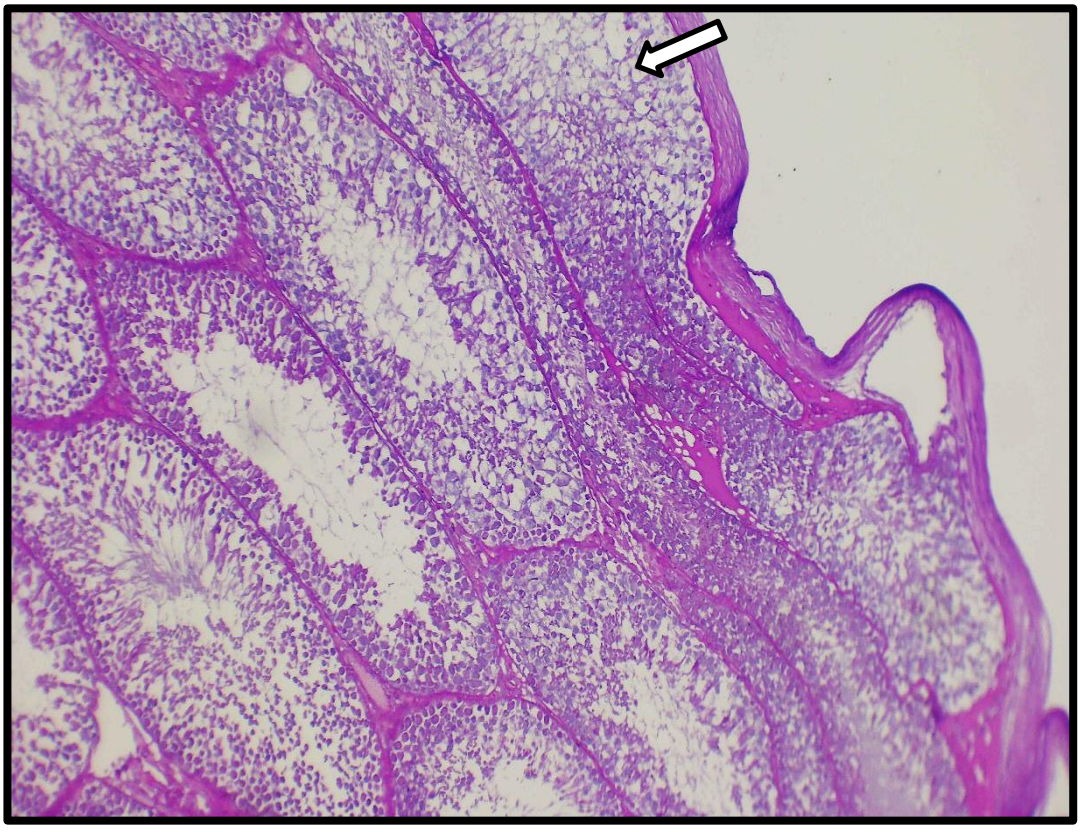

Figure (4-22): Histological section of the testis **from the pimaricin trated group** at 50 days post-exposed are showed degenerative changes with vaculations of cells **(white arrow)(PAS stain 10 X)**

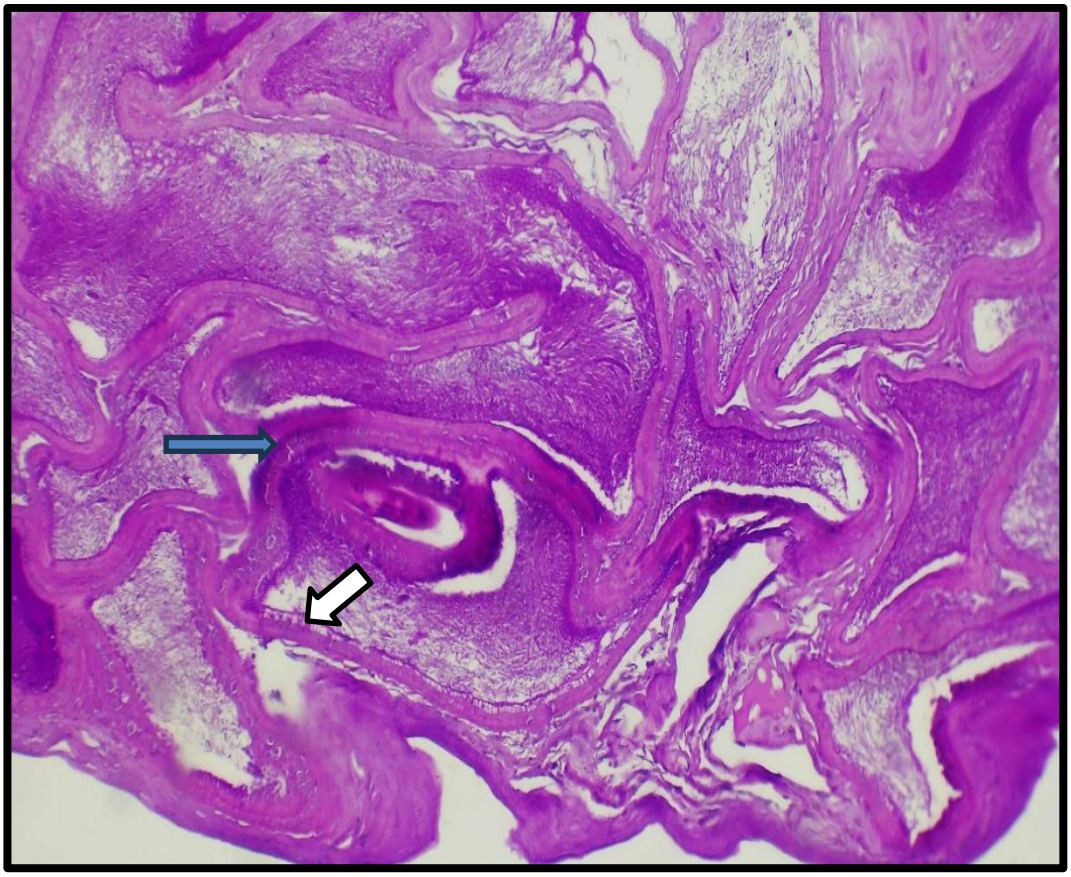

Figure (4-23): Histological section of epididymis **from pimaricin treated group** at 50 days post exposure, showed obvious increase in the thickness of basement membrane **(blue arrow)** with loose of normal tissue appearance intact thin apical PAS reaction in the lining epithelial cells **(white arrow),** (PAS stain, 10 X).

Figure (4-24): Histological section of the testis **from the pimaricin treated group** at 50 days post exposure, showed disorganization in the seminiferous tubules with increase in the thickness of tunica Albuginea due to overproduction of fibrous connective tissue stained with blue color **(yellow arrow),** (Masson Trichrome stain, 10 X).

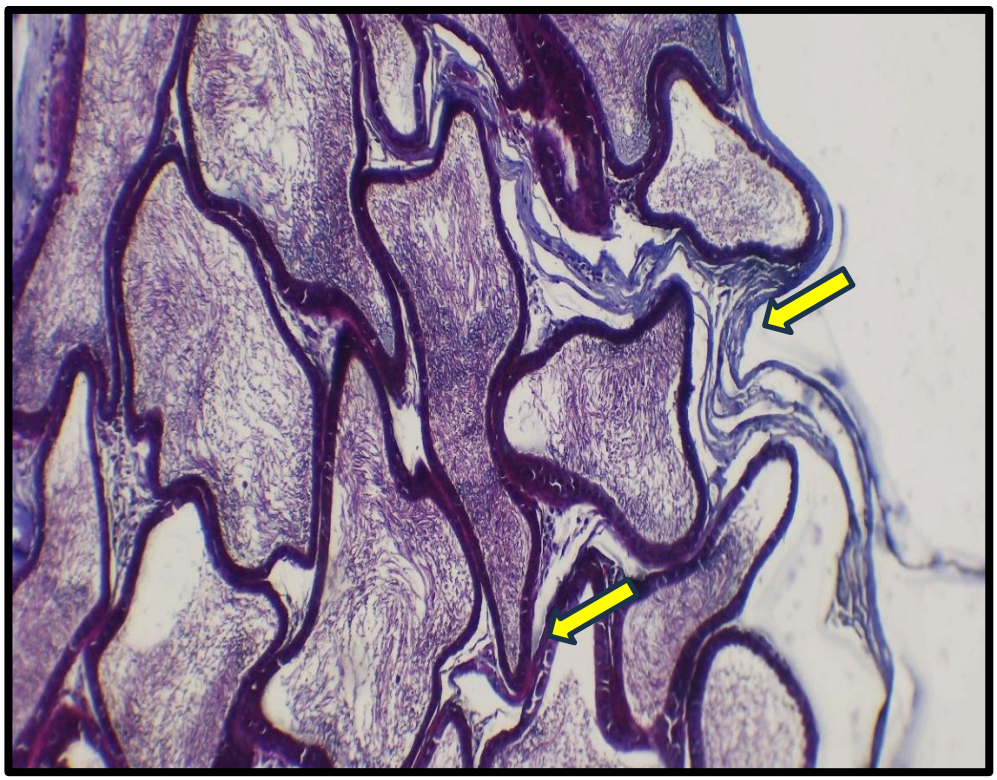

Figure (4-25): Histological section of the epididymis **from the pimaricin treated group** at 50 days post exposure, showed irregular outlines with degeneration of the ductal epithelium and increased collagen fibers surrounding the epididymal ducts stained with blue color **(yellow arrows), (Masson Trichrome stain, 10 X).**

Figure (4-26): Histological section of the epididymis from the **pimaricin treated group** at 50 days post exposure showed increased fibrous connective tissue in the tunica Albuginea stained with blue color **(yellow arrow) with irregular tubules structure (Masson Trichrome stain 10 X)**

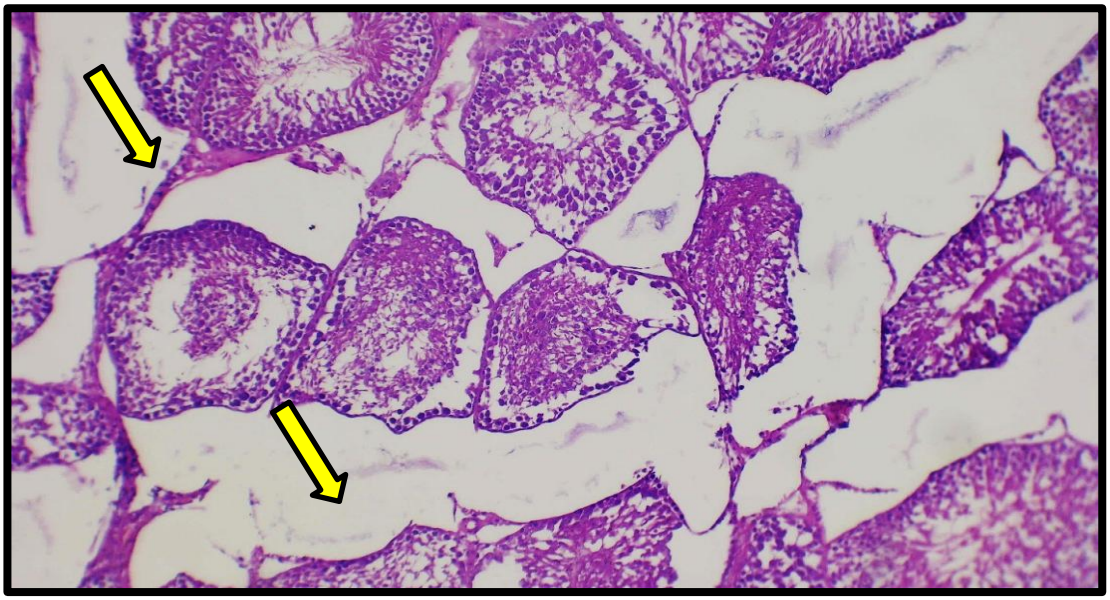

Figure (4-27): Histological section of the testis **from the mixed treated group** at 50 days post-exposure, exhibited seminiferous tubules atrophy with clear dilatation of interstitial spaces **(yellow arrows)** and decrease in number of Leydig cells **(H&E stain 10 X)**

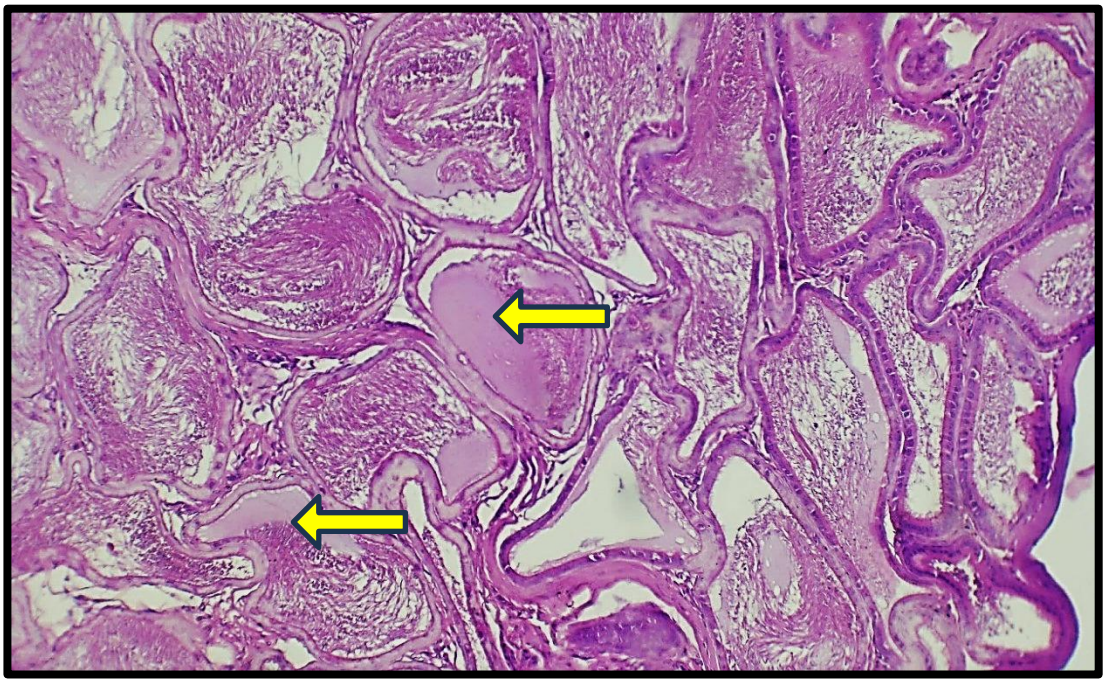

Figure (4-28): Histological section **of the epididymis from the mixed treated group** at 50 days post-exposed showed hyalinization of epididymal lumen **(yellow arrows)** (H&E stain 10 X)

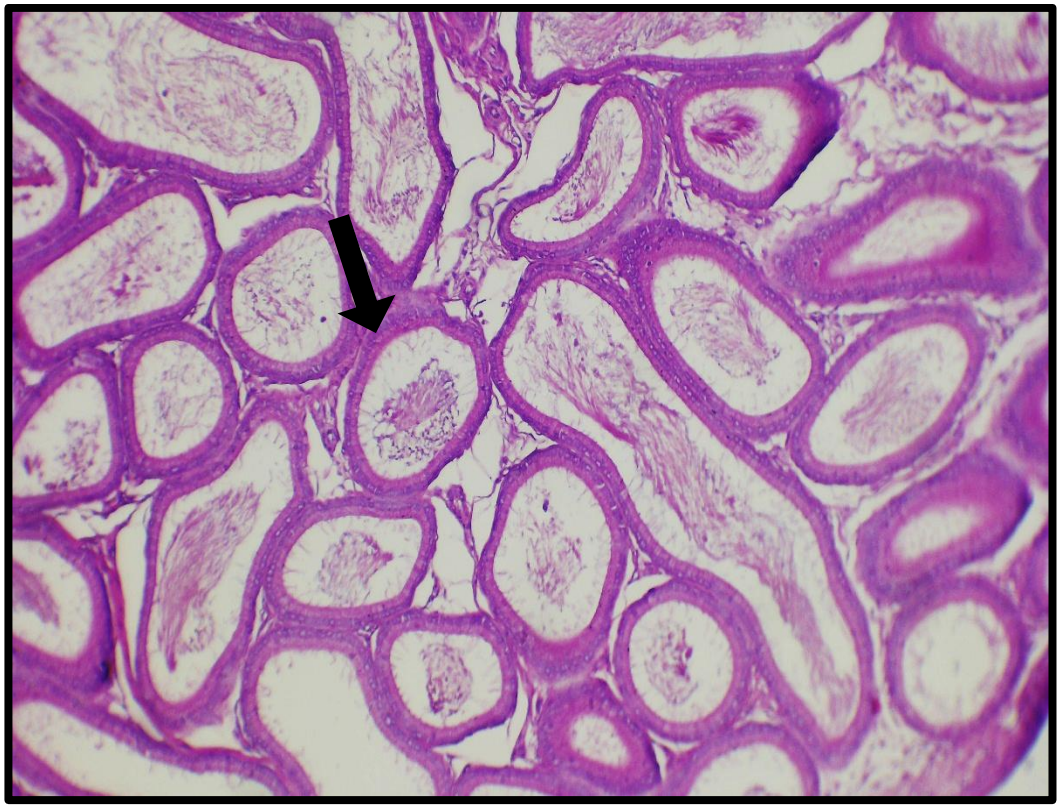

Figure (4-29): Histological section of the cauda epididymis **from the mixed treated group** at 50 days post exposure showed irregular arrangement of tubules surrounded by stroma with an increase thickness of basement membrane **(black arrow) (H&E stain 10 X).**

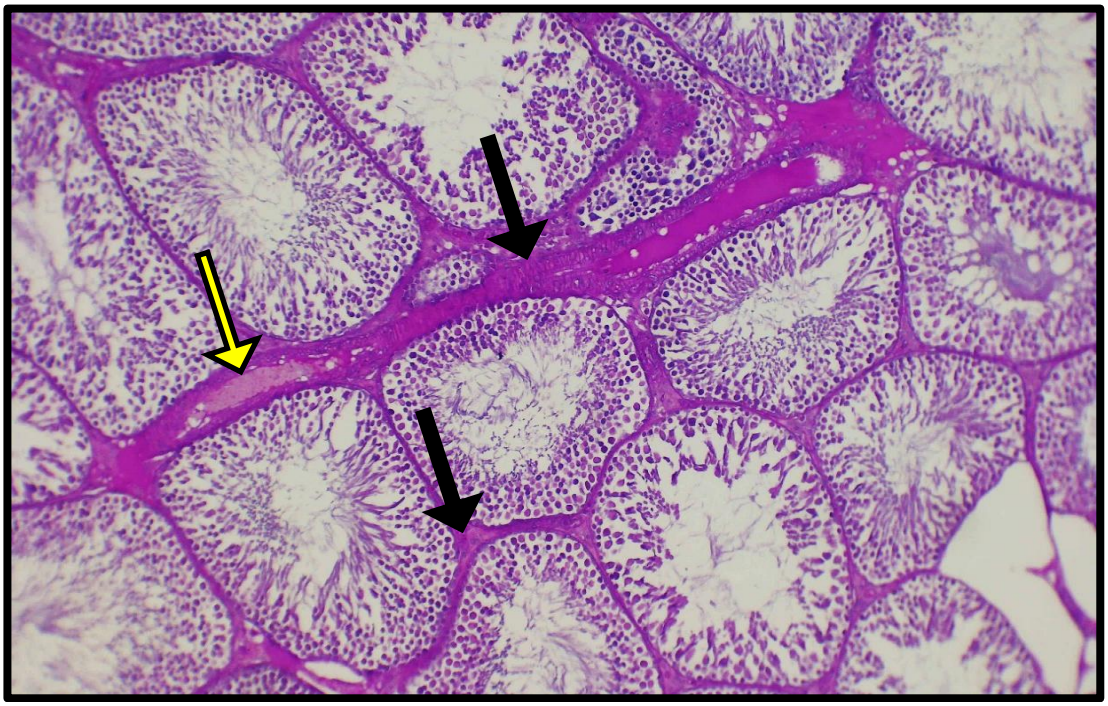

Figure (4-30): Histological section of the testis **from the mix treated group** at 50 days post-exposed are showed edema **(yellow arrow)** and a marked increase in thickness of interstitial tissues and basement membrane with stained purplish color **(black arrow)** with low number of Leyding cells**(PAS& 10 X)**

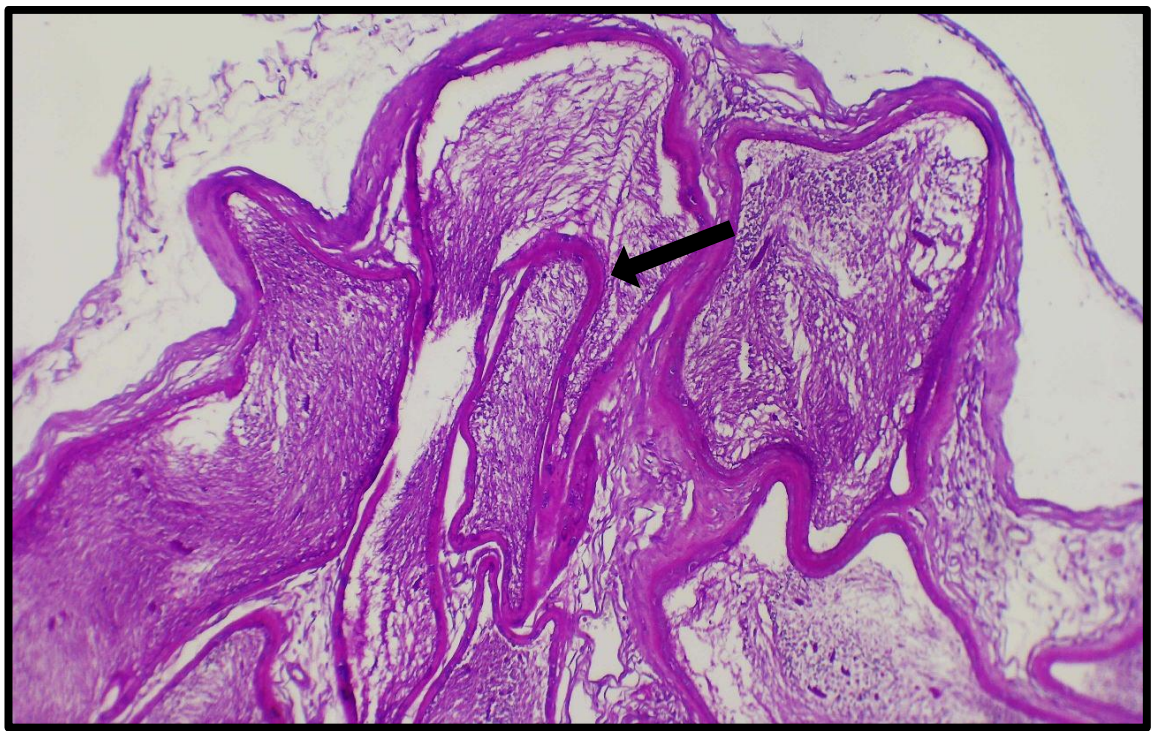

Figure (4-31): Histological section of the epididymis **from the mixed treated treatment** group at 50 days post exposure showed irregular tubular structure and marked increase in thickness of tunica albuginea & basement membrane stained with purplish color **(black arrow), (PAS stain ; 10 X).**

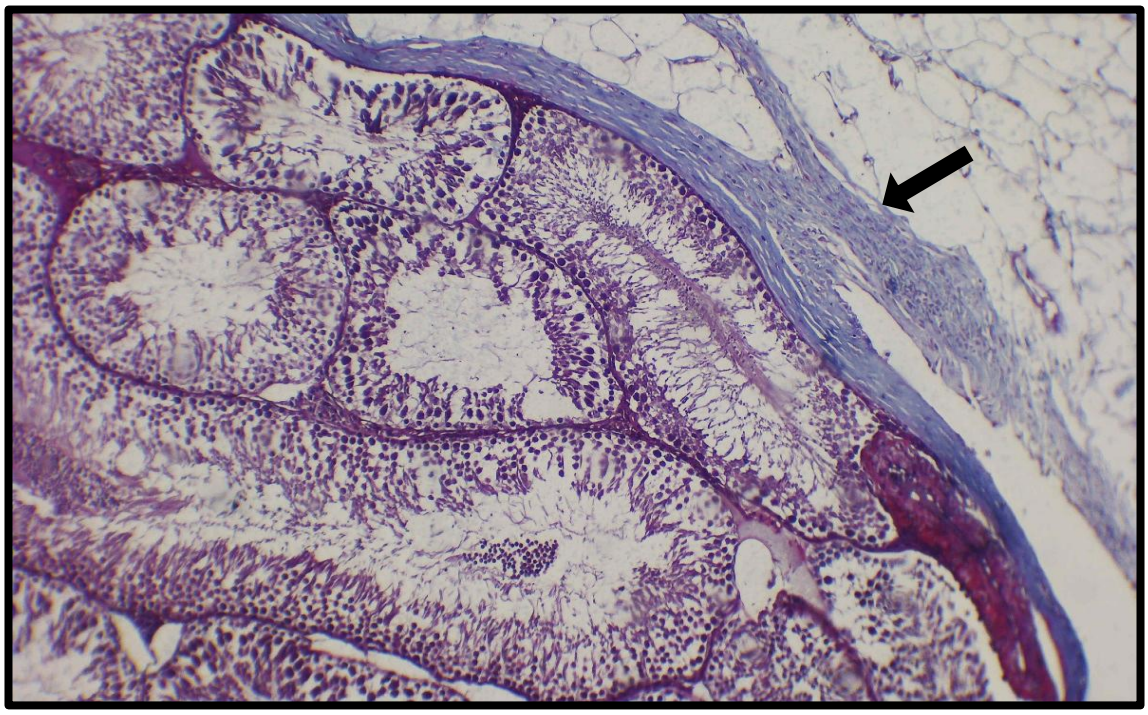

Figure (4-32): Histological section of the testis **from the mix treated group** at 50 days post-exposure are showed loose of normal tissue appearance and a marked increase in the thickness of tunica Albuginea due to increased fibrous connective tissue stained with blue color **(black arrow), (Masson Trichrome stain 10 X).**

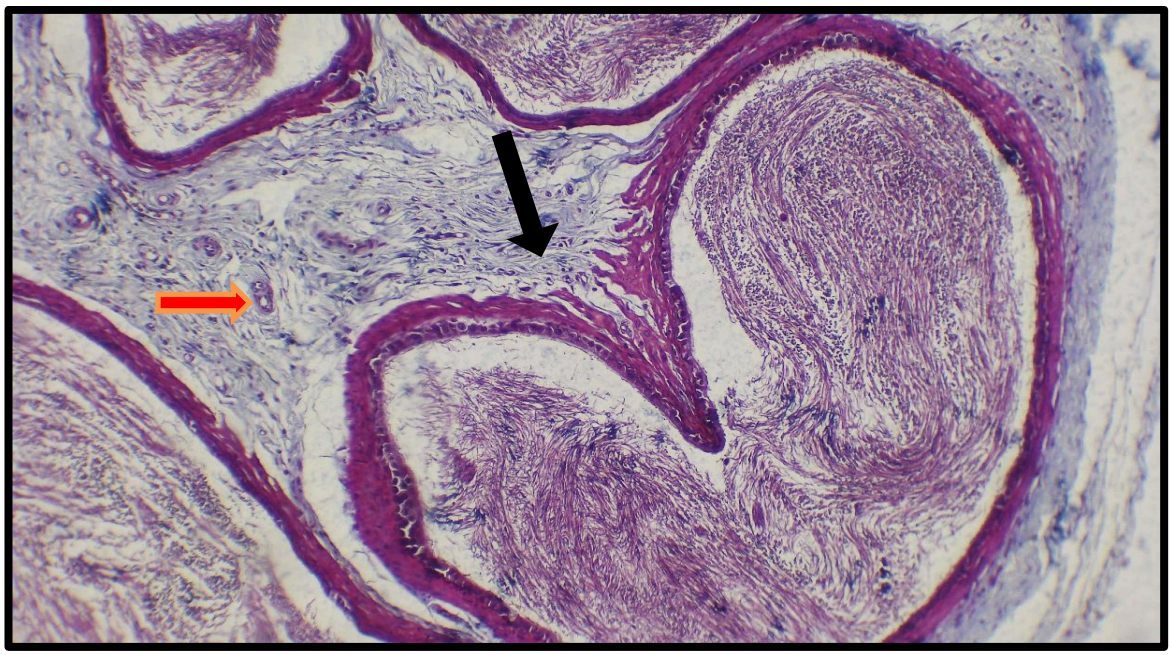

Figure (4-33): Histological section of the epididymis from **mixed treatment group** at 50 days post-exposure, showed marked fibrosis in tunica Albuginea and proliferation of collagen fibers surrounding the epididymal ducts **(black arrow)** and small blood vessels stained with blue color **(red arrow), (Masson Trichrome stain 40 X).**

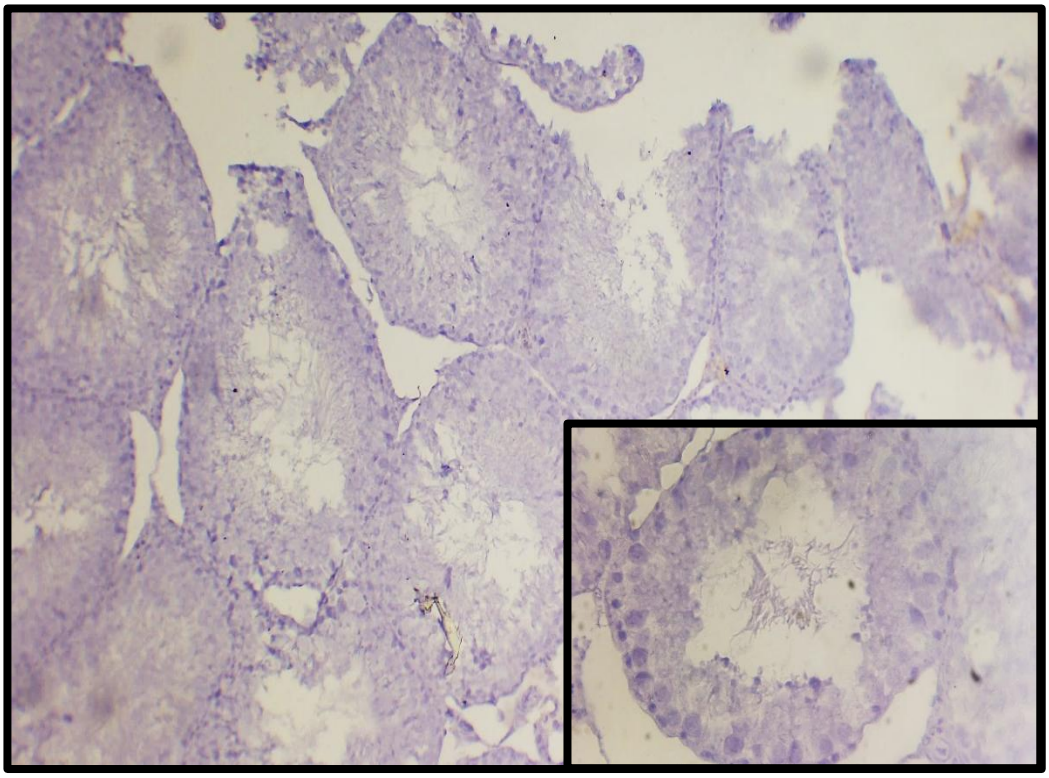

Figure (4-34): Immunohistochemistry analysis of MDA in formalin fixed testis sections **from the normal control** rats at day 50 of experiment. Representative photomicrographs showing no immune reactive cells in the negative control without primary antibody. (Negative MDA immunostaining 40 X +10 X)

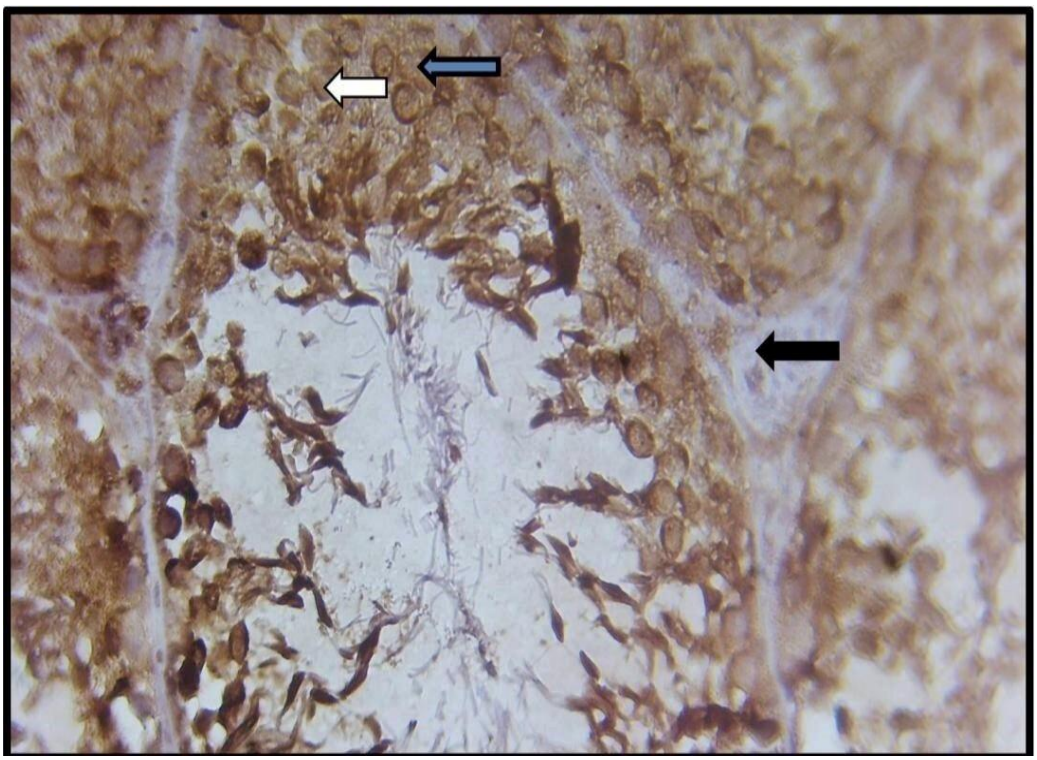

Figure (4-35): Immunohistochemistry analysis of MDA in formalin fixed testis sections **from the normal control** rats at day 50 of experiment. Representative photomicrographs demonstrated the presence of MDA immunoexpression in the spermatogenic **(white arrow),** Sertoli cells **(blue arrow)**in the seminiferous tubules& Leydig cells in the interstitial tissue **(black arrow)** (MDA immunostaining 40 X)

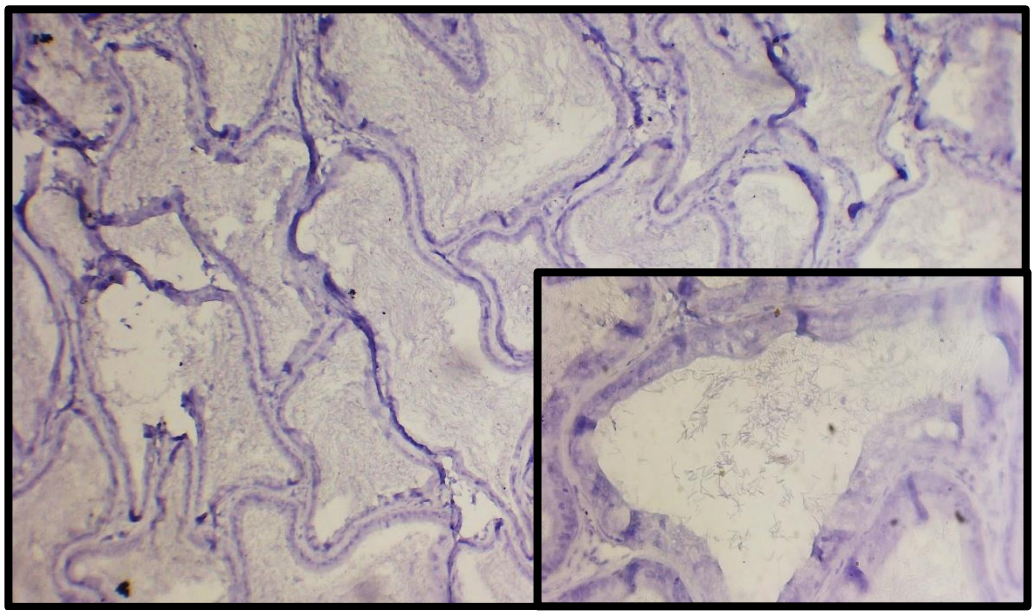

Figure (4-36): Immunohistochemistry analysis of MDA in formalin fixed cauda epididymis sections **from the normal control** rats at day 50 of experiment. Representative photomicrographs showing no (MDA) immunostaining in the negative control without primary antibody. (Negative MDA immunostaining 40 X +10 X).

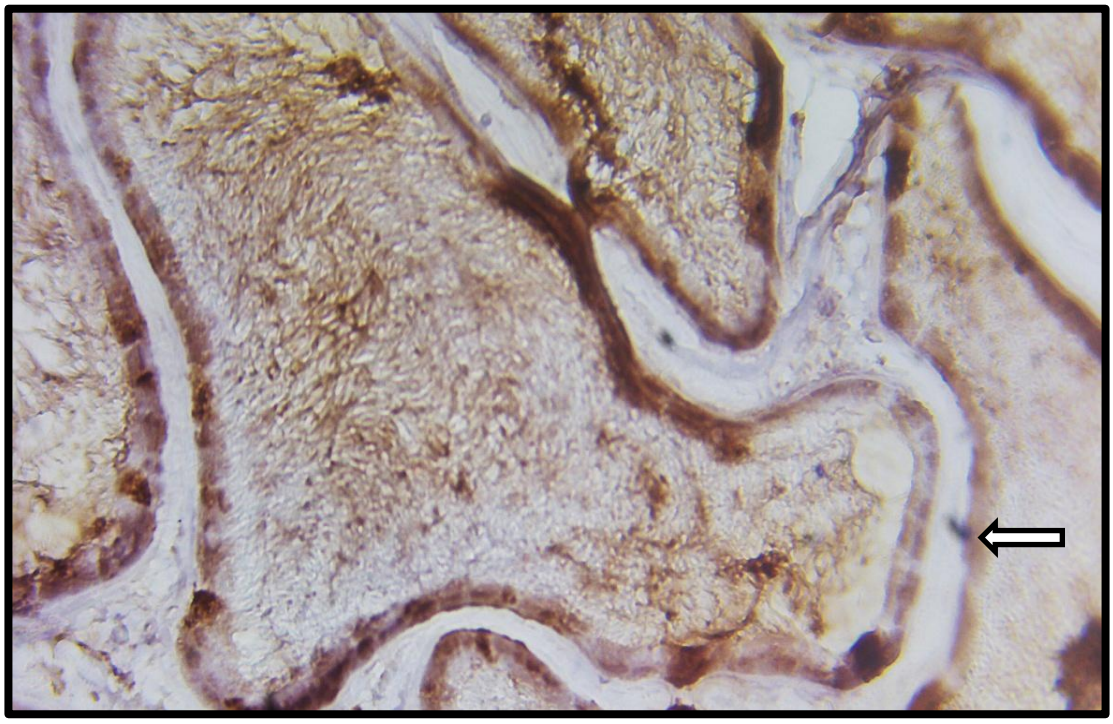

Figure (4-37): Immunohistochemistry analysis of MDA in formalin fixed cauda epididymis sections **from the normal control** rats at day 50 of experiment. Representative photomicrographs demonstrate the presence of MDA in the nuclear and cytoplasm of the epithelial cells lining the epididymal ducts **(white arrow).** (MDA immunostaining 40 X).

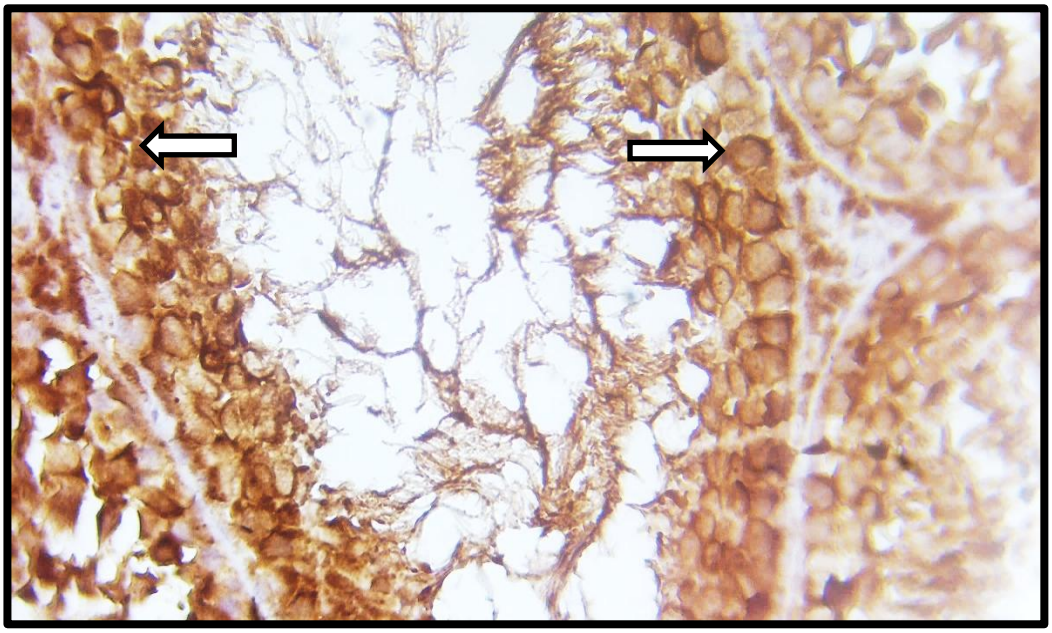

Figure (4-38): Immunohistochemistry analysis of MDA in formalin fixed testis sections **from the sodium group** at day 50 of experiment. Representative photomicrographs showing positive (MDA) immunoexpression in the spermatogenic in the seminiferous tubules **(white arrow).**(MDA immunostaining, 40 X)

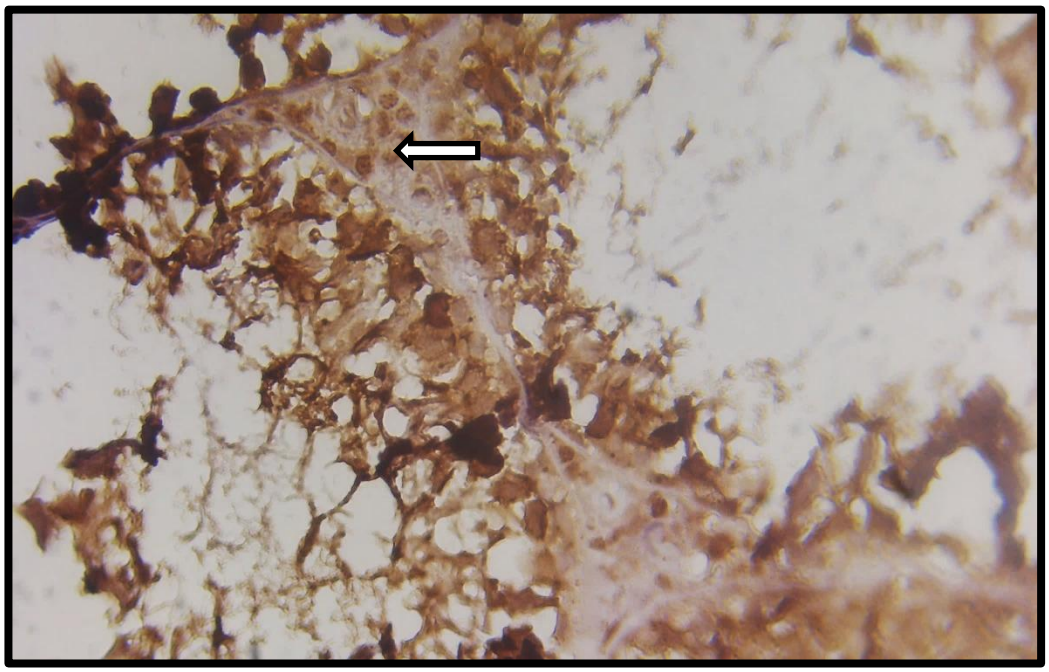

Figure (4-39): Immunohistochemistry analysis of MDA in formalin fixed testis sections **from the sodium group** at day 50 of experiment. Representative photomicrographs showing positive (MDA) immunoexpression in Leydig cells in the interstitial tissue **(white arrow**) (MDA immunostaining 40 X)

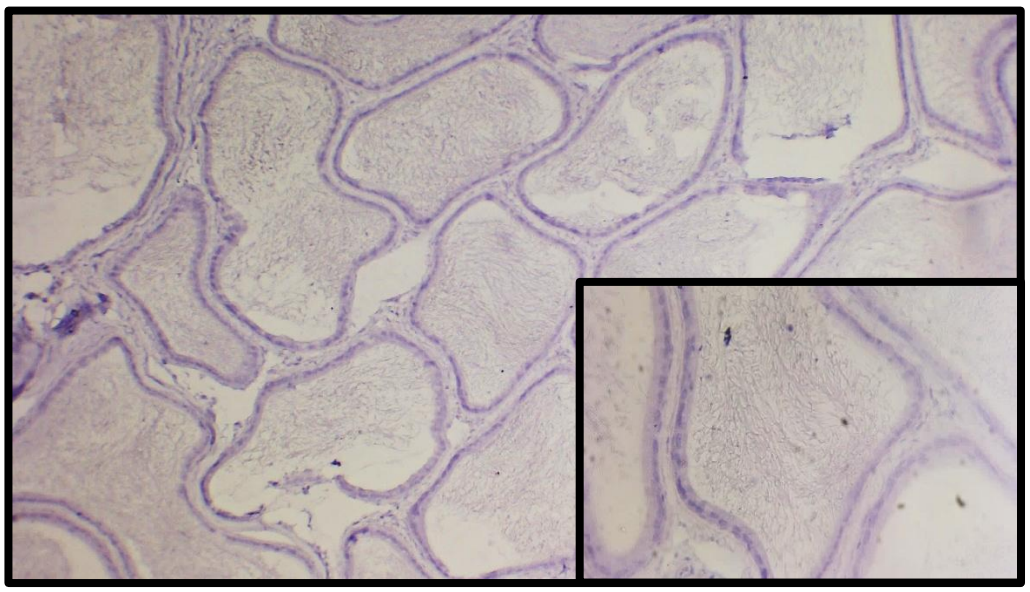

Figure (4-40): Immunohistochemistry analysis of MDA in formalin fixed cauda epididymis **from the sodium group** at day 50 of experiment. Representative photomicrographs showing no (MDA) immunostaining in the negative control without primary antibody. (Negative MDA immunostaining 40 X +10 X).

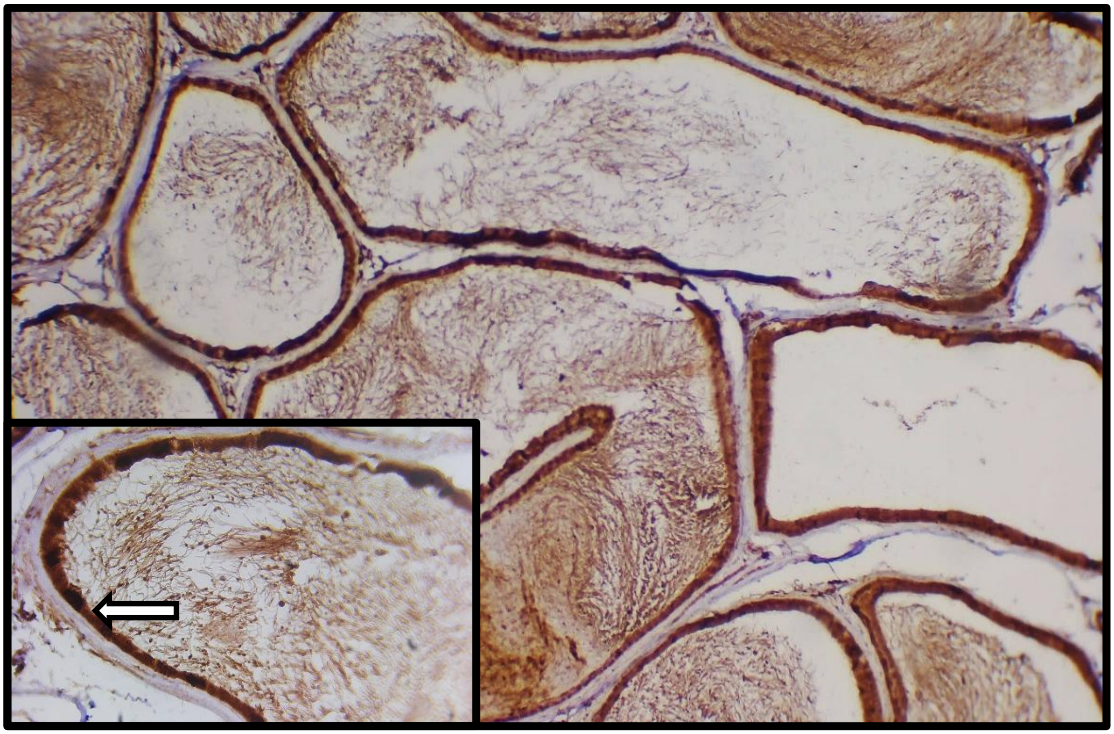

Figure (4-41): Immunohistochemistry analysis of MDA in formalin fixed cauda epididymis **from the sodium group** at day 50 of experiment**.** Representative photomicrographs showing mild nuclear and cytoplasmic MDA immunoreaction in the epithelial cells lining the epididymal ducts**(white arrow).** (MDA immunostaining 10 X +40 X).

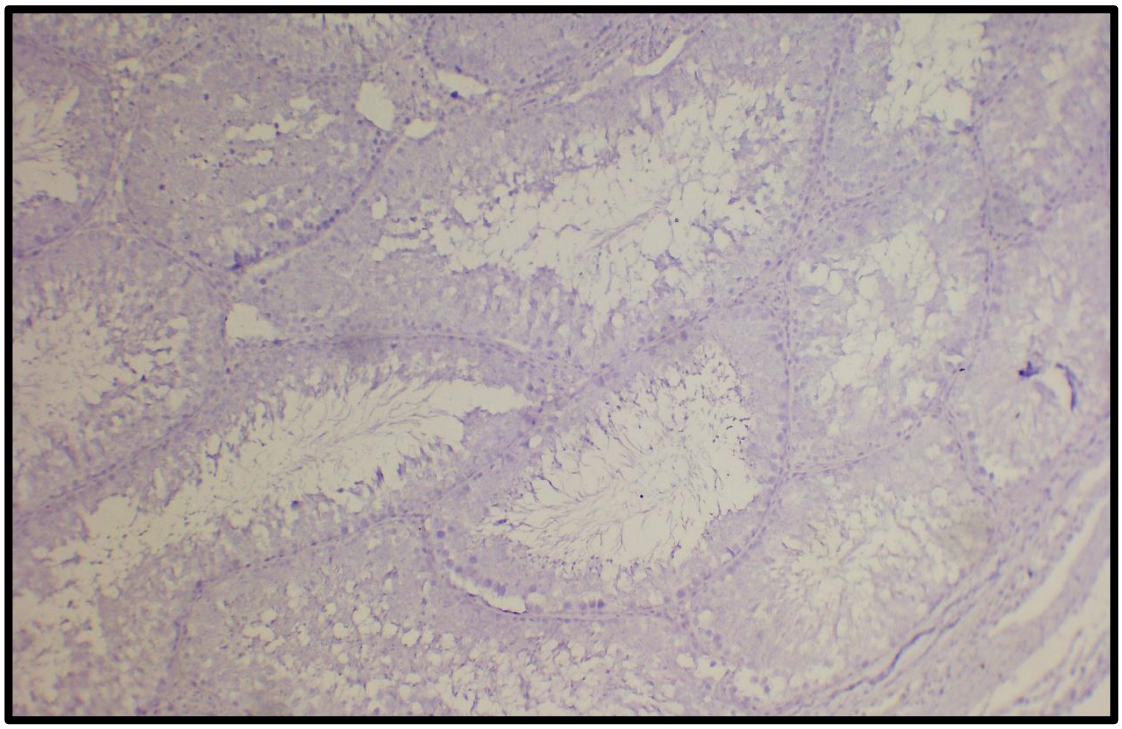

Figure (4-42): Immunohistochemistry analysis of MDA in formalin fixed testis sections **from the pimaricin group** rats at day 50 of experiment. Representative photomicrographs showing no immune reactive cells in the negative control without primary antibody. (Negative MDA immunostaining 10 X)

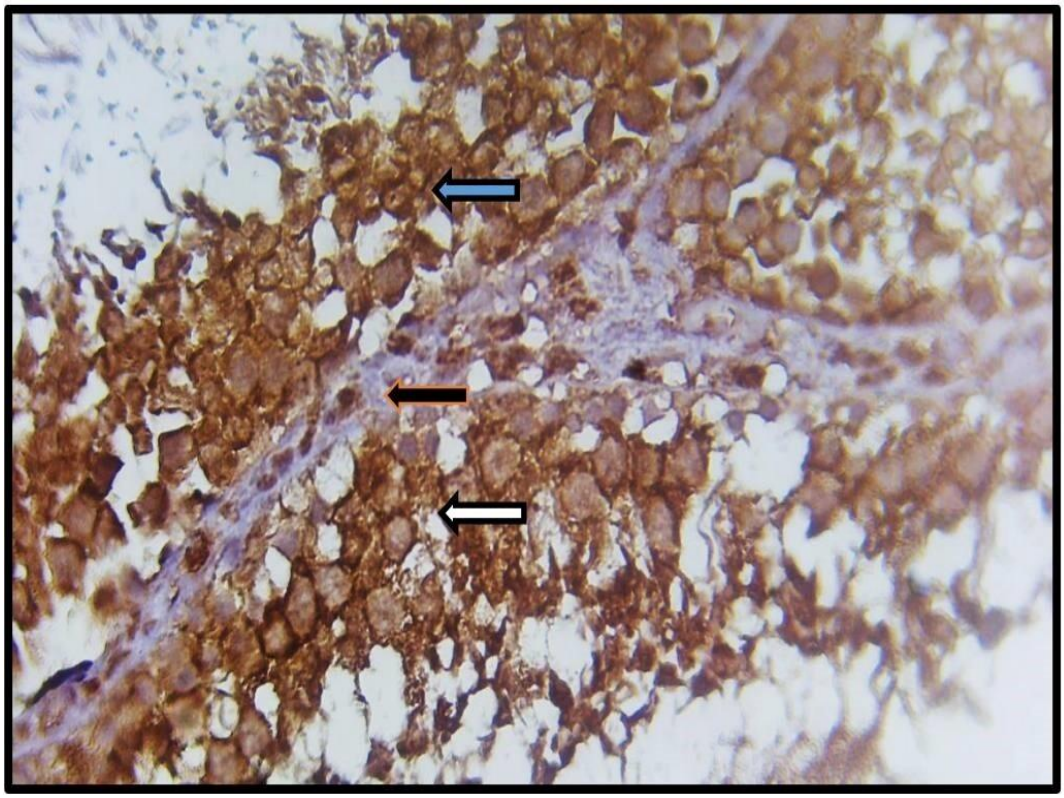

Figure (4-43): Immunohistochemistry analysis of MDA in formalin fixed cauda epididymis **from the pimaricin treated group** at day 50 of experiment. Representative photomicrographs showing mild (MDA) immunoexpression in the spermatogenic **(white arrow)** when compared with other treated group, and moderate reaction Sertoli cells **(blue arrow)** in the seminiferous tubules& Leydig cells in the interstitial tissue **(black arrow**) (MDA immunostaining 40 X)

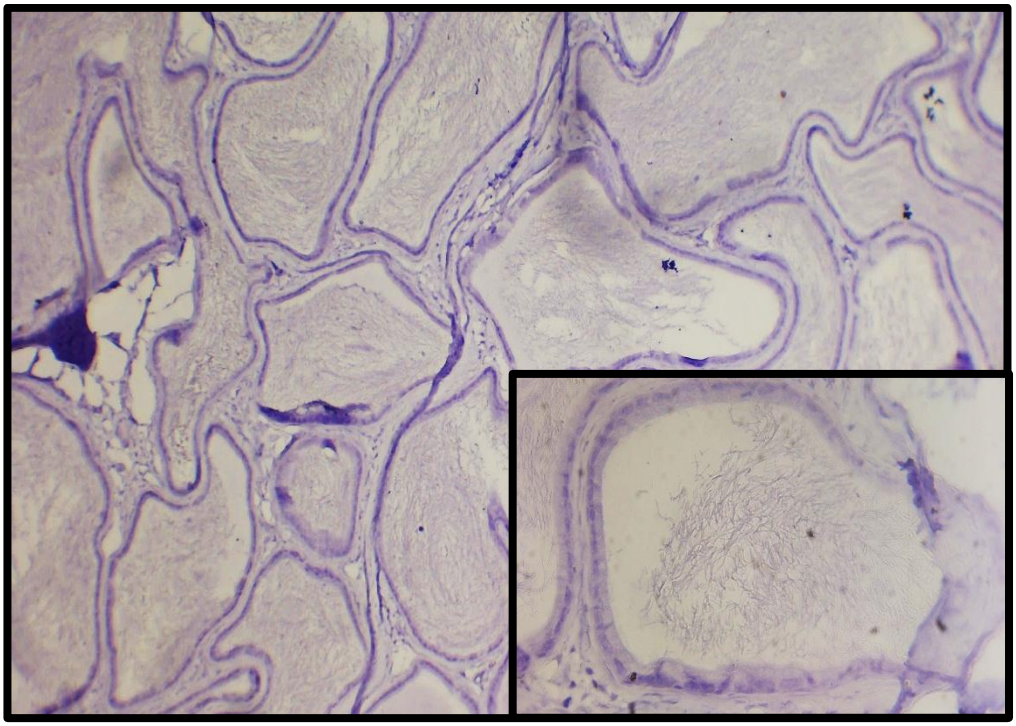

Figure (4-44): Immunohistochemistry analysis of MDA in formalin fixed cauda epididymis **from the pimaricin group** at day 50 of experiment. Representative photomicrographs showing no (MDA) immunostaining in the negative control without primary antibody.**(negative MDA immunostaining 40 X +10 X)**

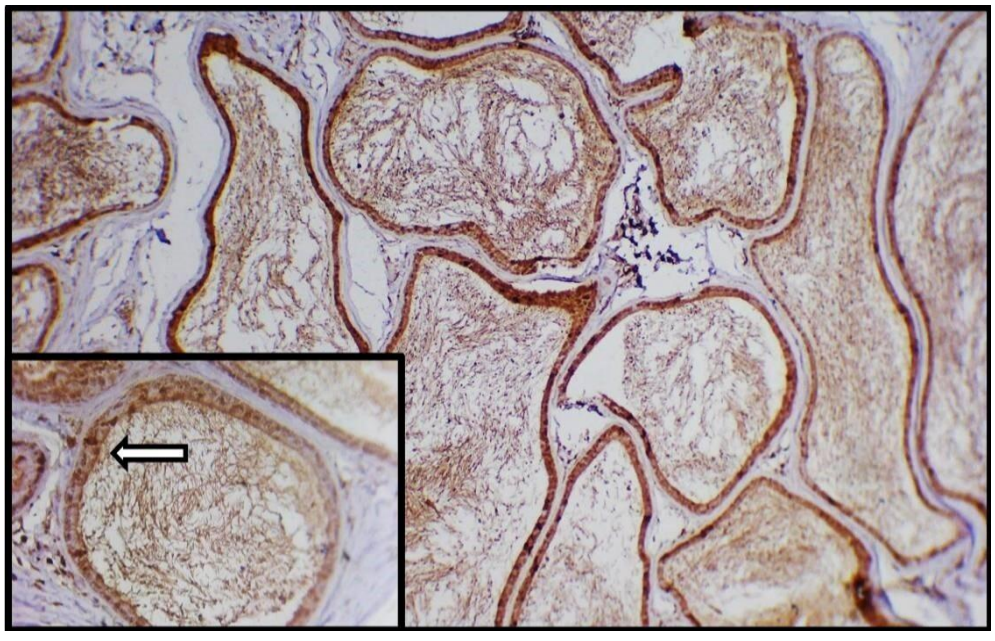

Figure (4-45): Immunohistochemistry analysis of MDA in formalin fixed cauda epididymis **from the pimaricin group** at day 50 of experiment. Representative photomicrographs showing moderate nuclear and cytoplasmic MDA immunoreaction in the epithelial cells lining the epididymal ducts**(white arrow)** when compared with mix group (MDA immunostaining 10 **X** +40 **X**)

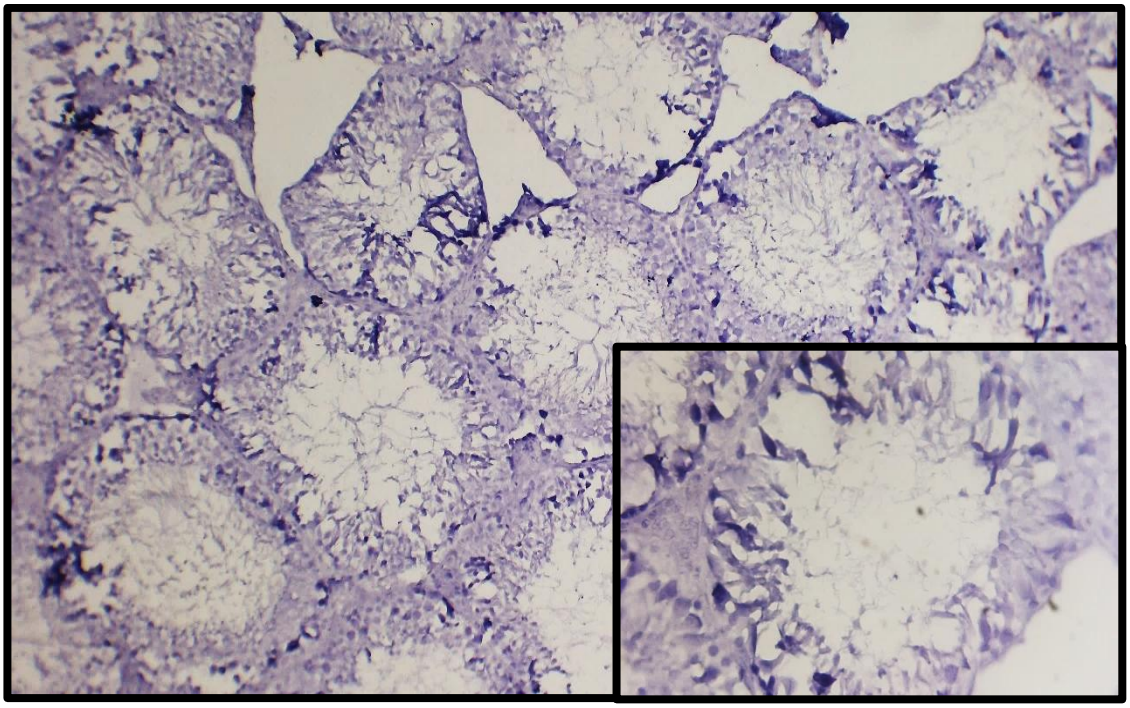

Figure (4-46):Immunohistochemistry analysis of MDA in formalin fixed testis sections **from the mix group (Sodium + Pimaricin)** at day 50 of experiment. Representative photomicrographs showing no immune reactive cell (negative MDA immunostaining) in the negative control without primary antibody. Magnification 40 X +10 X.

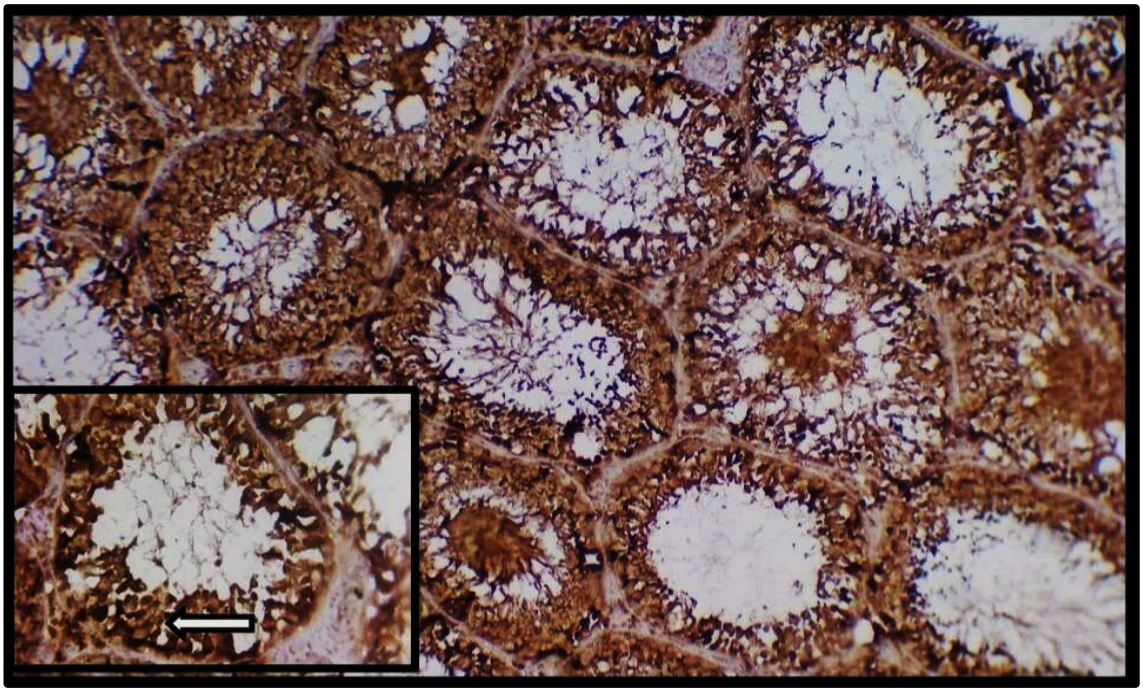

Figure (4-47): Immunohistochemistry analysis of MDA in formalin fixed cauda epididymis **from the mix group (Sodium + Pimaricin)** at day 50 of experiment. Representative photomicrographs showing strong nuclear and cytoplasmic MDA immunoreaction in the epithelial cells lining the epididymal ducts **(white arrow). (** Magnification 10 X +40 X).

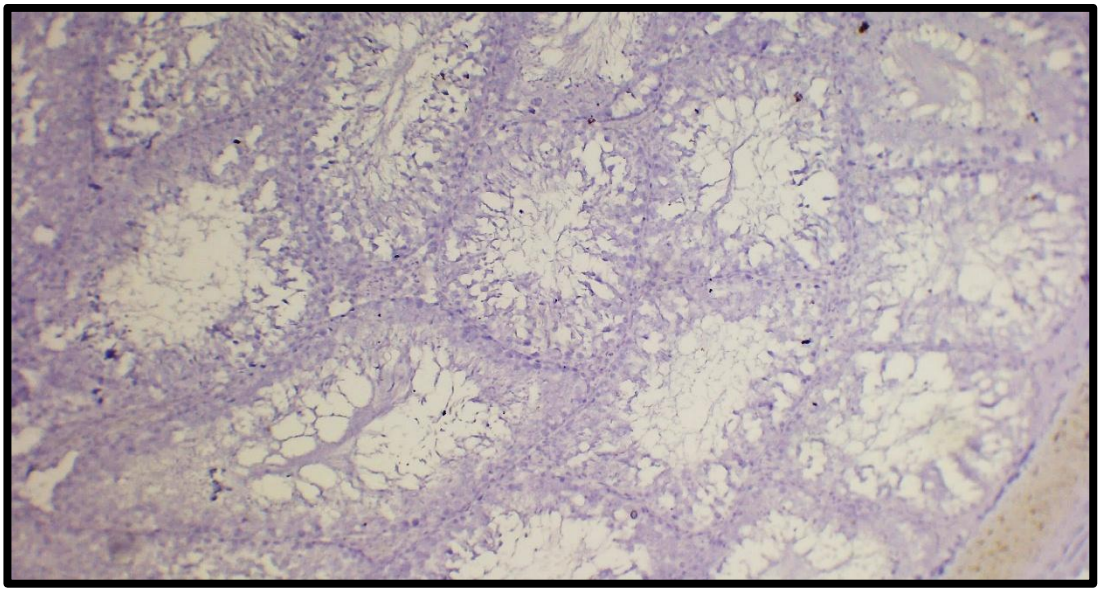

Figure (4-48): Immunohistochemistry analysis of MDA in formalin fixed testis sections **from the mix group (Sodium + Pimaricin)** at day 50 of experiment. Representative photomicrographs showing no (MDA) immunostaining in the negative control without primary antibody. Magnification 10 X.

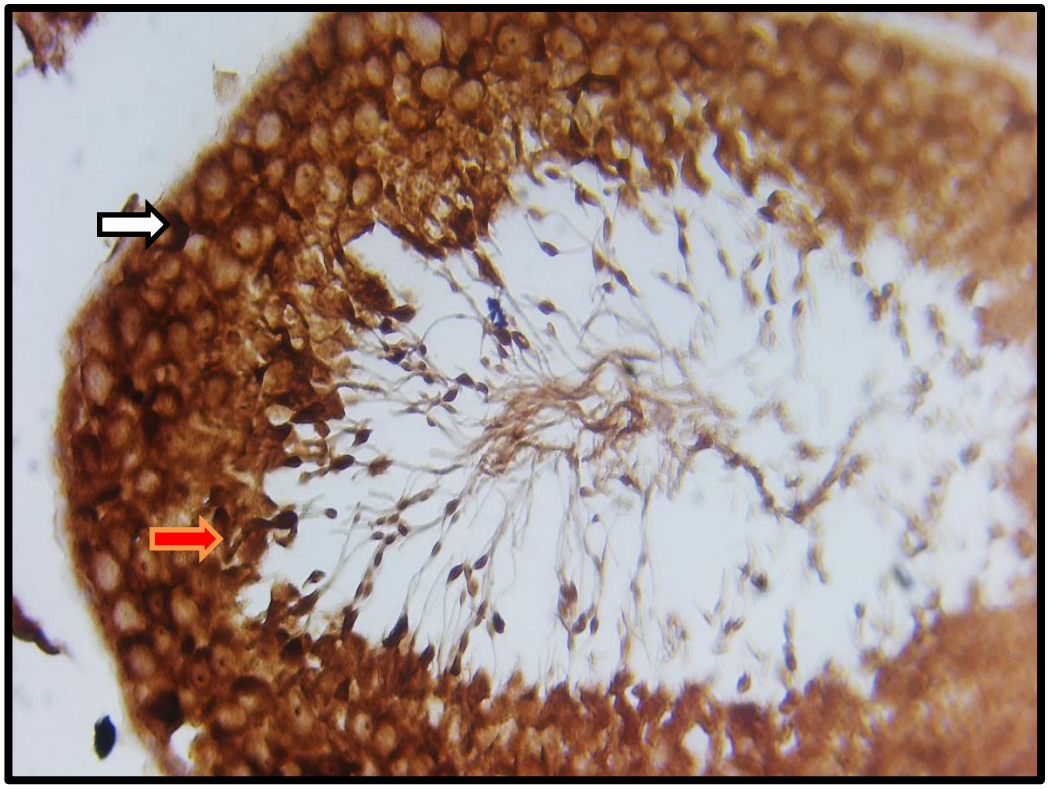

Figure (4-49): Immunohistochemistry analysis of MDA in formalin fixed testis sections **from the mix group (Sodium + Pimaricin)** at day 50 of experiment. Representative photomicrographs showing strong nuclear and cytoplasmic positivity staining for MDA in germ cells **(red arrow**) & Sertoli cells **(white arrow)** in seminiferous ducts. Magnification 40 X).

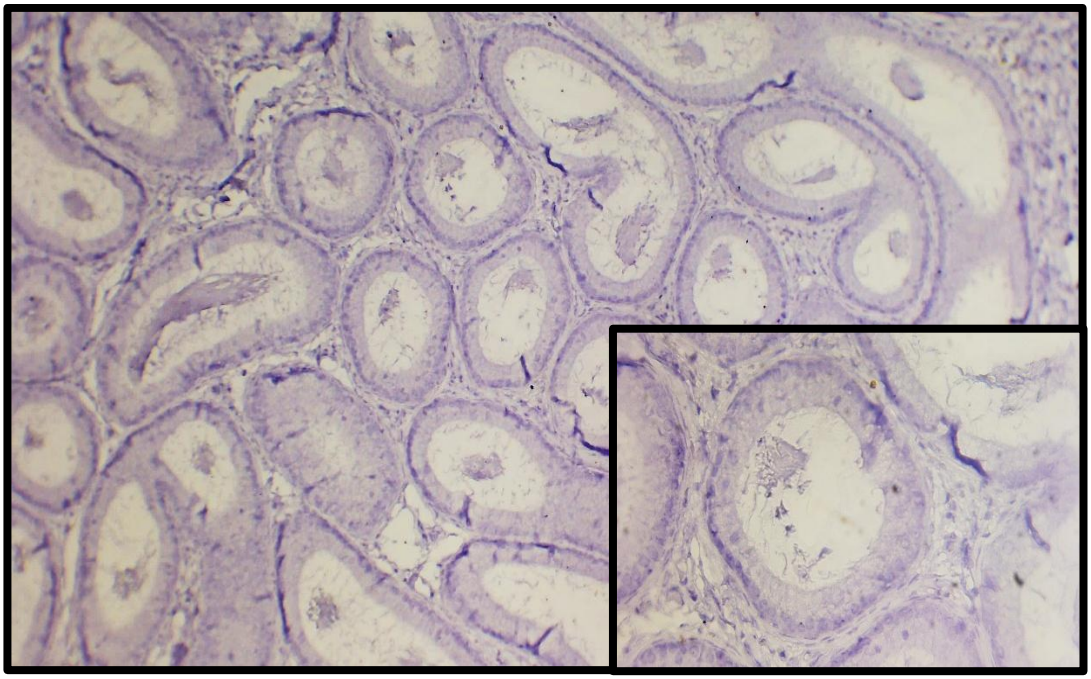

Figure (4-50): Immunohistochemistry analysis of MDA in formalin fixed cauda epididymis **from the mix group (Sodium + Pimaricin)** at day 50 of experiment. Representative photomicrographs showing no (MDA) immunostaining in the negative control without primary antibody. (Magnification 10X +40X).

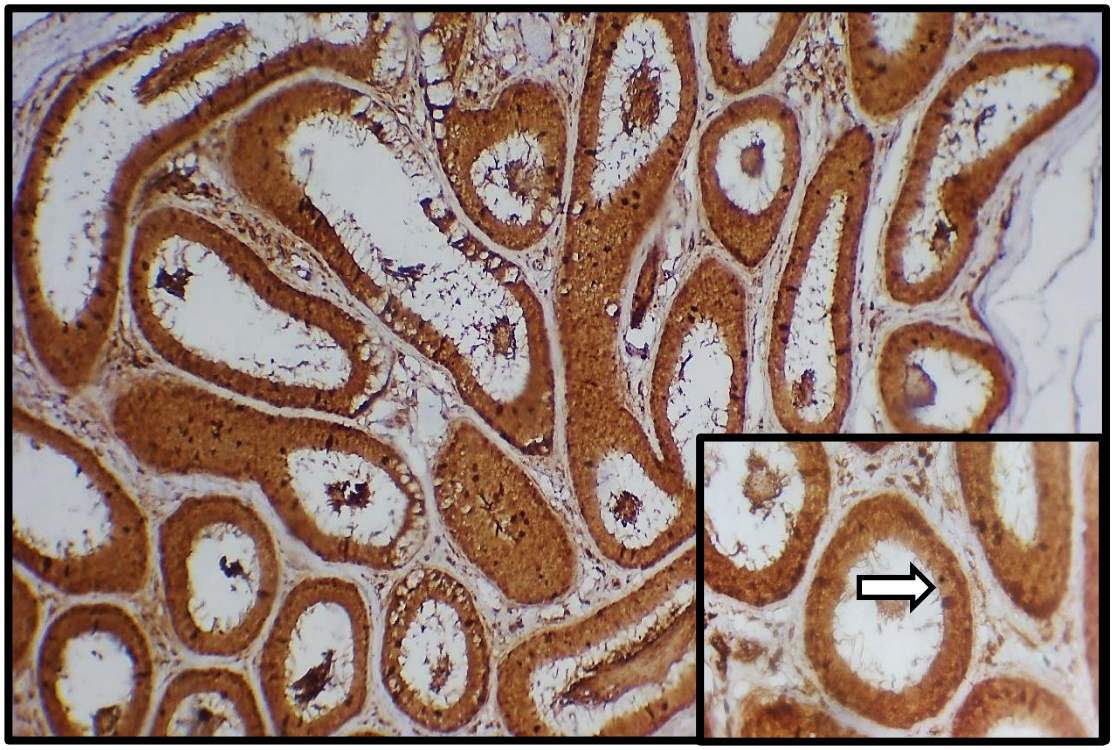

Figure (4-51): Immunohistochemistry analysis of MDA in formalin fixed cauda epididymis **from the mix group (Sodium + Pimaricin)** at day 50 of experiment. Representative photomicrographs showing strong nuclear and cytoplasmic MDA immunoreaction in the epithelial cells lining the epididymal ducts **(white arrow).** Magnification 10 X +40 X.

Discussion

The our finding results of histological pattern in control group majority of the tissues in the epididymal tubules, that's mean these tubules appeared normal in their architecture and clearly displayed a packet mass of spermatozoa in their lumen. The testicular parenchyma was composed of packed, well organized seminiferous tubules and separated by narrow interstitial that contained clusters of interstitial cells and blood vessels. These results are in agreement with those of **(El Gharabawy *et al.*, 2019) .** The our finding result these tubules were surrounded by thin and regular abasement membrane formed of connective tissue fibers and myoid cells and lined by stratified germinal epithelium including many layers of spermatogenic cells and Sertoli cells. The same results were reported by **Singh (2011).** So the spermatogenic cells in our result included: spermatogonia, primary spermatocytes, spermatids and spermatozoa. Spermatogonia were of different types and resting on thin and regular basement membrane. These results are in concomitant with those described by **(El-azab and El-mahalaway, 2019)**. The basement membrane is considered as a nutritional and functional support for both germ and somatic Sertoli cell.

Our results of histochemical study with PAS stain in control group in the testis and epididymis showed tunica albuginea &basement membrane gave positive reaction and stained purplish color & vivd positive reaction for elongated spermatids with acrosomal caps in some developing spermatids . The basal lamina of the epididymal ducts give pronounced PAS substance reaction and stained more purplish with intact thin apical PAS reaction in the lining epithelial cells The same results were reported by **(Hasanin *et al.*, 2018)** they showed PAS‑stained sections of the testicles of the control rats

showed intense magenta red (PAS + ve) material in the basement membrane of the seminiferous tubules. The nuclei of early spermatids showed + ve PAS's particles at one pole. They were recognized as the acrosomic vesicles. Numerous elongated spermatids were observed attached to the apex of Sertoli cell with strong PAS +ve reaction.

PAS-stained sections from control group showed a dense characteristic magenta red PAS reaction in the basal laminae of the epididymal ducts associated with intact thin apical PAS reaction in the lining epithelial cells **(Elbakry and Ibrahim, 2019).** control groups showing mild deposition of collagen fibers in the capsule (tunica albuginea), epididymal tubules, interstitial space and basal lamina .The same results were obtained by **(Qasim and Numman Waheed, 2023)** they reported marked deposition of collagen fibers in the capsule the collagen fibers with corrugation epididymal tubules, interstitial spaces and basal lamina.

Histological examination of testicular tissues in sodium benzoate revealed thrombus and congestion formation with degenerative, necrosis of spermatic cells, with a reduction in interstitial Leydig cells. These results support the findings of some previous researcher **(Hadi and Mahdi, 2019)** have shown that administration of sodium benzoate could alter the testicular architecture of testicular characterized by slight congestion in the interstitial tissue with thrombus, and atrophy in some seminal tissues.

Additionally, the sperm follicles exhibited reduced numbers of primary and secondary sperm cells. Leydig cells appear in very few numbers in the interstitial testicular tissue and blood vessels of the interstitial tissue showed signs of thrombus formation and edema in interstitial tissue & the sub tunica albuginea. These our findings are consistent with those reported

by **(Azouz, el al.,, 2023)** who observed mild congestion in the interstitial and tunica albuginea blood vessels accompanied by mild interstitial edema, slight testicular degeneration in a few seminiferous tubules,

The histological sections of the epididymis sodium benzoate treated groups revealed an increase of interstitial tissue containing mononuclear inflammatory cell. This observation was also detected in a previous study by **(Elbakry and Ibrahim, 2019).** who documented the presence of inflammatory cell infiltration and interstitial changes in the epididymal tissue. During this study, abnormal number of sperms was also detected in the lumen, with degeneration of lining epithelia, detachment of stereocilia and vascular congestion these results aligh with those of (**Azouz, el al.,, 2023**)who reported vacuolar degeneration in few epithelial cells lining epididymal tubules with mild interstitial edema and congestion.

our results staining of The basement membrane and apical parts of the lining epithelial cells suggested increased glycoprotein content and possible cellular stress. was also detected in a previous study by **(Elbakry and Ibrahim, 2019)** reported a strong PAS reaction in the basal laminae of the epididymal ducts with intact thin apical PAS reaction in the lining epithelial cells.

Pimaricin, a polyene macrolide antifungal agent widely used in the food and pharmaceutical industries **(Meena *et al.*, 2021),** is generally regarded as safe due to its poor gastrointestinal absorption**.** However, the chronic effects of low-dose systemic exposure, particularly on reproductive organs, remain poorly understood.

Our findings demonstrate that prolonged intake of pimaricin-containing food induces significant degenerative changes in the testis and epididymis,

suggesting a potential risk to male fertility. These changes are similar to those reported in other toxicological studies, where exposure to environmental toxins led to similar testicular dysfunction such as those by **(Mathur, Saradha and Vaithinathan, 2008),**who reported that exposure to environmental toxins induces testicular damage through steroidogenesis inhibition and oxidative stress, leading to impaired male fertility.

These findings align with our results showing pimaricin-induced degenerative changes in the testis and epididymis.

Our result showed that testicular toxicity, resulting in structural disruption of seminiferous tubules and impaired spermatogenesis, is a common outcome of exposure to various chemicals and environmental pollutants.

The main testicular observation showed clear increase in fibrosis evidenced by stained blue color in the tunica Albuginea and surrounding the epididymal ducts. This result aligns with other findings **(Qasim and Numman Waheed, 2023)** They investigated the impact of monosodium glutamate on mature male albino rats' epididymis. According to the study, seminiferous tubules were packed with connective tissue that contained blood vessels, clusters of Leydig cells, and a sharp rise in collagen fibers around the epididymal ducts. The masson trichrome stain was used to color the tunica albuginea blue. The identical outcomes were reported by **(El Gharabawy *et al.*, 2019),** showed that interstitial cells of Leydig were rounded or polygonal in shape with acidophilic cytoplasm and rounded or oval vesicular nuclei.

The Mix group showed an irregular arrangement of tubules with increased thickness of basement membrane .This result is consistent with **(Hadi and Mahdi, 2019)** who reported an irregular arrangement of tubules surrounded by stroma with the reduced epithelium. The main features of

fibrotic disorders affecting the testis and epididymis are thickening of the basement membrane and excessive extracellular matrix protein deposition. This finding is supported by what is stated by **(Faddladdeen, Murad and Ali, 2019)**and **(Sardar *et al.*, 2023)** who reported that such pathological changes are often associated with chronic inflammation and oxidative stress, which in turn stimulate fibroblast activation and collagen synthesis. These alterations can impair spermatogenesis and disrupt the normal architecture of the seminiferous tubules and epididymal ducts, ultimately leading to compromised male fertility

additionally, the current study also found a reduced PAS reaction in the apical regions of the epididymal epithelial cells, which may be attributed to the loss of the pseudostratified epithelium lining the epididymis. In contrast **(Jarjees, 2022)** reported a strong PAS reaction in the basal laminae of the epididymal tubules, along with a thin but intact apical PAS reaction in the lining epithelial cells.

Our results, showed marked collagen fiber deposition within the epididymal tubules, basal lamina, and interstitial spaces. Additionally, the basal lamina, tunica albuginea, and interstitial cells exhibited a strong PAS reaction. These findings are consistent with the results reported by several previous investigators**. (Qasim and Numman Waheed, 2023)** , who showed basal lamina and interstitial cells in the MSG, MSG +Vit.C, and MSG +Vit.E groups showed a high PAS reaction. The also reported increase inexpression and thickening of tunica albuginea and basement membrane, as evidenced by a positive PAS reaction and thickening of these structures in the testis**. (El Gharabawy *et al.*, 2019)** reported robust PAS-positive responses in the thickened and irregular basement membrane, interstitial, and thickened vascular walls in the group intoxicated with cyclophosphamide.

Masson trichrome-staining section, of epididymis demonstrated varying degrees of collagen fiber deposition among the study groups. The mix treated group exhibited the most extensive accumulation of collagen fiber was observed in the mix treated group followed by the pimaricin treated group with sodium benzoate group showing a comparatively lower extent collagen deposition was localized in the capsule (tunica albuginea), epididymal tubules, interstitial space and basal lamina in all treated group. While the control group exhibited minimal collagen presence indication normal histological structure these findings are in agreement with the reported by **(Qasim and Numman Waheed, 2023)** they documented marked deposition of collagen fibers in tunica albuginea along with corrugation of surrounding epididymal tubules interstitial spaces and basal lamina .

Administration of antioxidant influenced the severity of collagen deposition.this suggested potential protective effect of combined antioxidant therapy against fibrosis the observed fibrotic changes may contribute to structural alterations and shrinkage of seminiferous and epididymal tubules, possibly impairing reproductive function These findings are in agreement with **(Sarhan, 2018)** who suggested that the cause of this fibrosis is due to oxidative stress and the formation of ROS which can induce the transformation of fibroblasts to myofibroblasts and increase the deposition of collagen fibers in liver, kidney, and testicular tissues. While **(Sabour and Ibrahim, 2019)** attributed the cause of fibrosis to the diminished production of glutathione peroxidase.

Chapter Five

Conclusions and Recommendations

Conclusion

This study demonstrates that exposure to sodium benzoate and pimaricin, individually and in combination, induces significant histopathological and oxidative changes in the testicular and epididymal tissues of adult male albino rats.

While sodium benzoate caused mild degenerative and inflammatory changes, pimaricin led to more pronounced tissue damage, including fibrosis and necrosis. The combined exposure resulted in the most severe effects, indicating a potential synergistic toxicity.

Immunohistochemical analysis using MDA staining confirmed elevated oxidative stress levels, particularly in the mix-treated group.

Moreover, hormonal evaluation revealed a marked reduction in serum LH and FSH levels, reflecting impaired hypothalamic–pituitary–gonadal axis function and contributing to the observed disruption of spermatogenesis.

These findings suggest that chronic intake of these food additives, especially in combination, may pose a significant risk to male reproductive health.

Recommendations

• Reassess the safety limits of sodium benzoate and pimaricin for long-term use, especially regarding reproductive health.

• Encourage further research on dose-dependent effects, reversibility of tissue damage, and the protective strategies like antioxidants.

• Promote the use of safer, natural alternatives to these additives in food and pharmaceuticals.

• Increase public awareness of potential reproductive risks through education and improved product labeling

References

References

European Food Safety Authority (EFSA) (2009) Scientific Opinion on the use of natamycin (E 235) as a food additive. EFSA Journal, 7(12), p.1412. Wiley Online Library.

European Food Safety Authority (EFSA) (2010) Scientific Opinion on the use of Basic Methacrylate Copolymer as a food additive. EFSA Journal, 8(2), p.1513. Wiley Online Library.

Adelakun, S. A. *et al.* (2019) 'Nitrite-induced testicular toxicity in rats: Therapeutic potential of walnut oil', *Jornal Brasileiro de Reproducao Assistida*, 23(1), pp. 15–23. doi: 10.5935/1518-0557.20180062.

Afshar, M. *et al.* (2012) 'Effect of long term consumption of sodium benzoat before and during pregnancy on growth indexes of fetal balb/c mice'. MODERN CARE JOURNAL.

Afshar, M. *et al.* (2014) 'Fetal malformations due to long term consumption of Sodium Benzoate in pregnant balb/c mice', *AJPT*, 2, pp. 1–7.

Agarwal, A. *et al.* (2016) 'Histological profile of liver of albino rats on oral administration of sodium benzoate', *J. Anat. Sci*, 24(2), pp. 29–32.

Al-Shelash, A. A. and Gomaa, H. F. (2023) 'Research Article Prospective Effect of Nano-Selenium Particles on Thyroid Dysfunction and Oxidative Stress Induced by Sodium Benzoate in Male Albino Rats'.

Alabi, O. A. *et al.* (2022) 'Comparative study of the reproductive toxicity and modulation of enzyme activities by crude oil-contaminated soil before and after bioremediation', *Chemosphere*. Elsevier, 299, p. 134352.

Altunkaynak, P. and Avuloglu-Yilmaz, E. (2024) 'Analysis of genotoxic effects of food preservatives sodium acetate (E262) and sodium sulfite (E221) in human lymphocytes', *Food Science and Biotechnology*. Springer, pp. 1–10.

Arima, A. A. *et al.* (2014) 'The negligible effects of the antifungal natamycin on cholesterol-dipalmitoyl phosphatidylcholine monolayers may explain its low oral and topical toxicity for mammals', *Colloids and Surfaces B: Biointerfaces*. Elsevier, 122, pp. 202–208.

Asejeje, F. O. *et al.* (2022) 'Sodium benzoate induces neurobehavioral deficits and brain oxido-inflammatory stress in male Wistar rats: Ameliorative role of ascorbic acid', *Journal of Biochemical and Molecular Toxicology*, 36(5).

Azouz, R. A., Korany, R. M. S. and Noshy, P. A. (2023) 'Silica Nanoparticle-Induced Reproductive Toxicity in Male Albino Rats via Testicular Apoptosis and Oxidative Stress.', *Biological trace element research*. United States, 201(4), pp. 1816–1824. doi: 10.1007/s12011-022-03280-w.

Bancroft, J. D. and Gamble, M. (2008) *Theory and practice of histological techniques*. Elsevier health sciences.

Bielohuby, M., Popp, S. and Bidlingmaier, M. (2012) 'A guide for measurement of circulating metabolic hormones in rodents: Pitfalls

during the pre-analytical phase', *Molecular Metabolism*. Elsevier, 1(1–2), pp. 47–60. doi: 10.1016/j.molmet.2012.07.004.

De Boer, E. and Stolk-Horsthuis, M. (1977) 'Sensitivity to natamycin (pimaricin) of fungi isolated in cheese warehouses', *Journal of food protection*. Elsevier, 40(8), pp. 533–536.

Brik, H. (1994) 'Natamycin (supplement)', in *Analytical Profiles of Drug Substances and Excipients*. Elsevier, pp. 399–419.

Caldinelli, L. *et al.* (2010) 'Effect of ligand binding on human D-amino acid oxidase: implications for the development of new drugs for schizophrenia treatment', *Protein Science*. Wiley Online Library, 19(8), pp. 1500–1512.

Cedillo-Olivos, A. E. *et al.* (2024) 'Natural preservatives used in foods: a review.', *Critical reviews in food science and nutrition*. United States, pp. 1–17. doi: 10.1080/10408398.2024.2403000.

Cinar, A. and Onbaşı, E. (2019) 'Mycotoxins: The hidden danger in foods', *Mycotoxins and food safety*. IntechOpen Boston, MA, pp. 1–21.

Creasy, D. M. (2001) 'Pathogenesis of male reproductive toxicity', *Toxicologic pathology*. Sage Publications Sage CA: Los Angeles, CA, 29(1), pp. 64–76.

Dalhoff, A. A. H. and Levy, S. B. (2015) 'Does use of the polyene natamycin as a food preservative jeopardise the clinical efficacy of amphotericin B? A word of concern', *International Journal of Antimicrobial Agents*. Elsevier, 45(6), pp. 564–567.

Davidson, P. M., Sofos, J. N. and Branen, A. L. (2005) *Antimicrobials in food*. CRC press.

Davoodi, F. *et al.* (2021) 'Leech therapy (Hirudo medicinalis) attenuates testicular damages induced by testicular ischemia/reperfusion in an animal model', *BMC Veterinary Research*. BMC Veterinary Research, 17(1), pp. 1–15. doi: 10.1186/s12917-021-02951-5.

Debbasch, C. *et al.* (2001) 'Quaternary ammoniums and other preservatives' contribution in oxidative stress and apoptosis on Chang conjunctival cells', *Investigative ophthalmology & visual science*. The Association for Research in Vision and Ophthalmology, 42(3), pp. 642–652.

DÖHLER, K. D. and WUTTKE, W. (1974) 'Serum LH, FSH, prolactin and progesterone from birth to puberty in female and male rats', *Endocrinology*. Oxford University Press, 94(4), pp. 1003–1008.

El-azab, N. E. and El-mahalaway, A. M. (2019) 'A Histological and Immunohistochemical Study on Testicular Changes Induced by Sliver Nanoparticles in Adult Rats and the Possible Protective Role of Camel Milk', pp. 1044–1058.

El-Shennawy, L. *et al.* (2020) 'Dose-dependent reproductive toxicity of sodium benzoate in male rats: Inflammation, oxidative stress and apoptosis', *Reproductive Toxicology*. Elsevier, 98, pp. 92–98.

Elbakry, R. H. and Ibrahim, M. A. (2019) 'Histological, immunohistochemical and biochemical study of the effect of triclosan and its withdrawal on cauda epididymis of adult albino rat', *Egyptian Journal of Histology*. Egyptian Society of Histology and Cytology in Cooperation with The Egyptian …, 42(1), pp. 84–

98.

Emon, S. T. *et al.* (2015) ‘Effects of the popular food additive sodium benzoate on neural tube development in the chicken embryo.’, *Turkish Neurosurgery*, 25(2), pp. 294–297.

Faddladdeen, K. A., Murad, H. A. and Ali, S. S. (2019) ‘Improved histoarchitectural changes with angiotensin receptor blockers in early testicular and cauda toxicity in rats’, *International Journal of Morphology*, 37(2), pp. 515–521.

Food and Drug Administration, H. H. S. (2016) ‘Food additives permitted for direct addition to food for human consumption; folic acid. Final rule’, *Federal register*, 81(73), pp. 22176–22183.

Foot, N. C. (1933) ‘The Masson trichrome staining methods in routine laboratory use’, *Stain technology*. Taylor & Francis, 8(3), pp. 101–110.

Fujitani, T. (1993) ‘Short-term effect of sodium benzoate in F344 rats and B6C3F1 mice’, *Toxicology letters*. Elsevier, 69(2), pp. 171–179.

El Gharabawy, G. S. *et al.* (2019) ‘Histological and immunohistochemical study of the effect of cyclophosphamide on testis of male adult albino rats and the possible protective role of vitamin E’, *The Egyptian Journal of Hospital Medicine*. Pan Arab League of Continuous Medical Education, 77(6), pp. 5930–5946.

Hadi, M. M. and Mahdi, W. T. (2019) ‘I NTERNATIONAL J OURNAL OF R ESEARCH IN’, 10(1), pp. 98–105.

Hasanin, N. A. *et al.* (2018) 'Histological and ultrastructure study of the testes of acrylamide exposed adult male albino rat and evaluation of the possible protective effect of vitamin E intake', *Journal of microscopy and ultrastructure*. Medknow, 6(1), pp. 23–34.

Hu, Z. *et al.* (2018) 'Effects of natamycin on growth performance, serum biochemical parameters and antioxidant capacity in broiler chickens', *Pakistan Journal of Zoology*. AsiaNet Pakistan (Pvt) Ltd., 50(3), pp. 969–976.

Ibekwe, S. E., Uwakwe, A. A. and Monanu, M. O. (2007) 'In vivo effects of sodium benzoate on plasma aspartate amino transferase and alkaline phosphatase of wistar albino rats', *Sci. Res. Essays*, 2, pp. 10–12.

Jarjees, E. H. (2022) 'Iraqi Journal of Veterinary Sciences Effect of sodium benzoate on some biochemical , physiological and histopathological aspects in adult male rats', 36(2), pp. 267–272. doi: 10.33899/ijvs.2021.129935.1705.

Jewo, P. I. *et al.* (2020) 'Histological and biochemical studies of germ cell toxicity in male rats exposed to sodium benzoate', *J. Adv. Med. Pharm. Sci*, 22, pp. 51–69.

Kehinde, O. S., Christianah, O. I. and Oyetunji, O. A. (2018) 'Ascorbic acid and sodium benzoate synergistically aggravates testicular dysfunction in adult Wistar rats', *International journal of physiology, pathophysiology and pharmacology*. e-Century Publishing Corporation, 10(1), p. 39.

Khan, I. S. *et al.* (2022) ‘Toxicological impact of sodium benzoate on inflammatory cytokines, oxidative stress and biochemical markers in male Wistar rats’, *Drug and Chemical Toxicology*. Taylor & Francis, 45(3), pp. 1345–1354.

Khodaei, F. *et al.* (2019) ‘Effect of sodium benzoate on liver and kidney lipid peroxidation and antioxidant enzymes in mice’, *Journal of Reports in Pharmaceutical Sciences*. Medknow, 8(2), pp. 217–223.

Mahmoud, G. S. *et al.* (2019) ‘Positive effects of systemic sodium benzoate and olanzapine treatment on activities of daily life, spatial learning and working memory in ketamine-induced rat model of schizophrenia’, *International Journal of Physiology, Pathophysiology and Pharmacology*. e-Century Publishing Corporation, 11(2), p. 21.

Maier, E. *et al.* (2010) ‘Food preservatives sodium benzoate and propionic acid and colorant curcumin suppress Th1-type immune response in vitro’, *Food and chemical toxicology*. Elsevier, 48(7), pp. 1950–1956.

Martínez, M. A. *et al.* (2013) ‘Effect of natamycin on cytochrome P450 enzymes in rats’, *Food and chemical toxicology*. Elsevier, 62, pp. 281–284.

Mathur, P. P. and D’cruz, S. C. (2011) ‘The effect of environmental contaminants on testicular function’, *Asian journal of andrology*. Wolters Kluwer--Medknow Publications, 13(4), p. 585.

Mathur, P. P., Saradha, B. and Vaithinathan, S. (2008) 'Impact of environmental toxicants on testicular function', *Immunology, Endocrine & Metabolic Agents in Medicinal Chemistry (Formerly Current Medicinal Chemistry-Immunology, Endocrine and Metabolic Agents)*. Bentham Science Publishers, 8(1), pp. 79–90.

Matsumoto, A. M. *et al.* (1983) 'Reinitiation of sperm production in gonadotropin-suppressed normal men by administration of follicle-stimulating hormone', *The Journal of clinical investigation*. American Society for Clinical Investigation, 72(3), pp. 1005–1015.

Meena, M. *et al.* (2021) 'Natamycin: a natural preservative for food applications-a review.', *Food science and biotechnology*. Korea (South), 30(12), pp. 1481–1496. doi: 10.1007/s10068-021-00981-1.

Merino, G. *et al.* (1999) 'Relationship between hormone levels and testicular biopsies of azoospermic men', *Archives of andrology*. Taylor & Francis, 42(3), pp. 145–149.

Mohammed AL-Haar (2011) 'Effect of Lead Acetate in Some Physiological & Genetic Parameters in White Male Rat Rattus rattus', *University of Kerbala–College of Education Department of Biology*.

Mohiuddin, M. *et al.* (2021) 'Sodium benzoate in locally available soft drinks and its effect on DNA damage and liver function in rats', *Dhaka University Journal of Biological Sciences*, pp. 371–383.

Moniruzzaman, M. and Min, T. (2020) 'Curcumin, curcumin nanoparticles and curcumin nanospheres: A review on their pharmacodynamics based on monogastric farm animal, poultry and

fish nutrition', *Pharmaceutics*. Multidisciplinary Digital Publishing Institute, 12(5), p. 447.

Ogunro, O. B. and Babatunde, O. T. (2023) 'Epigenetics in reproductive aging: involvement of oxidative stress', in *Epigenetics-Regulation and New Perspectives*. IntechOpen.

Ojeda, S. R. and Ramirez, V. D. (1972) 'Plasma level of LH and FSH in maturing rats: response to hemigonadectomy', *Endocrinology*. Oxford University Press, 90(2), pp. 466–472.

Oyewole, O. I., Dere, F. A. and Okoro, O. E. (2012) 'Sodium benzoate mediated hepatorenal toxicity in wistar rat: Modulatory effects of azadirachta indica (neem) leaf', *European Journal of Medicinal Plants*. SCIENCEDOMAIN International, 2(1), p. 11.

Oyola, M. G. and Handa, R. J. (2017) 'Hypothalamic–pituitary–adrenal and hypothalamic–pituitary–gonadal axes: sex differences in regulation of stress responsivity', *stress*. Taylor & Francis, 20(5), pp. 476–494.

Paradis, V. *et al.* (1997) 'In situ detection of lipid peroxidation in chronic hepatitis C: Correlation with pathological features', *Journal of Clinical Pathology*, 50(5), pp. 401–406. doi: 10.1136/jcp.50.5.401.

Qasim, A. S. and Numman Waheed, I. (2023) 'Protective Effects of Vitamin C and E Against Monosodium Glutamate Induced Histological Changes in The Epididymis of Adult Male Albino Rats', *Egyptian Journal of Veterinary Sciences*. National Information and Documentation Center (NIDOC), Academy of Scientific …, 54(3), pp. 525–540.

Qian, X. L. *et al.* (2013) 'Syndecan Binding Protein (SDCBP) Is Overexpressed in Estrogen Receptor Negative Breast Cancers, and Is a Potential Promoter for Tumor Proliferation', *PLoS ONE*, 8(3), pp. 1–9. doi: 10.1371/journal.pone.0060046.

Radwan, E. H. *et al.* (2020) 'The possible effects of sodium nitrite and sodium benzoate as food additives on the liver in male rats', *J. Adv. Biol*, 13, pp. 14–30.

RasGele, P. and KaymaK, F. (2013) 'EffEcts of food preservative natamycin on liver enzymes and total protein in Mus Musculus', *Bulgarian Journal of Agricultural Science*. Citeseer, 19(2), pp. 298–302.

RD, H. (1948) 'A microchemical reaction resulting in the staining of polysaccharide structure in fixed tissue preparations', *Archives Biocheme*, 16, pp. 131–141.

Rezaei, A., Amirahmadi, A. and Poozesh, V. (2022) 'Herbal research: Gaps affecting the quality and validity of research findings', *Journal of Chemical Health Risks*. Islamic Azad University, Damghan Branch, Islamic Republic of Iran.

Sabour, A. N. and Ibrahim, I. R. (2019) 'Effect of Sodium Benzoate on Corticosterone Hormone Level, Oxidative Stress Indicators and Electrolytes in Immature Male Rats'.

Sardar, A. *et al.* (2023) 'Determination of biochemical and histopathological changes on testicular and epididymis tissues induced by exposure to insecticide Imidacloprid during postnatal development in rats', *BMC Pharmacology and Toxicology*. Springer, 24(1), p. 68.

Sarhan, N. (2018) ‘The Ameliorating Effect of Sodium Selenite on the Histological Changes and Expression of Caspase-3 in the Testis of Monosodium Glutamate-Treated Rats: Light and Electron Microscopic Study’, *Journal of Microscopy and Ultrastructure*, 6, p. 105. doi: 10.4103/JMAU.JMAU_2_18.

Shaffer, C. B. and Toxicity, A. (1966) ‘Acute and Chronic of Pimaricin ’’, 109, pp. 97–109.

Shahmohammadi, M., Javadi, M. and Nassiri-Asl, M. (2016) ‘An overview on the effects of sodium benzoate as a preservative in food products’, *Biotechnology and Health Sciences*. qums, 3(3), pp. 7–11.

Silva, M. M. and Lidon, F. C. (2016) ‘Food preservatives-An overview on applications and side effects’, *Emirates Journal of Food and Agriculture*. Pensoft Publishers, 28(6), p. 366.

Sohrabi, D., Alipour, M. and Gholami, M. R. (2008) ‘The effect of sodium benzoate on testicular tissue, gonadotropins and thyroid hormones level in adult (Balb/C) mice’, *Feyz Medical Sciences Journal*. Feyz Medical Sciences Journal, 12(3), pp. 7–11.

Stoy, N. *et al.* (2005) ‘Tryptophan metabolism and oxidative stress in patients with Huntington’s disease’, *Journal of neurochemistry*. Wiley Online Library, 93(3), pp. 611–623.

Taheri, S. and Sohrabi, D. (2002) ‘Teratogenic effects of sodium benzoate on the rat fetus’, *Journal of Advances in Medical and Biomedical Research*. Journal of Advances in Medical and Biomedical Research, 10(39), pp. 1–4.

Tietz, N. W. (1995) ‘Clinical guide to laboratory tests’, in *Clinical guide to laboratory tests*, p. 1096.

Turner, P. V *et al.* (2011) ‘Administration of substances to laboratory animals: routes of administration and factors to consider’, *Journal of the American Association for Laboratory Animal Science*. American Association for Laboratory Animal Science, 50(5), pp. 600–613.

Walczak-Nowicka, Ł. J. and Herbet, M. (2022) ‘Sodium benzoate—Harmfulness and potential use in therapies for disorders related to the nervous system: A review’, *Nutrients*. MDPI, 14(7), p. 1497.

Weaver, D. *et al.* (2020) ‘Alzheimer’s disease as a disorder of tryptophan metabolism (2745)’, *Neurology*. AAN Enterprises, 94(15_supplement), p. 2745.

Te Welscher, Y. M. *et al.* (2008) ‘Natamycin blocks fungal growth by binding specifically to ergosterol without permeabilizing the membrane’, *Journal of Biological Chemistry*. ASBMB, 283(10), pp. 6393–6401.

Zeghib, K. and Boutlelis, D. A. (2021) ‘Food additive (sodium benzoate)-induced damage on renal function and glomerular cells in rats; modulating effect of aqueous extract of Atriplex halimus L.’, *Iranian Journal of Pharmaceutical Research: IJPR*. Brieflands, 20(1), p. 296.

Appendix

Appendix (1): Procedure of Hematoxylin and Eosin (H&E) Staining

Purpose:

To stain tissue sections for routine histological examination, allowing differentiation of nuclei (blue/purple) and cytoplasm or extracellular matrix (pink/red).

Materials Required:

• Deparaffinized and rehydrated tissue sections (on glass slides)

• Hematoxylin stain (Harris, Mayer's, or Gill's)

• Eosin Y (1% alcoholic or aqueous)

• Acid alcohol (1% HCl in 70% ethanol)

• Ammonia water (or saturated lithium carbonate) – for blueing

• Distilled water

• Ethanol (70%, 95%, 100%)

• Xylene

• DPX or other mounting medium

Staining Procedure:

1. Deparaffinization:

• Place slides in xylene for 2 changes, 5 minutes each.

2. Rehydration:

• Pass through descending ethanol series:

• 100% ethanol: 2 min × 2

• 95% ethanol: 1 min

• 70% ethanol: 1 min

• Rinse in distilled water: 1–2 min

3. Hematoxylin Staining:

• Stain in hematoxylin: 5–10 minutes (depending on type used)

• Rinse in running tap water: 2–5 minutes

• Differentiate in 1% acid alcohol (few seconds, optional)

• Rinse in water

• Blueing in ammonia water or lithium carbonate: 30 seconds – 1 minute

• Rinse in tap water again

4. Eosin Counterstain:

• Stain in 1% Eosin Y: 30 seconds – 1 minute

• Rinse briefly in 70% ethanol to remove excess eosin

5. Dehydration and Clearing:

• Dehydrate in ascending ethanol series:

• 95% ethanol: 1 min

• 100% ethanol: 2 min × 2

• Clear in xylene: 2 min × 2

6. Mounting:

• Mount using DPX or synthetic resin mounting medium.

• Cover with coverslip and allow to dry.

Result Interpretation:

Tissue Component Stain Color

Nuclei Blue to purple

Cytoplasm Pink

Muscle fibers Pink to red

Red blood cells (RBCs) Bright red

Collagen Pale pink

Appendix (2): Procedure of Periodic Acid–Schiff (PAS) Staining

Purpose:

To detect polysaccharides such as glycogen, mucosubstances, and basement membranes in tissue sections.

Materials Required:

• Periodic acid (0.5–1%)

• Schiff's reagent (commercially prepared or freshly made)

• Sulfite rinse solution (e.g., 0.5% sodium metabisulfite)

• Distilled water

• Hematoxylin (optional, for nuclear counterstain)

• Ethanol (70%, 95%, 100%)

• Xylene

• Mounting medium (e.g., DPX)

Staining Procedure:

1. Deparaffinization and Rehydration:

• Xylene: 2 changes, 5 min each

• Descending ethanol series: 100%, 95%, 70%, 1–2 min each

• Rinse in distilled water

2. Oxidation:

• Place slides in 0.5–1% periodic acid for 5–10 minutes

• Rinse in distilled water: 2 min

3. Schiff's Reagent:

• Immerse slides in Schiff's reagent: 10–15 minutes in the dark

• Rinse in running tap water or 0.5% sodium metabisulfite: 5–10 minutes until pink color develops

4. Counterstain (Optional):

• Stain nuclei with hematoxylin: 1–2 minutes

• Rinse in tap water and blue in alkaline water if needed

5. Dehydration and Clearing:

• Pass through ascending ethanol series (70%, 95%, 100%)

• Clear in xylene: 2 changes, 2 minutes each

6. Mounting:

• Mount using DPX or other suitable medium

• Apply coverslip

Result Interpretation:

Tissue Component Staining Color

Glycogen, mucins, glycoproteins Magenta (deep pink)

Basement membranes Magenta

Nuclei (with hematoxylin) Blue/purple

Cytoplasm Pale to colorless

Appendix (3): Procedure of Masson's Trichrome Staining

Purpose:

To differentiate collagen fibers from muscle and cytoplasm, commonly used to assess fibrosis in tissue sections.

Materials Required:

- Bouin's solution (for mordanting – optional but improves staining)
- Weigert's iron hematoxylin (for nuclear staining)
- Biebrich scarlet-acid fuchsin solution (stains cytoplasm/muscle)
- Phosphomolybdic/phosphotungstic acid (differentiation)
- Aniline blue (collagen stain)
- Acetic acid (1%)
- Ethanol (70%, 95%, 100%)
- Xylene
- Mounting medium (e.g., DPX)

Staining Procedure:

1. Deparaffinization and Rehydration:

- Xylene: 2 × 5 min
- Descending ethanol series (100% → 70%)
- Rinse in distilled water

2. Optional Mordanting:

- Bouin's solution at 56°C: 1 hour

• Cool and rinse in running tap water (10 min)

3. Nuclear Staining:

• Weigert's iron hematoxylin: 10 min

• Rinse in water

4. Cytoplasm Staining:

• Biebrich scarlet-acid fuchsin: 10–15 min

• Rinse briefly in water

5. Differentiation:

• Phosphomolybdic/phosphotungstic acid: 10–15 min (removes red from collagen)

6. Collagen Staining:

• Aniline blue: 5–10 min

• Rinse in 1% acetic acid: 2–3 min

7. Dehydration and Clearing:

• Ethanol 95%, then 100%: 1–2 min each

• Clear in xylene: 2 changes × 2 min

8. Mounting:

• Mount with DPX or resin medium

• Coverslip and allow to dry

Result Interpretation:

Tissue Component Staining Color

Nuclei Dark blue/black

Cytoplasm, muscle Red

Collagen, connective tissue Blue

RBCs Red

Appendix (4): Immunohistochemistry Procedure for Detection of MDA (Oxidative Stress Marker)

Objective:

To detect malondialdehyde (MDA) expression in testicular tissue as a marker of oxidative stress using immunohistochemical staining.

Materials and Reagents:

- Formalin-fixed, paraffin-embedded tissue blocks
- Xylene and graded alcohol solutions
- Citrate buffer (pH 6.0)
- Primary antibody: SDCBP Polyclonal Antibody (E-AB-17209)
- Immunohistochemistry Kit (Elabscience, USA)
- Goat anti-mouse linker and rabbit antibody
- Horseradish peroxidase (HRP)-conjugated secondary antibody
- DAB chromogen
- Hematoxylin
- Phosphate-buffered saline (PBS)

Procedure:

1. Sectioning and Deparaffinization:

- Sections of 5 μm thickness were cut from paraffin blocks.

• Slides were deparaffinized in xylene and rehydrated through descending alcohol series.

2. Antigen Retrieval:

• Antigen retrieval was performed using citrate buffer (pH 6.0) in an autoclave at 121°C for 10–15 minutes.

• Slides were cooled and rinsed with PBS.

3. Blocking:

• Tissue sections were incubated with blocking solution provided in the kit to prevent nonspecific binding.

4. Primary Antibody Incubation:

• The primary antibody (SDCBP, E-AB-17209) was applied and incubated at 37°C for 2 hours.

5. Secondary Antibody Application:

• Goat anti-mouse linker and rabbit antibody were added and incubated for 30 minutes.

• Slides were washed, followed by application of the HRP-conjugated secondary antibody.

6. Chromogen Development:

• DAB substrate was applied for signal visualization.

• Slides were monitored for appropriate staining intensity.

7. Counterstaining and Mounting:

• Sections were counterstained with hematoxylin, dehydrated, cleared in xylene, and mounted with DPX.

Controls:

• Negative Control: Tissue sections treated with PBS instead of primary antibody.

• Positive Control: Tissue known to express MDA.

الخلاصة

تهدف هذه الدراسة إلى تقييم التأثيرات النسجية و الكيميائية لمادتي بنزوات الصوديوم والبيماريسين على الخصى والبربخ في ذكور الجرذان البيضاء، وذلك لتحديد سميتهما المحتملة على الجهاز التناسلي. أُجريت التجربة في مختبرات فرع التشريح والأنسجة، كلية الطب البيطري / جامعة كربلاء، خلال الفترة من تشرين الثاني 2024 إلى كانون الثاني 2025.

تم تقسيم أربعين جرذاً ذكراً بصورة عشوائية إلى أربع مجموعات (10 حيوانات/مجموعة): مجموعة سيطرة، وثلاث مجموعات تجريبية تم معاملتها على التوالي ببنزوات الصوديوم (600 ملغم/كغم)، والبيماريسين (0.3 ملغم/كغم)، والمجموعة المختلطة (بنزوات الصوديوم + بيماريسين). استمر الإعطاء الفموي يومياً لمدة 50 يوماً. وعند نهاية التجربة، تم جمع الدم و النماذج النسجية وتجهيزها للفحص المجهري.

• **الفحص النسجي**: أظهرت صبغة الهيماتوكسيلين والإيوزين (H&E) درجات متفاوتة من التغيرات التنكسية والنخرية في الخصى والبربخ لجميع المجموعات المعالجة، حيث أظهرت مجموعة بنزوات الصوديوم وجود خثار وعائي، ووذمة بينية، وتنكس في الظهارة المنوية، وتكون فجوات في الخلايا المولدة للنطاف، مع انخفاض واضح في عدد خلايا ليدك. كما بدت قنوات البربخ غير منتظمة مع ارتشاح التهابي ونخر ونقص في محتوى الحيوانات المنوية داخل التجويف. أما التعرض للبيماريسين فقد أدى إلى تنكس خصوي بؤري واضح، واحتقان وعائي، وتليف بيني، وتنكس في التجويف البربخ مما يعكس ضعف نضوج الحيوانات المنوية.

سُجِّلت أشد التغيرات النسيجية في المجموعة المختلطة، حيث ظهر ضمور في الأنابيب المنوية، ونخر في الخلايا المولدة للنطاف، وانفصال في الغشاء القاعدي، تلايف بيني ممتد، وزيادة في سمك الغلالة البيضاء. كما كانت قنوات البربخ محاطة ليفي كثيف، مع تلايف في البربخ وتشوه في البنية الهيكلية وتثخن في الغشاء القاعدي.

أكدت صبغة PAS تراكم الكلايكوبروتين، وتثخن في الأغشية القاعدية، وأظهرت زيادة ملحوظة في الألياف الكولاجينية وتطور واضح للتليف، خصوصاً في المجموعة المختلطة. أما صبغة ماسون ثلاثية الألوان فقد أظهرت تغيرات ليفية، تضمنت تثخن الغلالة البيضاء وزيادة في ترسيب ألياف الكولاجين، خاصة في مجموعة المعالجة المشتركة.

• **التحليل الكيميائي:** استخدم المالوندي ألدهيد (MDA) كمؤشر للإجهاد التأكسدي، وقد أظهر تعبيراً متزايداً في جميع المجموعات المعالجة، مع أقوى استجابة في المجموعة المختلطة، مما يشير إلى وجود ضرر تأكسدي واضح في الأنسجة التناسلية.

من جهة أخرى، أظهرت نتائج التحليل الهرموني في هذه الدراسة انخفاضاً ملحوظاً في مستويات كل من الهرمون المحفز للجريبات (FSH) والهرمون اللوتيني (LH) في جميع المجموعات المعالجة مقارنةً بمجموعة السيطرة. وقد تفاقم هذا التثبيط الهرموني مع مرور الوقت، حيث سجلت المجموعة المختلطة أشد الانخفاضات في اليوم الخمسين.

تشير نتائج هذه الدراسة إلى أن التعرض طويل الأمد لبنزوات الصوديوم والبيماريسين، خاصة عند استخدامهما معاً، قد يؤدي إلى تغيرات نسيجية في الخصى والبربخ، مصحوبة باضطراب هرموني، مما قد يُضعف الخصوبة الذكرية.

جمهورية العراق وزارة التعليم العالي والبحث العلمي- كلية الطب البيطري

عنوان الرسالة

دراسة مظهرية وكيمياء نسيجية لتأثير المواد الحافظة (بنزوات الصوديوم والبيماريسين) على النسيج الخصوي في ذكور الجرذان البيضاء

رسالة

مقدمة إلى مجلس كلية الطب البيطري / جامعة كربلاء كجزء من متطلبات نيل درجة الماجستير في اختصاص علوم الطب البيطري/ فرع التشريح والانسجة

تقدم بها

عبد الأمير احمد اموري حسون الكلش

بأشراف

المشرف الاول

أ.د. منى حسين حسن العاملي

المشرف الثاني

أ.د. وفاق جبوري البازي

1446 هـ

2025م